DISSERTATION

# MECHANISMS OF TRANSPOSABLE ELEMENT TRANSCRIPT DYSREGULATION IN BRAIN AGING AND ALZHEIMER'S DISEASE

Submitted by

Cali Madison McEntee

Department of Health and Exercise Science

In partial fulfillment of the requirements

For the Degree of Doctor of Philosophy

Colorado State University

Fort Collins, Colorado

Summer 2025

Doctoral Committee:

Advisor: Thomas J. LaRocca

Daniel S. Lark
Julie A. Moreno
Ronald B. Tjalkens

ABSTRACT

MECHANISMS OF TRANSPOSABLE ELEMENT TRANSCRIPT DYSREGULATION IN BRAIN AGING AND ALZHEIMER'S DISEASE

Transposable element (TE) transcript accumulation may significantly contribute to neuroinflammation in brain aging and Alzheimer's disease; however, the mechanisms underlying TE dysregulation in this context have not been well characterized. The studies in this dissertation investigate two possible causes of TE dysregulation: 1) reduced expression and/or activity of the adenosine deaminase acting on RNA 1 (ADAR1) enzyme; and 2) increased chromatin accessibility in repressed regions of the genome. Guided by my mentoring team, I investigated these hypotheses in various experimental models and datasets throughout four studies. First, I examined changes in inflammatory signaling and TE transcript expression with ADAR1 suppression in primary human astrocytes. Second, I attempted to upregulate ADAR1 in the brains of older mice to prevent age-related cognitive decline and neuroinflammation. Third, I identified TE transcripts that form double-stranded RNA in the absence of ADAR1, and those that are most likely to stimulate inflammation, through cell culture experiments and RNA immunoprecipitation analyses. Finally, I analyzed cell-type-specific changes in TE transcript expression and chromatin accessibility in Alzheimer's disease using prefrontal cortex single-nucleus RNA-seq data. These studies also addressed the potential pro-inflammatory signaling pathways activated by TE transcripts, potentially driving neuroinflammation with brain aging and Alzheimer's disease. In summary, this work may serve as a foundation for future studies examining mechanisms of TE transcript dysregulation, and it suggests potential therapeutic targets to modulate their expression.

ACKNOWLEDGEMENTS

First, I would like to sincerely thank my dissertation committee members—Drs. Dan Lark, Julie Moreno, and Ron Tjalkens—for their time, thoughtful feedback, and support throughout the projects in this dissertation. Your guidance has been instrumental in shaping the development and execution of my work. Most importantly, I am deeply grateful to my PhD advisor and scientific mentor, Dr. Tom LaRocca. You have played a pivotal role in my growth as a scientist, and I attribute much of what I am today to your mentorship. I truly believe I would not be where I am now without your unwavering support and guidance.

I also want to thank the past and current members of the Healthspan Biology Laboratory. I could not have asked for a better group of people to navigate the highs and lows of graduate school—from long, grueling days of sample preparation and failed experiments to the rewarding moments of paper publications and successful grant applications. You all made this journey worthwhile. Additionally, I am grateful to the Department of Health and Exercise Science at Colorado State University for the opportunity to advance my research training, and to the National Institute of Aging for providing the funding that made my work possible.

Finally, this dissertation would not have been possible without the support of those outside of academia. To my best friends from undergrad, the friends I made during my PhD, and my partner—you all have reminded me to enjoy life outside of the lab during this process. Most of all, I want to thank my family: my mom, Casey; my dad, Roland; my sister, Caitlin; and (maybe the most important) my dog, Addy. I am endlessly grateful for all the sacrifices you have made to help me reach this point.

TABLE OF CONTENTS

ABSTRACT ..... ii
ACKNOWLEDGEMENTS ..... iii
CHAPTER 1 – INTRODUCTION AND EXPERIMENTAL AIMS ..... 1
BRAIN AGING AS A PRECURSOR TO ALZHEIMER'S DISEASE (AD) ..... 1
TRANSPOSABLE ELEMENT TRANSCRIPTS AS A SOURCE OF NEUROINFLAMMATION 5
MECHANISMS OF TRANSPOSABLE ELEMENT DYSREGULATION ..... 10
DISSERTATION AIMS ..... 12
REFERENCES ..... 13
CHAPTER 2 – ADAR1 SUPPRESSION CAUSES INTERFERON SIGNALING AND TRANSPOSABLE ELEMENT TRANSCRIPT ACCUMULATION IN HUMAN ASTROCYTES ... 22
INTRODUCTION ..... 22
METHODS ..... 24
RESULTS ..... 28
DISCUSSION ..... 37
REFERENCES ..... 41
CHAPTER 3 – AN AAV APPROACH TO INCREASE ADAR1 EXPRESSION IN THE BRAINS OF AGED MICE ..... 44
INTRODUCTION ..... 44
METHODS ..... 45
RESULTS ..... 48
DISCUSSION ..... 52
REFERENCES ..... 55
CHAPTER 4 – THE IDENTIFICATION OF TRANSPOSABLE ELEMENT-DERIVED DOUBLE-STRANDED RNAS THAT ARE MODULATED BY ADAR1 AND ACTIVATE INFLAMMATORY SIGNALING ..... 57
INTRODUCTION ..... 57
METHODS ..... 58
RESULTS ..... 61
DISCUSSION ..... 70
REFERENCES ..... 74
CHAPTER 5 – SINGLE-CELL TRANSCRIPTOME PATTERNS OF TRANSPOSABLE ELEMENTS IN ALZHEIMER'S DISEASE ..... 77
INTRODUCTION ..... 77
METHODS ..... 78
RESULTS ..... 82

DISCUSSION ..... 92
REFERENCES ..... 97
CHAPTER 6 – ADAR1 vs. CHROMATIN ACCESSIBILITY: WHICH DRIVES TRANSPOSABLE ELEMENT TRANSCRIPT ACCUMULATION IN AGING AND AD? ..... 102
INTRODUCTION ..... 102
GENERAL APPROACH ..... 104
AIM 1: IDENTIFY ACTIVATORS OF ADAR1 ACTIVITY THAT REDUCE TE TRANSCRIPT ACCUMULATION AND NEUROINFLAMAMTION WITH AGING AND AD. ..... 105
AIM 2: DETERMINE IF AGE-ASSOCIATED CHANGES IN TE TRANSCRIPT ACCUMULATION AND ACCESSIBILITY PRECEDE AD IN ALL CELL TYPES OF THE BRAIN ..... 110
FUTURE DIRECTIONS ..... 114
REFERENCES ..... 115
APPENDIX A – CHAPTER 2 SUPPLEMENTAL DATA ..... 118
APPENDIX B – CHAPTER 3 SUPPLEMENTAL DATA ..... 121
APPENDIX C – CHAPTER 4 SUPPLEMENTAL DATA ..... 123
APPENDIX D – CHAPTER 5 SUPPLEMENTAL DATA ..... 126
APPENDIX E – CHAPTER 6 SUPPLEMENTAL DATA ..... 134

# CHAPTER 1 – INTRODUCTION AND EXPERIMENTAL AIMS

## BRAIN AGING AS A PRECURSOR TO ALZHEIMER'S DISEASE (AD)

Alzheimer's disease (AD) is a neurodegenerative disease broadly characterized by cognitive impairment and changes in biological processes that result in neuronal dysfunction, neuroinflammation, and cellular death/degeneration in the brain [1]. Common neuropathological features of AD include aggregations of amyloid beta (Aβ) plaques and neurofibrillary tangles composed of tau [2, 3]. AD is also associated with excessive activation of glial cells (gliosis), which contributes to neuroinflammation [4]. Both pathological protein aggregations and gliosis are hallmark features of neurodegenerative diseases, representing cellular and molecular processes that drive disease development and progression [5]. AD also exhibits other hallmarks of neurodegenerative diseases, including neuronal cell death, altered energy homeostasis, and synaptic network defects [5]. Importantly, many hallmark processes of AD also occur progressively with aging, but to a lesser degree [6-11], and older age remains the most significant risk factor for developing AD and may even be a potential cause [12, 13]. According to the Alzheimer's Association, more than 13 million adults above the age of 65 are projected to be diagnosed with AD by 2060, with even higher prevalence anticipated among adults 85 years old and older [14]. Despite these connections between AD and aging, the precise mechanisms underlying age-related AD remain unknown.

The global population is rapidly aging, and older adults (>65 years old) will represent a quarter of all Americans in the next 30 years [15]. As such, understanding the processes and consequences of aging are a key priority. Aging results from the progressive decline of biological functions and adverse cellular changes that are known as the "Hallmarks of Aging" (e.g., mitochondrial dysfunction, stem cell exhaustion) [16, 17], and these hallmarks are implicated in many age-related diseases [18, 19]. Importantly, many of these hallmark processes also occur during brain aging, which also includes a set of brain-specific processes

(e.g., glial cell activation and inflammation, dysregulated neuronal calcium homeostasis) [20]. Notably, several of these processes mirror those observed in neurodegenerative diseases, including AD [5]. Many of the hallmarks of aging have been linked to declines in cognitive function [21-26], a precursor and significant risk factor for AD [27]. Collectively, these studies support the rationale for a link between brain aging and AD, but the specific mechanisms connecting the two remain poorly understood.

Given the points above, in order to understand the mechanism(s) by which brain aging leads to AD, it is crucial to characterize the similarities (and potential links) between the hallmarks of aging and neurodegenerative diseases. While many hallmark processes are shared between the two, those that are most relevant to the studies in this dissertation include neuroinflammation and genome/transcriptome alterations.

*Neuroinflammation*

Neuroinflammation is closely linked to AD pathology and reduced cognitive function with aging and AD [28, 29], and it is characterized by the activation of pro-inflammatory pathways within the innate immune system [30]. Innate immune signaling increases in the brain and periphery with aging and AD [31-33], suggesting that the immune activation that occurs with aging may precede the onset of AD. Chronic low-grade inflammation with aging driven by innate immune signaling—referred to as “inflammaging”—may predispose the brain to AD-specific cellular changes, like tau and Aβ aggregations (pathological features of AD) [34, 35]. Innate immune activation can originate from many sources, including AD pathology, injury, reactive oxygen species, senescent cells, peripheral immune cells, all of which are linked with the activation of inflammatory pathways in the brain [29, 36-41]. Of particular relevance to this dissertation, other innate immune activators include damage-associated and pathogen-associated molecular patterns (DAMPs and PAMPs, respectively), which may accumulate as a result of aging and even exacerbate AD pathology and symptoms. DAMPs, derived from dying

or dead cells (e.g., ATP, nucleic acids, cytokines) [42], and PAMPs, which include pathogen-derived molecules (e.g., bacterial LPS, viral nucleic acids), both activate innate immune signaling pathways [43]. The age-related increase in DAMPs and PAMPs is driven by cellular changes (e.g., mitochondrial dysfunction, cellular senescence, and epigenetic alterations) [16, 17, 44], and their presence typically results in the activation of the nuclear factor kappa-B (NF-κB) pathway [45]. DAMPs have also been detected in the brains of AD patients [46-48], likely a result of disease-specific cellular degeneration, further amplifying the inflammatory response in AD [49, 50]. Additionally, evidence also suggests that viral-like signatures (e.g., nucleic acids, proteins) may act as critical PAMPs in AD. For example, active herpes simplex virus has been identified in the brains of AD patients [51, 52], potentially driving a chronic inflammatory response that accelerates disease progression [53, 54]. However, the exact sources of innate immune activation in AD have yet to be comprehensively documented.

Many cell types contribute to neuroinflammation; however, glial cells—particularly microglia and astrocytes—play major roles in its development [55, 56]. Microglia serve as the brain's resident immune cells [57, 58], while astrocytes maintain homeostasis and support neuronal function [59]. Although the role of microglia in neuroinflammation with aging and AD has been extensively studied and reviewed [60-63], this dissertation focuses on astrocytes, a cell type increasingly implicated in neuroinflammation with aging and AD [64], primarily through NF-κB activation [65]. Pro-inflammatory astrocytes release cytokines (e.g., IL-1β, TNF-α, CXCL10, CCL5, and others) that act as positive feedback loops to amplify inflammatory signaling and activate neighboring cells [64, 66]. These astrocytes can also stimulate microglia, reduce oligodendrocyte myelination, disrupt synaptic activity, compromise blood brain barrier integrity, and recruit peripheral immune cells to the brain [67-71]. Astrocytes respond to a variety of stimuli, including cytokines (e.g., released by microglia or other cells), DAMPs (e.g., from neuronal loss or AD pathology), and PAMPs (i.e., via viral infection), to trigger an

inflammatory phenotype in both aging and AD [72-76]. Together, these findings suggest that astrocytes play a crucial role in neuroinflammation associated with aging and AD.

Beyond glia, other cell types in the brain, including neurons, also contribute to neuroinflammation with aging and AD. Neurofibrillary tangles of tau, primarily originating from neurons, can elicit an inflammatory response in microglia and astrocytes [77]. Additionally, DAMPs released due to neuronal death or dysfunction can further intensify inflammatory responses [38]. NF-κB signaling is also highly active in inflammatory neurons [78], and is activated by common inflammatory stimuli (e.g., tau, Aβ, cytokines) [38, 79]. However, the specific role of neurons as a source of inflammation is not well characterized. Evidence also suggests other CNS cell types, like oligodendrocytes, endothelial cells, and peripheral mononuclear blood cells, may be sources of inflammatory activation in the brain [80-85]. Despite the involvement of multiple cell types in the progression of neuroinflammation with aging and AD, this dissertation focuses on astrocytes and neurons as contributors to aging- and AD-related neuroinflammation, aiming to identify the upstream drivers that may originate from endogenous sources.

*Genome/transcriptome alterations*

Key biological processes involved in the regulation of DNA (e.g., DNA damage, impaired DNA repair processes, and epigenetic changes) are closely associated with aging, and their dysfunction can lead to genomic alterations [86, 87]. These age-related changes may reshape the chromatin structure by modifying the chromatin landscape, allowing for regions of the genome that are typically suppressed to be newly expressed [88]. DNA sequences that reside in repressed regions often are non-coding, as much of the non-coding genome is involved in maintaining chromatin structure [89]. The derepression of the non-coding genome has been linked to aging and many age-related diseases [90, 91], including AD [92, 93]. The increased expression of the non-coding genome may result from complex epigenetic alterations, including

DNA methylation and histone modifications (e.g., methylation, acetylation) [94-98], that lead to chromatin relaxation. These changes to the epigenome may occur as a consequence of normal aging (i.e., “epigenetic drift”, or the gradual loss of control of the epigenome) and may contribute to AD development [99, 100]. In parallel, impaired RNA degradation and homeostasis pathways may permit the accumulation of non-coding RNAs that act as inflammatory stimuli, as observed in normal aging and other neurodegenerative diseases [101-103]. In some cases, non-coding RNA may aggregate in stress granules—collections of excess RNA and cellular debris that impair proper cell function [104], and are linked with neuroinflammation, aging, and neurogenerative diseases, including AD [105-107]. Collectively, these genomic and transcriptomic changes may lead to unregulated expression and accumulation of non-coding RNAs that are normally suppressed, along with altered expression of protein-coding genes, potentially serving as a source of neuroinflammation with aging and/or AD.

*Summary and Hypothesis*

Together, the observations described above suggest that age-related neuroinflammation and genome/transcriptome changes may play a significant and interconnected role in the development of AD. However, It remains uncertain whether these aging-associated changes directly *cause* AD or *predispose* the brain to develop AD in later life. Based on the evidence presented, I hypothesize that dysregulated expression of non-coding RNAs (i.e., transposable elements transcripts, described below) may serve as a pro-inflammatory trigger for neuroinflammation during aging, ultimately making the brain more vulnerable to AD.

## TRANSPOSABLE ELEMENT TRANSCRIPTS AS A SOURCE OF NEUROINFLAMMATION

Only 2% of the human genome encodes protein-coding genes [108], leaving the vast majority composed of non-coding elements [108]. Among these non-coding elements, transposable elements (TEs) make up ~45% of the entire human genome and were historically

regarded as “junk DNA” [109, 110], but more recent evidence suggests they may have important roles in cellular function [111, 112]. TEs are composed of two major classes, transposons and retrotransposons, and they propagate throughout the genome through transposition (in which transposons “cut-and-paste” from one region of the genome to another) and retrotransposition (in which retrotransposons “copy-and-paste”, inserting into new genomic locations) [110, 113]. TEs are repetitive in nature, both throughout the genome and in their sequences, and are thought to be remnants of ancient viruses that have accumulated and persisted in the genome through evolution [114], possibly to stimulate a greater inflammatory response during an infection [115]. Under normal conditions, TEs are typically hyperchromatinized (via epigenetic silencing), thus preventing their expression [89]. However, our lab and others have reported increased TE transcript levels with aging [90, 91], and this may be driven by age-related epigenetic changes and altered chromatin accessibility that enhance transcription [116, 117]. TE transcripts are also elevated in neurodegenerative diseases [92, 118, 119], particularly in AD [120, 121], and are associated with cognitive decline and AD pathology [116, 122-124]. Additionally, TE transcripts have been linked with AD-related neuroinflammation [122, 123, 125], although the exact mechanisms underlying TE-associated neuroinflammation are not fully understood.

There are several potential mechanisms by which TEs could contribute to neuroinflammation. First, TE-associated inflammation may result from cytoplasmic DNA (cDNA), a PAMP that resembles viral nucleic acids. TE-derived cDNA is produced by retrotransposons, whose RNA transcripts are reversed transcribed into cDNA prior to being inserted into new genomic locations [126]. However, before insertion, retrotransposon cDNA can activate antiviral response pathways, such as cGAS-STING [127]. Briefly, cDNA binds to cyclic GMP-AMP synthase (cGAS) to trigger the formation of cyclic GMP-AMP (cGAMP) [127]. cGAMP then binds to the stimulator of interferon genes (STING), triggering inflammatory signaling via TANK-binding kinase 1 (TBK1) and interferon regulatory factor 3 (IRF3) phosphorylation [127]. Recent

studies have demonstrated activation of the cGAS-STING pathway in mouse models of aging and AD [128-130], but these observations have yet to be translated to human subjects. Importantly, this signaling pathway only applies to a subset of TEs (i.e., retrotransposons), and therefore, only represents one of several mechanism in which TEs contribute to inflammation.

TEs are also associated with DNA damage due to the double-stranded DNA breaks (a DAMP) that are generated during TE propagation (e.g., transposition or retrotransposition) [131]. This TE-associated DNA damage may amplify inflammatory responses in the context of aging or AD, where DNA repair processes are often impaired [132-135]. Additionally, TE insertions may induce chromatin rearrangements that lead to genetic mutations and alter RNA splicing, potentially resulting in dysfunctional proteins [136]. Although these events are plausible, it remains unclear whether chromatin rearrangements caused by TE insertions significantly impact biological processes associated with aging and/or AD. Like cDNA and the cGAS-STING pathway, these inflammatory mechanisms only apply to active TEs, which comprise <5% of TEs in the human genome [137]. Thus, it is likely that these response pathways also only apply to a small portion of TEs.

Lastly, TE-associated inflammation may be the result of endogenous double-stranded RNA (dsRNA; a viral-like PAMP) coming from TE transcripts. Due do their repetitive nature, TE transcripts may form intra-strand dsRNA (palindromic, double-stranded secondary RNA structures within a single transcript) and inter-strand dsRNA (complimentary binding between sense and antisense transcripts) that activate innate immune signaling pathways (e.g., pattern recognition receptors) in any cell type [138-140]. Growing evidence supports a role for dsRNA and TE transcripts in neurodegenerative diseases [92, 118, 141-144], particularly in AD and its associated neuroinflammation [119, 122, 145]. TE-derived dsRNA likely triggers neuroinflammation through dsRNA sensor proteins (a type of innate immune sensor, described in detail below) [146]. However, the precise mechanisms by which TE-derived dsRNA contribute to inflammation are incompletely understood.

The above points collectively suggest that TEs and their transcripts can trigger inflammatory signaling through multiple pathways, many of which can be aggravated by declines/hallmark changes associated with aging and AD (e.g., increased DNA damage). Moreover, while certain inflammatory mechanisms may be specific to certain TEs subsets (e.g., cGAS-STING signaling occurs only in response to TE-derived cDNA, depending on class and type), most TEs have the potential to form pro-inflammatory dsRNA. TE-derived dsRNA can activate a variety of response pathways that lead to inflammation. For instance, common pathways include those mediated by RIG-I-like receptors (RLRs) and protein kinase R (PKR) [146]. Other sensors, such as oligoadenylate synthases, NOD-, LRR- and pyrin domain-containing 1, and Toll-like receptors, may also respond to endogenous dsRNA [146-149], although it remains unclear whether they bind to TE-derived dsRNA, a topic beyond the scope of this dissertation. Below, the signaling pathways of RLRs and PKR in dsRNA sensing and the potential roles in brain aging and AD are discussed.

*RIG-I-like Receptors (RLRs)*

The RIG-I-like receptor (RLR) signaling pathway involves the dsRNA sensor proteins retinoic acid-inducible gene I (RIG-I) and melanoma differentiation-associated protein 5 (MDA5). The binding of dsRNA to RIG-I or MDA5 activates mitochondrial antiviral-signaling protein (MAVS), and the signal is transduced through TBK1 and IκB kinase-ε (IKKε) [150]. TBK1 and IKKε then phosphorylate IRF3 and IRF7, leading to increased production of type I interferons and other pro-inflammatory cytokines [150]. While this pathway is typically activated in response to viral infections, endogenous RNAs (including from TE transcripts) can also trigger the same response. In particular, RLRs have been shown to bind to TE transcripts in models of inflammation and cancer [151, 152], and our lab has provided evidence of a relationship between transcripts of TEs and MDA5 in aging-related inflammation [153]. Moreover, RIG-I expression is elevated in patients with mild cognitive impairment and is associated with AD

pathology [154], but the RNAs that bind to RIG-I in cognitive impairment and if MDA5 is involved in AD are unknown. Together, these observations suggest that RLRs may play a crucial role as sensor proteins in TE-associated neuroinflammation with brain aging and AD, possibly by binding to TE-derived dsRNAs.

*Protein Kinase R (PKR)*

PKR is a key regulator of several critical cellular functions, including cell growth, apoptosis, translation, and inflammation [155]. PKR was first identified as an antiviral protein due to its ability to bind to viral dsRNA to trigger an inflammatory response and inhibit viral replication [156]. Upon binding to dsRNA, PKR is auto-phosphorylated into its active form, which then phosphorylates eukaryotic translation initiation factor 2A (eIF2α) and inhibitor of nuclear factor kappa-αβ-kinase (iKKαβ) to induce translational arrest and stimulate an inflammatory response, respectively [155]. Additionally, activated PKR induces the FADD/Caspase 8 pathway to initiate apoptosis [155], and it also colocalizes with excess RNA in stress granules during viral infection [157]. Importantly, PKR activation and its associated signaling pathways can be inhibited by the compound C16, a potential therapeutic approach to modulate PKR-related inflammation [158, 159]. While limited data suggest that TE-derived dsRNA may bind to PKR [160], PKR has been shown to bind to mitochondrial dsRNA (another endogenous dsRNA source) [161], indicating that PKR may also bind to TE-derived dsRNA. Importantly, RLR signaling may be dependent on PKR, as evidence suggests that PKR acts downstream of MDA5 [162], but this relationship has not been well characterized. Furthermore, PKR signaling is associated with aging and linked with Aβ toxicity, tau phosphorylation, inflammation, insulin resistance, and cognitive impairment in AD [163, 164]. However, it remains unclear whether TE transcripts, as a result of aging and/or AD, activate PKR.

## MECHANISMS OF TRANSPOSABLE ELEMENT DYSREGULATION

The accumulation of TE-derived dsRNA with aging and/or AD could result from: 1) a decline in cytoplasmic dsRNA degradation pathways; and 2) an increase in TE transcription due to changes to the epigenome. Importantly, both possibilities are closely linked to the hallmarks of aging and neurodegenerative diseases (e.g., impaired molecular waste disposal, DNA and RNA defects, and genome instability) [5, 16, 17].

### *Reduced expression/activity of double-stranded RNA-specific adenosine deaminases*

Key regulators of endogenous dsRNA degradation include the family of enzymes called adenosine deaminase acting on RNA (ADARs) [165]. The ADAR family consists of the catalytically active ADAR1 and ADAR2, as well as the catalytically inactive ADAR3 [166]. ADAR1 and ADAR2 convert adenosines to inosines (referred to as A-to-I editing), which disrupts base-pairing and unwinds dsRNA, preventing the activation of type I interferon signaling via RLRs [167-171]. ADAR1 is reportedly more active than ADAR2 [166], suggesting that it likely plays a greater role in regulating endogenous dsRNA and modulating pro-inflammatory signaling [172]. Additionally, ADAR1 exists in two isoforms: the nuclear p110 and the cytoplasmic, interferon-inducible p150 [166]. Evidence suggests that the p110 isoform may be more crucial for development, whereas the p150 isoform plays a bigger role in regulating inflammation [169, 173]. Mutations in ADAR1 have been implicated in the autoimmune disorder Aicardi-Goutières syndrome (AGS), which is characterized by elevated type I interferon activity in the brain, immune system, and skin [174-176]. Furthermore, ADAR1 may also be implicated in neurodegenerative diseases (e.g., Multiple Sclerosis, Parkinson's disease) [177, 178]. Based on this evidence, it is plausible that ADAR1 could play a direct role in brain aging and age-related neurodegenerative diseases, like AD, although this hypothesis has yet to be explored.

The validation of ADAR1 as a key mediator of neuroinflammation has proven challenging. ADAR1 is essential for suppressing inflammation in various human cells lines [179-

181], but homozygous knockout (KO) of the *Adar1* gene in mice is embryonically lethal due to aberrant apoptosis is multiple tissues [182]. Heterozygous *Adar1* (*Adar1*$^{+/-}$) KO mice display increased RLR-mediated type I interferon signaling and inflammation, and evidence suggests that this is occurring in the brain [169, 170, 183]. Additionally, the loss of ADAR1 editing may specifically drive the RLR inflammatory response, whereas the loss of the cytoplasmic p150 isoform of ADAR1 may drive PKR signaling [184]. In brain-like tissue, Adar *Drosophila melanogaster* mutants exhibit elevated innate immune signaling, impaired locomotion, and neurodegeneration [185]. Lastly, ADAR1 has been associated with TEs, particularly by reducing retrotransposon activity [186, 187], though whether this reduction in activity was due to A-to-I editing by ADAR1 remains unclear. Collectively, these studies suggest that ADAR1 may play a significant role in neuroinflammation during brain aging and AD, possibly by modulating TE-derived dsRNA.

*Changes to chromatin accessibility*

Changes to the epigenome may underlie increases in TE transcript expression. TEs reside in typically repressed regions of the genome [89], but alterations in the epigenome with brain aging and/or AD could lead to the derepression of TEs (e.g., via changes in DNA methylation and/or histone modifications). In particular, chromatin accessibility is a key hallmark of aging and been linked with TE transcript expression [16, 17, 88]. Recent preprint data suggest that increased chromatin accessibility, resulting from epigenetic changes, leads to the upregulation of retrotransposon transcripts, which are associated with an accelerated aging phenotype [188]. Additionally, in AD *Drosophila melanogaster* mutants, tau has been shown to increase TE transcript expression by altering the chromatin landscape [116], and some of these TE transcripts even form dsRNA [122]. While these TE-specific findings have not yet to be translated to humans, tau has been linked to chromatin relaxation in human postmortem brain samples [189, 190], suggesting that tau's interaction with chromatin could be a driver of TE

transcript expression in human AD brains. Thus, it is possible that aging-related chromatin accessibility and increased TE transcript expression could precede AD, but this whether this is true remains unknown.

## DISSERTATION AIMS

As described in the sections above, the current literature provides justification for investigating TE transcripts as contributors to neuroinflammation in aging and/or AD, as well as for examining the dysregulation of the mechanisms that normally prevent excessive expression of these transcripts (e.g., ADAR1, chromatin accessibility) in this context. Therefore, the aims of this dissertation were as follows:

**Aim 1:** Determine the role of ADAR1 in preventing TE-associated inflammation in primary human astrocytes.

**Aim 2**: Investigate the role of ADAR1 in protecting against the accumulation of TE-derived dsRNA that contribute to age-related neuroinflammation and cognitive decline.

**Aim 3:** Identify endogenous, TE-derived dsRNA and the inflammatory signaling pathways activated by reduced ADAR1 expression.

**Aim 4:** Analyze cell-type specific changes in TE transcript dysregulation to identify which cell type(s) are TE transcripts most dysregulated in the AD brain.

REFERENCES


1. Scheltens, P., et al., *Alzheimer's disease.* Lancet, 2021. **397**(10284): p. 1577-1590.
2. Trejo-Lopez, J.A., A.T. Yachnis, and S. Prokop, *Neuropathology of Alzheimer's Disease.* Neurotherapeutics, 2022. **19**(1): p. 173-185.
3. DeTure, M.A. and D.W. Dickson, *The neuropathological diagnosis of Alzheimer's disease.* Mol Neurodegener, 2019. **14**(1): p. 32.
4. De Sousa, R.A.L., *Reactive gliosis in Alzheimer's disease: a crucial role for cognitive impairment and memory loss.* Metab Brain Dis, 2022. **37**(4): p. 851-857.
5. Wilson, D.M., 3rd, et al., *Hallmarks of neurodegenerative diseases.* Cell, 2023. **186**(4): p. 693-714.
6. Singh, A., et al., *Aging and Inflammation.* Cold Spring Harb Perspect Med, 2024. **14**(6).
7. Mostany, R., et al., *Altered synaptic dynamics during normal brain aging.* J Neurosci, 2013. **33**(9): p. 4094-104.
8. Rodrigue, K.M., K.M. Kennedy, and D.C. Park, *Beta-amyloid deposition and the aging brain.* Neuropsychol Rev, 2009. **19**(4): p. 436-50.
9. Li, Y., et al., *Interactions between mitochondrial dysfunction and other hallmarks of aging: Paving a path toward interventions that promote healthy old age.* Aging Cell, 2024. **23**(1): p. e13942.
10. Hartl, F.U., A. Bracher, and M. Hayer-Hartl, *Molecular chaperones in protein folding and proteostasis.* Nature, 2011. **475**(7356): p. 324-32.
11. Saha, P. and N. Sen, *Tauopathy: A common mechanism for neurodegeneration and brain aging.* Mech Ageing Dev, 2019. **178**: p. 72-79.
12. Wyss-Coray, T., *Ageing, neurodegeneration and brain rejuvenation.* Nature, 2016. **539**(7628): p. 180-186.
13. Guerreiro, R. and J. Bras, *The age factor in Alzheimer's disease.* Genome Med, 2015. **7**: p. 106.
14. *2023 Alzheimer's disease facts and figures.* Alzheimers Dement, 2023. **19**(4): p. 1598-1695.
15. Vespa, J.M., L. Armstrong, D.M., *Demographic Turning Points for the United States: Population Projections for 2020 to 2060* in *Population Estimates and Projections*. 2020, United States Census Bureau.
16. López-Otín, C., et al., *The hallmarks of aging.* Cell, 2013. **153**(6): p. 1194-217.
17. López-Otín, C., et al., *Hallmarks of aging: An expanding universe.* Cell, 2023. **186**(2): p. 243-278.
18. Guo, J., et al., *Aging and aging-related diseases: from molecular mechanisms to interventions and treatments.* Signal Transduct Target Ther, 2022. **7**(1): p. 391.
19. Tenchov, R., et al., *Aging Hallmarks and Progression and Age-Related Diseases: A Landscape View of Research Advancement.* ACS Chem Neurosci, 2024. **15**(1): p. 1-30.
20. Mattson, M.P. and T.V. Arumugam, *Hallmarks of Brain Aging: Adaptive and Pathological Modification by Metabolic States.* Cell Metab, 2018. **27**(6): p. 1176-1199.
21. Murman, D.L., *The Impact of Age on Cognition.* Semin Hear, 2015. **36**(3): p. 111-21.
22. Languren, G., et al., *Neuronal damage and cognitive impairment associated with hypoglycemia: An integrated view.* Neurochem Int, 2013. **63**(4): p. 331-43.
23. Mather, K.A., et al., *The role of epigenetics in cognitive ageing.* Int J Geriatr Psychiatry, 2014. **29**(11): p. 1162-71.
24. Chou, Y.H., et al., *Cortical excitability and plasticity in Alzheimer's disease and mild cognitive impairment: A systematic review and meta-analysis of transcranial magnetic stimulation studies.* Ageing Res Rev, 2022. **79**: p. 101660.

25. Song, T., et al., *Mitochondrial dysfunction, oxidative stress, neuroinflammation, and metabolic alterations in the progression of Alzheimer's disease: A meta-analysis of in vivo magnetic resonance spectroscopy studies.* Ageing Res Rev, 2021. **72**: p. 101503.
26. Teylan, M., et al., *Cognitive trajectory in mild cognitive impairment due to primary age-related tauopathy.* Brain, 2020. **143**(2): p. 611-621.
27. Janoutová, J., et al., *Is Mild Cognitive Impairment a Precursor of Alzheimer's Disease? Short Review.* Cent Eur J Public Health, 2015. **23**(4): p. 365-7.
28. Andronie-Cioara, F.L., et al., *Molecular Mechanisms of Neuroinflammation in Aging and Alzheimer's Disease Progression.* Int J Mol Sci, 2023. **24**(3).
29. Heneka, M.T., et al., *Neuroinflammation in Alzheimer's disease.* Lancet Neurol, 2015. **14**(4): p. 388-405.
30. Mukhara, D., U. Oh, and G.N. Neigh, *Neuroinflammation.* Handb Clin Neurol, 2020. **175**: p. 235-259.
31. Hearps, A.C., et al., *Aging is associated with chronic innate immune activation and dysregulation of monocyte phenotype and function.* Aging Cell, 2012. **11**(5): p. 867-75.
32. Cribbs, D.H., et al., *Extensive innate immune gene activation accompanies brain aging, increasing vulnerability to cognitive decline and neurodegeneration: a microarray study.* J Neuroinflammation, 2012. **9**: p. 179.
33. Le Page, A., et al., *Role of the peripheral innate immune system in the development of Alzheimer's disease.* Exp Gerontol, 2018. **107**: p. 59-66.
34. Cullen, N.C., et al., *Accelerated inflammatory aging in Alzheimer's disease and its relation to amyloid, tau, and cognition.* Sci Rep, 2021. **11**(1): p. 1965.
35. Giunta, B., et al., *Inflammaging as a prodrome to Alzheimer's disease.* J Neuroinflammation, 2008. **5**: p. 51.
36. Sulhan, S., et al., *Neuroinflammation and blood-brain barrier disruption following traumatic brain injury: Pathophysiology and potential therapeutic targets.* J Neurosci Res, 2020. **98**(1): p. 19-28.
37. Teleanu, D.M., et al., *An Overview of Oxidative Stress, Neuroinflammation, and Neurodegenerative Diseases.* Int J Mol Sci, 2022. **23**(11).
38. Zhang, W., et al., *Role of neuroinflammation in neurodegeneration development.* Signal Transduct Target Ther, 2023. **8**(1): p. 267.
39. Zhang, W., et al., *Cellular senescence, DNA damage, and neuroinflammation in the aging brain.* Trends Neurosci, 2024. **47**(6): p. 461-474.
40. Gaikwad, S., et al., *Senescence, brain inflammation, and oligomeric tau drive cognitive decline in Alzheimer's disease: Evidence from clinical and preclinical studies.* Alzheimers Dement, 2024. **20**(1): p. 709-727.
41. Zang, X., et al., *The Emerging Role of Central and Peripheral Immune Systems in Neurodegenerative Diseases.* Front Aging Neurosci, 2022. **14**: p. 872134.
42. Roh, J.S. and D.H. Sohn, *Damage-Associated Molecular Patterns in Inflammatory Diseases.* Immune Netw, 2018. **18**(4): p. e27.
43. Li, D. and M. Wu, *Pattern recognition receptors in health and diseases.* Signal Transduct Target Ther, 2021. **6**(1): p. 291.
44. Feldman, N., A. Rotter-Maskowitz, and E. Okun, *DAMPs as mediators of sterile inflammation in aging-related pathologies.* Ageing Res Rev, 2015. **24**(Pt A): p. 29-39.
45. Salminen, A., et al., *Activation of innate immunity system during aging: NF-kB signaling is the molecular culprit of inflamm-aging.* Ageing Res Rev, 2008. **7**(2): p. 83-105.
46. Van Eldik, L.J. and W.S. Griffin, *S100 beta expression in Alzheimer's disease: relation to neuropathology in brain regions.* Biochim Biophys Acta, 1994. **1223**(3): p. 398-403.
47. Lassmann, H., et al., *Synaptic pathology in Alzheimer's disease: immunological data for markers of synaptic and large dense-core vesicles.* Neuroscience, 1992. **46**(1): p. 1-8.

48. de la Monte, S.M., et al., *Mitochondrial DNA damage as a mechanism of cell loss in Alzheimer's disease.* Lab Invest, 2000. **80**(8): p. 1323-35.
49. Mangalmurti, A. and J.R. Lukens, *How neurons die in Alzheimer's disease: Implications for neuroinflammation.* Curr Opin Neurobiol, 2022. **75**: p. 102575.
50. Venegas, C. and M.T. Heneka, *Danger-associated molecular patterns in Alzheimer's disease.* J Leukoc Biol, 2017. **101**(1): p. 87-98.
51. Itzhaki, R.F., et al., *Herpes simplex virus type 1 in brain and risk of Alzheimer's disease.* Lancet, 1997. **349**(9047): p. 241-4.
52. Lin, W.R., et al., *Herpesviruses in brain and Alzheimer's disease.* J Pathol, 2002. **197**(3): p. 395-402.
53. Wang, Z., et al., *Herpes simplex virus 1 accelerates the progression of Alzheimer's disease by modulating microglial phagocytosis and activating NLRP3 pathway.* J Neuroinflammation, 2024. **21**(1): p. 176.
54. Cairns, D.M., et al., *A 3D human brain-like tissue model of herpes-induced Alzheimer's disease.* Sci Adv, 2020. **6**(19): p. eaay8828.
55. Singh, D., *Astrocytic and microglial cells as the modulators of neuroinflammation in Alzheimer's disease.* J Neuroinflammation, 2022. **19**(1): p. 206.
56. Al-Ghraiybah, N.F., et al., *Glial Cell-Mediated Neuroinflammation in Alzheimer's Disease.* Int J Mol Sci, 2022. **23**(18).
57. Borst, K., A.A. Dumas, and M. Prinz, *Microglia: Immune and non-immune functions.* Immunity, 2021. **54**(10): p. 2194-2208.
58. Prinz, M., S. Jung, and J. Priller, *Microglia Biology: One Century of Evolving Concepts.* Cell, 2019. **179**(2): p. 292-311.
59. Sofroniew, M.V. and H.V. Vinters, *Astrocytes: biology and pathology.* Acta Neuropathol, 2010. **119**(1): p. 7-35.
60. Leng, F. and P. Edison, *Neuroinflammation and microglial activation in Alzheimer disease: where do we go from here?* Nat Rev Neurol, 2021. **17**(3): p. 157-172.
61. Subhramanyam, C.S., et al., *Microglia-mediated neuroinflammation in neurodegenerative diseases.* Semin Cell Dev Biol, 2019. **94**: p. 112-120.
62. Woodburn, S.C., J.L. Bollinger, and E.S. Wohleb, *The semantics of microglia activation: neuroinflammation, homeostasis, and stress.* J Neuroinflammation, 2021. **18**(1): p. 258.
63. Wang, C., et al., *The effects of microglia-associated neuroinflammation on Alzheimer's disease.* Front Immunol, 2023. **14**: p. 1117172.
64. Linnerbauer, M., M.A. Wheeler, and F.J. Quintana, *Astrocyte Crosstalk in CNS Inflammation.* Neuron, 2020. **108**(4): p. 608-622.
65. Sun, E., et al., *The Pivotal Role of NF-kB in the Pathogenesis and Therapeutics of Alzheimer's Disease.* Int J Mol Sci, 2022. **23**(16).
66. Choi, S.S., et al., *Human astrocytes: secretome profiles of cytokines and chemokines.* PLoS One, 2014. **9**(4): p. e92325.
67. Hu, X., et al., *Interactions Between Astrocytes and Oligodendroglia in Myelin Development and Related Brain Diseases.* Neurosci Bull, 2023. **39**(3): p. 541-552.
68. Wu, Y. and U.L.M. Eisel, *Microglia-Astrocyte Communication in Alzheimer's Disease.* J Alzheimers Dis, 2023. **95**(3): p. 785-803.
69. Lian, H., et al., *NFκB-activated astroglial release of complement C3 compromises neuronal morphology and function associated with Alzheimer's disease.* Neuron, 2015. **85**(1): p. 101-115.
70. Kim, H., et al., *Reactive astrocytes transduce inflammation in a blood-brain barrier model through a TNF-STAT3 signaling axis and secretion of alpha 1-antichymotrypsin.* Nat Commun, 2022. **13**(1): p. 6581.
71. Sanmarco, L.M., et al., *Functional immune cell-astrocyte interactions.* J Exp Med, 2021. **218**(9).

72. Thadathil, N., et al., *Necroptosis increases with age in the brain and contributes to age-related neuroinflammation.* Geroscience, 2021. **43**(5): p. 2345-2361.
73. Liddelow, S.A., et al., *Neurotoxic reactive astrocytes are induced by activated microglia.* Nature, 2017. **541**(7638): p. 481-487.
74. Latham, A.S., J.A. Moreno, and C.E. Geer, *Biological agents and the aging brain: glial inflammation and neurotoxic signaling.* Front Aging, 2023. **4**: p. 1244149.
75. Kumar, V., *Toll-like receptors in the pathogenesis of neuroinflammation.* J Neuroimmunol, 2019. **332**: p. 16-30.
76. Bajwa, E., C.B. Pointer, and A. Klegeris, *The Role of Mitochondrial Damage-Associated Molecular Patterns in Chronic Neuroinflammation.* Mediators Inflamm, 2019. **2019**: p. 4050796.
77. Chen, Y. and Y. Yu, *Tau and neuroinflammation in Alzheimer's disease: interplay mechanisms and clinical translation.* J Neuroinflammation, 2023. **20**(1): p. 165.
78. Soelter, T.M., et al., *Altered glia-neuron communication in Alzheimer's Disease affects WNT, p53, and NFkB Signaling determined by snRNA-seq.* Cell Commun Signal, 2024. **22**(1): p. 317.
79. Smith, J.A., et al., *Role of pro-inflammatory cytokines released from microglia in neurodegenerative diseases.* Brain Res Bull, 2012. **87**(1): p. 10-20.
80. Huang, L.T., et al., *Association of Peripheral Blood Cell Profile With Alzheimer's Disease: A Meta-Analysis.* Front Aging Neurosci, 2022. **14**: p. 888946.
81. Saresella, M., et al., *A complex proinflammatory role for peripheral monocytes in Alzheimer's disease.* J Alzheimers Dis, 2014. **38**(2): p. 403-13.
82. Grammas, P., *Neurovascular dysfunction, inflammation and endothelial activation: implications for the pathogenesis of Alzheimer's disease.* J Neuroinflammation, 2011. **8**: p. 26.
83. Charabati, M., et al., *MCAM+ brain endothelial cells contribute to neuroinflammation by recruiting pathogenic CD4+ T lymphocytes.* Brain, 2023. **146**(4): p. 1483-1495.
84. Papaneophytou, C., E. Georgiou, and K.A. Kleopa, *The role of oligodendrocyte gap junctions in neuroinflammation.* Channels (Austin), 2019. **13**(1): p. 247-263.
85. González-Alvarado, M.N., et al., *Oligodendrocytes regulate the adhesion molecule ICAM-1 in neuroinflammation.* Glia, 2022. **70**(3): p. 522-535.
86. Siametis, A., G. Niotis, and G.A. Garinis, *DNA Damage and the Aging Epigenome.* J Invest Dermatol, 2021. **141**(4s): p. 961-967.
87. Zhao, Y., et al., *DNA damage and repair in age-related inflammation.* Nat Rev Immunol, 2023. **23**(2): p. 75-89.
88. Pal, S. and J.K. Tyler, *Epigenetics and aging.* Sci Adv, 2016. **2**(7): p. e1600584.
89. Wood, J.G. and S.L. Helfand, *Chromatin structure and transposable elements in organismal aging.* Front Genet, 2013. **4**: p. 274.
90. LaRocca, T.J., A.N. Cavalier, and D. Wahl, *Repetitive elements as a transcriptomic marker of aging: Evidence in multiple datasets and models.* Aging Cell, 2020. **19**(7): p. e13167.
91. Gorbunova, V., et al., *The role of retrotransposable elements in ageing and age-associated diseases.* Nature, 2021. **596**(7870): p. 43-53.
92. Copley, K.E. and J. Shorter, *Repetitive elements in aging and neurodegeneration.* Trends Genet, 2023. **39**(5): p. 381-400.
93. Zhang, Y., et al., *The Role of Non-coding RNAs in Alzheimer's Disease: From Regulated Mechanism to Therapeutic Targets and Diagnostic Biomarkers.* Front Aging Neurosci, 2021. **13**: p. 654978.
94. Deniz, Ö., J.M. Frost, and M.R. Branco, *Regulation of transposable elements by DNA modifications.* Nat Rev Genet, 2019. **20**(7): p. 417-431.

95. Choi, J., et al., *DNA Methylation and Histone H1 Jointly Repress Transposable Elements and Aberrant Intragenic Transcripts.* Mol Cell, 2020. **77**(2): p. 310-323.e7.
96. Pal, D., et al., *H4K16ac activates the transcription of transposable elements and contributes to their cis-regulatory function.* Nat Struct Mol Biol, 2023. **30**(7): p. 935-947.
97. Reik, W., *Stability and flexibility of epigenetic gene regulation in mammalian development.* Nature, 2007. **447**(7143): p. 425-32.
98. Martens, J.H., et al., *The profile of repeat-associated histone lysine methylation states in the mouse epigenome.* Embo j, 2005. **24**(4): p. 800-12.
99. Wang, S.C., B. Oelze, and A. Schumacher, *Age-specific epigenetic drift in late-onset Alzheimer's disease.* PLoS One, 2008. **3**(7): p. e2698.
100. Wang, K., et al., *Epigenetic regulation of aging: implications for interventions of aging and diseases.* Signal Transduct Target Ther, 2022. **7**(1): p. 374.
101. Liu, E.Y., C.P. Cali, and E.B. Lee, *RNA metabolism in neurodegenerative disease.* Dis Model Mech, 2017. **10**(5): p. 509-518.
102. De Marchi, F., et al., *Emerging Trends in the Field of Inflammation and Proteinopathy in ALS/FTD Spectrum Disorder.* Biomedicines, 2023. **11**(6).
103. Gray, D.A. and J. Woulfe, *Structural disorder and the loss of RNA homeostasis in aging and neurodegenerative disease.* Front Genet, 2013. **4**: p. 149.
104. Khong, A., et al., *The Stress Granule Transcriptome Reveals Principles of mRNA Accumulation in Stress Granules.* Mol Cell, 2017. **68**(4): p. 808-820.e5.
105. Ghosh, S. and R.L. Geahlen, *Stress Granules Modulate SYK to Cause Microglial Cell Dysfunction in Alzheimer's Disease.* EBioMedicine, 2015. **2**(11): p. 1785-98.
106. Wolozin, B. and P. Ivanov, *Stress granules and neurodegeneration.* Nat Rev Neurosci, 2019. **20**(11): p. 649-666.
107. Sato, K., K.I. Takayama, and S. Inoue, *Stress granules sequester Alzheimer's disease-associated gene transcripts and regulate disease-related neuronal proteostasis.* Aging (Albany NY), 2023. **15**(10): p. 3984-4011.
108. Poliseno, L., M. Lanza, and P.P. Pandolfi, *Coding, or non-coding, that is the question.* Cell Res, 2024. **34**(9): p. 609-629.
109. Ayarpadikannan, S. and H.S. Kim, *The impact of transposable elements in genome evolution and genetic instability and their implications in various diseases.* Genomics Inform, 2014. **12**(3): p. 98-104.
110. Bourque, G., et al., *Ten things you should know about transposable elements.* Genome Biol, 2018. **19**(1): p. 199.
111. Hayward, A. and C. Gilbert, *Transposable elements.* Curr Biol, 2022. **32**(17): p. R904-r909.
112. Fueyo, R., et al., *Roles of transposable elements in the regulation of mammalian transcription.* Nat Rev Mol Cell Biol, 2022. **23**(7): p. 481-497.
113. Wells, J.N. and C. Feschotte, *A Field Guide to Eukaryotic Transposable Elements.* Annu Rev Genet, 2020. **54**: p. 539-561.
114. Biémont, C., *A brief history of the status of transposable elements: from junk DNA to major players in evolution.* Genetics, 2010. **186**(4): p. 1085-93.
115. Marasca, F., et al., *The Sophisticated Transcriptional Response Governed by Transposable Elements in Human Health and Disease.* Int J Mol Sci, 2020. **21**(9).
116. Sun, W., et al., *Pathogenic tau-induced piRNA depletion promotes neuronal death through transposable element dysregulation in neurodegenerative tauopathies.* Nat Neurosci, 2018. **21**(8): p. 1038-1048.
117. Rivera, L., et al., *Integrative Single-Cell Analysis Reveals the Regulation of Transposable Elements in HSPCs during the Aging Process.* Blood, 2024. **144**(Supplement 1): p. 5647-5647.

118. Jönsson, M.E., et al., *Transposable Elements: A Common Feature of Neurodevelopmental and Neurodegenerative Disorders.* Trends Genet, 2020. **36**(8): p. 610-623.
119. Saleh, A., A. Macia, and A.R. Muotri, *Transposable Elements, Inflammation, and Neurological Disease.* Front Neurol, 2019. **10**: p. 894.
120. Macciardi, F., et al., *A retrotransposon storm marks clinical phenoconversion to late-onset Alzheimer's disease.* Geroscience, 2022. **44**(3): p. 1525-1550.
121. Feng, Y., et al., *Widespread transposable element dysregulation in human aging brains with Alzheimer's disease.* Alzheimers Dement, 2024. **20**(11): p. 7495-7517.
122. Ochoa, E., et al., *Pathogenic tau-induced transposable element-derived dsRNA drives neuroinflammation.* Sci Adv, 2023. **9**(1): p. eabq5423.
123. Wahl, D., et al., *The reverse transcriptase inhibitor 3TC protects against age-related cognitive dysfunction.* Aging Cell, 2023. **22**(5): p. e13798.
124. Guo, C., et al., *Tau Activates Transposable Elements in Alzheimer's Disease.* Cell Rep, 2018. **23**(10): p. 2874-2880.
125. Frost, B. and J. Dubnau, *The Role of Retrotransposons and Endogenous Retroviruses in Age-Dependent Neurodegenerative Disorders.* Annu Rev Neurosci, 2024. **47**(1): p. 123-143.
126. Luqman-Fatah, A., et al., *Retrotransposon life cycle and its impacts on cellular responses.* RNA Biol, 2024. **21**(1): p. 11-27.
127. Chen, Q., L. Sun, and Z.J. Chen, *Regulation and function of the cGAS-STING pathway of cytosolic DNA sensing.* Nat Immunol, 2016. **17**(10): p. 1142-9.
128. Gulen, M.F., et al., *cGAS-STING drives ageing-related inflammation and neurodegeneration.* Nature, 2023. **620**(7973): p. 374-380.
129. Chung, S., et al., *Blockade of STING activation alleviates microglial dysfunction and a broad spectrum of Alzheimer's disease pathologies.* Exp Mol Med, 2024. **56**(9): p. 1936-1951.
130. Xie, X., et al., *Activation of innate immune cGAS-STING pathway contributes to Alzheimer's pathogenesis in 5×FAD mice.* Nat Aging, 2023. **3**(2): p. 202-212.
131. De Cecco, M., et al., *Transposable elements become active and mobile in the genomes of aging mammalian somatic tissues.* Aging (Albany NY), 2013. **5**(12): p. 867-83.
132. Nelson, T.J. and Y. Xu, *Sting and p53 DNA repair pathways are compromised in Alzheimer's disease.* Sci Rep, 2023. **13**(1): p. 8304.
133. Zhang, H., et al., *DNA double-strand break repair and nucleic acid-related immunity.* Acta Biochim Biophys Sin (Shanghai), 2022. **54**(6): p. 828-835.
134. Obulesu, M. and D.M. Rao, *DNA damage and impairment of DNA repair in Alzheimer's disease.* Int J Neurosci, 2010. **120**(6): p. 397-403.
135. Peze-Heidsieck, E., et al., *Retrotransposons as a Source of DNA Damage in Neurodegeneration.* Front Aging Neurosci, 2021. **13**: p. 786897.
136. Chénais, B., *Transposable Elements and Human Diseases: Mechanisms and Implication in the Response to Environmental Pollutants.* Int J Mol Sci, 2022. **23**(5).
137. Mills, R.E., et al., *Which transposable elements are active in the human genome?* Trends Genet, 2007. **23**(4): p. 183-91.
138. Cordaux, R. and M.A. Batzer, *The impact of retrotransposons on human genome evolution.* Nat Rev Genet, 2009. **10**(10): p. 691-703.
139. Zheng, R., et al., *hnRNPM protects against the dsRNA-mediated interferon response by repressing LINE-associated cryptic splicing.* Mol Cell, 2024. **84**(11): p. 2087-2103.e8.
140. Lee, K., et al., *Inverted Alu repeats: friends or foes in the human transcriptome.* Exp Mol Med, 2024. **56**(6): p. 1250-1262.
141. Saldi, T.K., et al., *Neurodegeneration, Heterochromatin, and Double-Stranded RNA.* J Exp Neurosci, 2019. **13**: p. 1179069519830697.

142. Lawlor, K.T., et al., *Double-stranded RNA is pathogenic in Drosophila models of expanded repeat neurodegenerative diseases.* Hum Mol Genet, 2011. **20**(19): p. 3757-68.
143. Ravel-Godreuil, C., et al., *Transposable elements as new players in neurodegenerative diseases.* FEBS Lett, 2021. **595**(22): p. 2733-2755.
144. Adler, G.L., et al., *Human Endogenous Retroviruses in Neurodegenerative Diseases.* Genes (Basel), 2024. **15**(6).
145. Polesskaya, O., et al., *The role of Alu-derived RNAs in Alzheimer's and other neurodegenerative conditions.* Med Hypotheses, 2018. **115**: p. 29-34.
146. Chen, Y.G. and S. Hur, *Cellular origins of dsRNA, their recognition and consequences.* Nat Rev Mol Cell Biol, 2022. **23**(4): p. 286-301.
147. Choi, U.Y., et al., *Oligoadenylate synthase-like (OASL) proteins: dual functions and associations with diseases.* Exp Mol Med, 2015. **47**(3): p. e144.
148. Chavarría-Smith, J. and R.E. Vance, *The NLRP1 inflammasomes.* Immunol Rev, 2015. **265**(1): p. 22-34.
149. Kawai, T. and S. Akira, *TLR signaling.* Cell Death Differ, 2006. **13**(5): p. 816-25.
150. Rehwinkel, J. and M.U. Gack, *RIG-I-like receptors: their regulation and roles in RNA sensing.* Nat Rev Immunol, 2020. **20**(9): p. 537-551.
151. Du, J., et al., *Transposable elements potentiate radiotherapy-induced cellular immune reactions via RIG-I-mediated virus-sensing pathways.* Commun Biol, 2023. **6**(1): p. 818.
152. Dhillon, P., et al., *Increased levels of endogenous retroviruses trigger fibroinflammation and play a role in kidney disease development.* Nat Commun, 2023. **14**(1): p. 559.
153. Smith, M.E., et al., *Repetitive element transcript accumulation is associated with inflammaging in humans.* Geroscience, 2024. **46**(6): p. 5663-5679.
154. de Rivero Vaccari, J.P., et al., *RIG-1 receptor expression in the pathology of Alzheimer's disease.* J Neuroinflammation, 2014. **11**: p. 67.
155. Gal-Ben-Ari, S., et al., *PKR: A Kinase to Remember.* Front Mol Neurosci, 2018. **11**: p. 480.
156. García, M.A., E.F. Meurs, and M. Esteban, *The dsRNA protein kinase PKR: virus and cell control.* Biochimie, 2007. **89**(6-7): p. 799-811.
157. Okonski, K.M. and C.E. Samuel, *Stress granule formation induced by measles virus is protein kinase PKR dependent and impaired by RNA adenosine deaminase ADAR1.* J Virol, 2013. **87**(2): p. 756-66.
158. LaRocca, T.J., et al., *TDP-43 knockdown causes innate immune activation via protein kinase R in astrocytes.* Neurobiol Dis, 2019. **132**: p. 104514.
159. Tronel, C., et al., *The specific PKR inhibitor C16 prevents apoptosis and IL-1β production in an acute excitotoxic rat model with a neuroinflammatory component.* Neurochem Int, 2014. **64**: p. 73-83.
160. Mangiavacchi, A., et al., *LINE-1 RNA triggers matrix formation in bone cells via a PKR-mediated inflammatory response.* Embo j, 2024. **43**(17): p. 3587-3603.
161. Kim, Y., et al., *PKR Senses Nuclear and Mitochondrial Signals by Interacting with Endogenous Double-Stranded RNAs.* Mol Cell, 2018. **71**(6): p. 1051-1063.e6.
162. Pham, A.M., et al., *PKR Transduces MDA5-Dependent Signals for Type I IFN Induction.* PLoS Pathog, 2016. **12**(3): p. e1005489.
163. Hugon, J., et al., *PKR involvement in Alzheimer's disease.* Alzheimers Res Ther, 2017. **9**(1): p. 83.
164. Lu, W., et al., *The role of PKC/PKR in aging, Alzheimer's disease, and perioperative neurocognitive disorders.* Front Aging Neurosci, 2022. **14**: p. 973068.
165. Samuel, C.E., *Adenosine deaminase acting on RNA (ADAR1), a suppressor of double-stranded RNA-triggered innate immune responses.* J Biol Chem, 2019. **294**(5): p. 1710-1720.

166. Savva, Y.A., L.E. Rieder, and R.A. Reenan, *The ADAR protein family.* Genome Biol, 2012. **13**(12): p. 252.
167. George, C.X., et al., *Editing of Cellular Self-RNAs by Adenosine Deaminase ADAR1 Suppresses Innate Immune Stress Responses.* J Biol Chem, 2016. **291**(12): p. 6158-68.
168. Eisenberg, E. and E.Y. Levanon, *A-to-I RNA editing - immune protector and transcriptome diversifier.* Nat Rev Genet, 2018. **19**(8): p. 473-490.
169. Kim, J.I., et al., *RNA editing at a limited number of sites is sufficient to prevent MDA5 activation in the mouse brain.* PLoS Genet, 2021. **17**(5): p. e1009516.
170. Liddicoat, B.J., et al., *RNA editing by ADAR1 prevents MDA5 sensing of endogenous dsRNA as nonself.* Science, 2015. **349**(6252): p. 1115-20.
171. Rehwinkel, J. and P. Mehdipour, *ADAR1: from basic mechanisms to inhibitors.* Trends Cell Biol, 2025. **35**(1): p. 59-73.
172. Zhang, F., et al., *SPRINT: an SNP-free toolkit for identifying RNA editing sites.* Bioinformatics, 2017. **33**(22): p. 3538-3548.
173. Pestal, K., et al., *Isoforms of RNA-Editing Enzyme ADAR1 Independently Control Nucleic Acid Sensor MDA5-Driven Autoimmunity and Multi-organ Development.* Immunity, 2015. **43**(5): p. 933-44.
174. Rice, G.I., et al., *Mutations in ADAR1 cause Aicardi-Goutières syndrome associated with a type I interferon signature.* Nat Genet, 2012. **44**(11): p. 1243-8.
175. Inoue, M., et al., *An Aicardi-Goutières Syndrome-Causative Point Mutation in Adar1 Gene Invokes Multiorgan Inflammation and Late-Onset Encephalopathy in Mice.* J Immunol, 2021. **207**(12): p. 3016-3027.
176. Guo, X., et al., *Aicardi-Goutières syndrome-associated mutation at ADAR1 gene locus activates innate immune response in mouse brain.* J Neuroinflammation, 2021. **18**(1): p. 169.
177. Cheng, L., et al., *A Wonderful Journey: The Diverse Roles of Adenosine Deaminase Action on RNA 1 (ADAR1) in Central Nervous System Diseases.* CNS Neurosci Ther, 2025. **31**(1): p. e70208.
178. Pozdyshev, D.V., et al., *Differential Analysis of A-to-I mRNA Edited Sites in Parkinson's Disease.* Genes (Basel), 2021. **13**(1).
179. Wang, H., et al., *ADAR1 Suppresses the Activation of Cytosolic RNA-Sensing Signaling Pathways to Protect the Liver from Ischemia/Reperfusion Injury.* Sci Rep, 2016. **6**: p. 20248.
180. Pujantell, M., et al., *RNA editing by ADAR1 regulates innate and antiviral immune functions in primary macrophages.* Sci Rep, 2017. **7**(1): p. 13339.
181. Yang, S., et al., *Adenosine deaminase acting on RNA 1 limits RIG-I RNA detection and suppresses IFN production responding to viral and endogenous RNAs.* J Immunol, 2014. **193**(7): p. 3436-45.
182. Wang, Q., et al., *Stress-induced apoptosis associated with null mutation of ADAR1 RNA editing deaminase gene.* J Biol Chem, 2004. **279**(6): p. 4952-61.
183. Guo, X., et al., *An AGS-associated mutation in ADAR1 catalytic domain results in early-onset and MDA5-dependent encephalopathy with IFN pathway activation in the brain.* J Neuroinflammation, 2022. **19**(1): p. 285.
184. Hu, S.B., et al., *ADAR1p150 prevents MDA5 and PKR activation via distinct mechanisms to avert fatal autoinflammation.* Mol Cell, 2023. **83**(21): p. 3869-3884.e7.
185. Deng, P., et al., *Adar RNA editing-dependent and -independent effects are required for brain and innate immune functions in Drosophila.* Nat Commun, 2020. **11**(1): p. 1580.
186. Ahmad, S., et al., *Breaching Self-Tolerance to Alu Duplex RNA Underlies MDA5-Mediated Inflammation.* Cell, 2018. **172**(4): p. 797-810.e13.
187. Orecchini, E., et al., *ADAR1 restricts LINE-1 retrotransposition.* Nucleic Acids Res, 2017. **45**(1): p. 155-168.

188. Martinez, J.C., et al., *cGAS deficient mice display premature aging associated with de-repression of LINE1 elements and inflammation.* bioRxiv, 2024.
189. Frost, B., et al., *Tau promotes neurodegeneration through global chromatin relaxation.* Nat Neurosci, 2014. **17**(3): p. 357-66.
190. Siano, G., et al., *Tau mediates the reshaping of the transcriptional landscape toward intermediate Alzheimer's disease stages.* Front Cell Dev Biol, 2024. **12**: p. 1459573.

# CHAPTER 2 – ADAR1 SUPPRESSION CAUSES INTERFERON SIGNALING AND TRANSPOSABLE ELEMENT TRANSCRIPT ACCUMULATION IN HUMAN ASTROCYTES[1]

## INTRODUCTION

Neuroinflammation is a major mechanism of brain aging and age-related neurodegenerative disorders like Alzheimer's disease (AD), and it is characterized by pro-inflammatory activation of glial cells [1, 2]. Astrocytes, the most common glial cell in the brain, interface closely with neurons and other central nervous system (CNS) cells [3], and pro-inflammatory astrocytes have been documented in both acute neuroinflammation and chronic, age-related neurodegenerative diseases like AD [4-6]. However, the upstream causes of pro-inflammatory activation in astrocytes during aging and/or AD are not fully understood.

One biologically important, intracellular driver of pro-inflammatory signaling is double-stranded RNA (dsRNA), which is a virus-associated molecular pattern. Cytoplasmic dsRNA binds to innate immune sensors that stimulate type I interferon and pro-inflammatory signaling pathways, a normal response to dsRNA virus infections [7]. However, cytoplasmic dsRNA may also originate from endogenous sources (e.g., genomic DNA/RNA). A key regulator of endogenous dsRNA is the enzyme adenosine deaminase acting on RNA 1 (ADAR1) [8], which regulates dsRNA through adenosine-to-inosine (A-to-I) editing that disrupts base-pairing to prevent the accumulation of dsRNA in the cytoplasm [9, 10]. ADAR1 is important in reducing type I interferon and pro-inflammatory signaling [11, 12], and although *Adar1* (mouse ortholog) knockout or editing inhibition in mice is embryonically lethal, this can be prevented by simultaneous knockout of the dsRNA sensor melanoma differentiation-associated protein 5 (MDA5) [13-15]. Recent data in *Drosophila* also show that catalytically inactive *Adar* (fly

[1]McEntee CM, Cavalier AN, LaRocca TJ. ADAR1 suppression causes interferon signaling and transposable element transcript accumulation in human astrocytes. *Front Mol Neurosci*. 2023;16:1263369. doi:10.3389/fnmol.2023.1263369. PMID: 38035265; PMCID: PMC10685929.

ortholog) causes innate immune activation in brain-like tissue [16], and mutations in human *ADAR1* result in Aicardi Goutières syndrome (AGS), which is characterized by type I interferon activation in the brain [17].

The role of ADAR1 in regulating type I interferon responses in the mammalian brain has not been comprehensively investigated, and the potential sources of dsRNA regulated by ADAR1 in glial cells are unknown. However, one possible source of dsRNA relevant to aging and AD is transposable elements (TEs). TEs, which include short and long interspersed nuclear elements (SINEs and LINEs), are non-coding repetitive DNA sequences that are often ignored as "junk DNA" [18], but growing evidence links TE transcripts with inflammation, aging, and AD [19-23]. While most work in this area has focused on the ability of select TE transcripts to form cytoplasmic DNA (another virus-associated molecular pattern) [24], TEs also have the potential to form both inter- and intra-strand dsRNA [25]. Recent data even show that TE-derived dsRNA induced by tau (a key pathological feature of AD) drives neuroinflammatory signaling in astrocytes [26].

Here, we extend on these recent findings by testing the hypothesis that ADAR1 inhibits pro-inflammatory signaling in human astrocytes, and that this may involve TE-derived dsRNA. Using a combination of transcriptomics (RNA-seq) and confirmatory molecular biology analyses, we show that ADAR1 suppression activates type I interferon and pro-inflammatory signaling pathways, and that this is associated with an increase in both dsRNA and TE transcripts with the potential form dsRNA. We also provide evidence that our *in vitro* data may be clinically relevant, as we find reduced *ADAR1* gene expression with aging and AD, along with a similar increase in TE transcripts, in existing human brain transcriptome data. Collectively, our data suggest that ADAR1 may regulate TE-derived dsRNA that stimulates type I interferon/inflammatory signaling, and that reductions in ADAR1 could be a novel mechanism of neuroinflammation in aging/AD.

METHODS

*Primary human astrocyte culture*

Primary fetal human astrocytes (to rule out potential age/pathology-related variables) were used for all experiments. Cells were purchased from ScienCell and grown according to standard procedures at 37 °C and 5% $CO_2$ in a humidified incubator using astrocyte-specific medium and poly-L-lysine coated tissue culture plates. All cells had typical astrocyte morphology and tested >90% positive for GFAP expression at passage 1 (**Figure A.1**). Cells were subcultured at ~90% confluency and used at passages 3-6 for all experiments. No passage-associated differences were observed in any experiments.

*siRNA transfection*

Astrocytes were transfected when 80% confluent using pre-designed siRNAs according to manufacturers' instructions. Lipofectamine RNAiMAX reagent (ThermoFisher, 13778-075) and siRNAs were diluted in Opti-MEM Medium (ThermoFisher, 31985-070), combined and incubated for 5 min, then applied to cells in fresh medium at a final concentration of 15 nM. siRNAs used included: ADAR1 siRNA (ThermoFisher Silencer Select, s1008, target sequence: GAGAUUCUCUCAGCCUAAAtt); scramble siRNA (Santa Cruz Control siRNA A, sc36869, non-targeting sequence). Cells were incubated for 48 h after transfection to allow for knockdown to proceed. Media was then replaced with serum-free media and cells were incubated for an additional 24 h, after which cells were either: 1) rinsed with DPBS and frozen for immunoblotting or RNA isolation; or 2) fixed in 4% paraformaldehyde for immunofluorescence staining or fluorescence *in situ* hybridization. All cells were 90-100% confluent for final analyses, and experiments were repeated at least three times, except for RNA-seq (one experiment with three replicates).

*Immunoblotting*

Cell samples were thawed on ice and lysed using RIPA lysis buffer containing phosphatase and protease inhibitors (ThermoFisher/Roche). 5-10 ug of protein was separated by electrophoresis on 4-12% Bis-Tris gels (Bio-Rad) then transferred to nitrocellulose membranes (Bio-Rad). Membranes were blocked using 5% milk in TBS-Tween or 5% BSA in TBS-Tween (for phospho-antibodies) for at least 1-2 h at room temperature or overnight at 4 °C. Primary antibodies were diluted in 5% milk in TBS-Tween or 5% BSA in TBS-Tween, added to membranes, and incubated overnight at 4 °C. Antibodies used included: ADAR1 (Novus Biologicals, NBP3-05500, 1:1000), ICAM-1 (Novus Biologicals, NBP1-88700, 1:1000), MDA5 (Novus Biologicals, NBP1-76760, 1:500), phosphorylated (p)-IRF3 (ABclonal, AP0995, 1:1000), pNF-κB (ABclonal, AP0123, 1:1000), RIG-I (Novus Biologicals, NBP1-76732, 1:1000), and TNF-α (Cell Signaling, 6945s, 1:500). Mouse and rabbit HRP-conjugated secondary antibodies (Cell Signaling, 7076s/7074s, 1:2000) were diluted in 5% milk in TBS-Tween or 5% BSA in TBS-Tween, added to membranes, and incubated for 1 h at room temperature. Proteins were detected using ECL chemiluminescent substrate (Thermo) on a FluorChem E imager (ProteinSimple). Protein levels (ECL signal intensities) were measured using ImageJ2/Fiji and normalized to GAPDH (Novus Biologicals, 1:2000).

*RNA isolation, sequencing, and bioinformatics*

Cells were lysed with Trizol (Zymo Research), and RNA was isolated using an RNA-specific spin column kit (Direct-zol RNA MicroPrep, Zymo Research, R2062) including a DNase I treatment according to the manufacturer's instructions. Ribosomal RNA-depleted total RNA libraries were generated using Zymo Total RNA library preparation kits, then sequenced on an Illumina NovaSeq6000 instrument to generate >60 M 151-bp paired-end fastq reads per sample. Reads were trimmed using fastp (v0.20.0) [27] and aligned to the hg38 genome using STAR (v2.7.3a) with default settings [28]. Differential gene expression from the gene counts

generated by STAR was analyzed using DESeq2 (v1.30.1) [29], and differentially expressed genes with an adjusted p-value (FDR) < 0.1, the standard DESeq2 cutoff, were used for gene ontology analyses in the g:Profiler program [30]. TEs were identified using RepeatMasker annotation files and the RepEnrich2 program with default settings [31], and differential expression of TEs was analyzed using DESeq2 with sample-specific size factors to normalize for library size. RNA editing was measured using SPRINT [32] with default parameters. To determine RNA edits within TEs, SPRINT output files were intersected with the human RepeatMasker annotation file. Changes in editing in response to ADAR1 knockdown (i.e., "Δ-edits") were calculated by subtracting the number of edits per TE in ADAR1 siRNA-treated cells from the number of edits per TE in scramble siRNA-treated cells. RNA secondary structures were generated using the RNAfold Webserver (v2.5.1) [33]. All data can be found on the Gene Expression Omnibus (GEO) website under accession number: GSE225369.

*Immunofluorescence staining*

Cells were cultured on poly-L-lysine-coated glass chamber slides (Nunc Lab-Tek). After fixation in 4% paraformaldehyde for 10 min, cells were washed with DPBS, permeabilized with 0.25% Triton-X and for 10 min, washed again and then blocked using 3% normal goat serum/3% fetal bovine serum (Jackson ImmunoResearch) in DPBS for 30 min. Primary antibodies were prepared in 0.1% tween/5% normal goat serum in DPBS and added to cells to incubate overnight at 4 °C. Primary antibodies used included: J2 (Novus Biologicals, NBP3-11395, 1:500) and MDA5 (Novus Biologicals, NBP1-76760, 1:500). After overnight incubation, cells were washed with DPBS and mouse/rabbit fluorescent probe-conjugated secondary antibodies (Invitrogen, A32731/A32727) diluted in 0.1% tween/5% normal goat serum were added to incubate for 1 hour at room temperature in the dark. Cells were washed with DPBS, mounted using Prolong mounting medium containing DAPI (ThermoFisher, P36935), and allowed to set overnight at room temperature. Images were generated using an EVOS M7000

fluorescence microscope at 40x magnification, and per cell fluorescence was measured in five images per slide well for each treatment and normalized to the mean of all conditions using ImageJ2/Fiji software, as previously reported [34].

*ELISA*

Cell culture media was collected following the switch to serum-free media. To measure levels of CXCL10, media samples were diluted 1:20 and analyzed using a sandwich ELISA according manufacturer's instructions (ABclonal, Ab83700). IFNβ was measured using undiluted cell culture media samples and a sandwich ELISA according manufacturer's instructions (R&D Systems, DIFNB0).

*Fluorescence in situ hybridization*

Fluorescence *in-situ* hybridization (FISH) probes for the transposable element L1MA6, a LINE with sequence similarity to several other L1 elements (to increase signal detection), were designed using Biosearch Technologies Stellaris Probe Designer Version 4.2, and 12.5 μM FISH probe stock solutions were prepared in TE buffer (10 mM Tris-HCL, 1mM EDTA, pH 8.0). Cells were washed with DPBS and fixed with 4% formaldehyde in RNase-free DPBS for 10min at room temperature, then washed again and permeabilized in 70% ethanol for 2 h at 4 °C. After permeabilization, cells were washed, and RNA FISH probe in hybridization buffer along with primary antibodies (same dilutions as above for immunofluorescence) was added and incubated for 16 h at 37 °C in the dark. Cells were washed again for 30 min at 37 °C in the dark, then incubated for 30 min with 5 ng/ml DAPI in wash buffer before a final 5 min wash per manufacturer's instructions. Slides were mounted using Prolong mounting medium (ThermoFisher) and imaged on an EVOS M7000 fluorescence microscope at 40x magnification.

*RNA-seq secondary analysis*

Existing RNA-seq data used in this study are available via the GEO accession number GSE153875. Bioinformatics analyses of these data were performed as described above. Raw counts were normalized using size factors generated from DESeq2 for downstream statistical analyses.

*Statistical analyses*

GraphPad Prism software was used for ANOVAs with post-hoc t-tests and unpaired t-tests for all experimental data, as well as normality testing and Pearson correlation analyses of RNA-seq data and chi-square analyses of increased versus decreased TE transcripts. DESeq2 was used for differential expression analyses as described above.

RESULTS

ADAR1 is a key regulator of cytoplasmic dsRNA and inflammatory signaling activation in many tissues, but its role and potential dsRNA targets in human astrocytes have not been comprehensively investigated. Therefore, we knocked down ADAR1 by siRNA transfection in primary human astrocytes and performed transcriptomics (RNA-seq) to broadly profile resulting changes in gene expression. We were able to achieve a knockdown efficiency of ~60% (**Figure 2.1A, Figure A.2A**), and differential gene expression analyses showed that ADAR1 knockdown resulted in 220 increased and 745 decreased RNA transcripts compared to a scramble siRNA control (**Figure 2.1B**). Many increased transcripts were interferon stimulating genes (ISGs) or related to interferon signaling pathways (**Figure 2.1C**). Although only several of these genes/transcripts were increased at FDR < 0.1, compared to average gene expression, ISGs as a group were significantly increased (**Figure A.2B**), consistent with other studies of dsRNA-induced interferon activation [35]. Moreover, gene ontology analysis indicated that up-regulated

biological processes with ADAR1 knockdown were related to immune responses and inflammation, whereas down-regulated biological processes were related to development and extracellular matrix organization (**Figure 2.1D**). We also found increased KEGG and REAC pathways reflecting pro-inflammatory and interferon signaling with ADAR1 knockdown, and decreased REAC pathways reflecting extracellular matrix organization (**Figure 2.1E and F**). These data show increases in pro-inflammatory/interferon-associated gene expression following ADAR1 knockdown, which is consistent with previous studies on ADAR1 suppression or dysfunction in other cell types [36], and with astrocyte-related neuroinflammation [37].

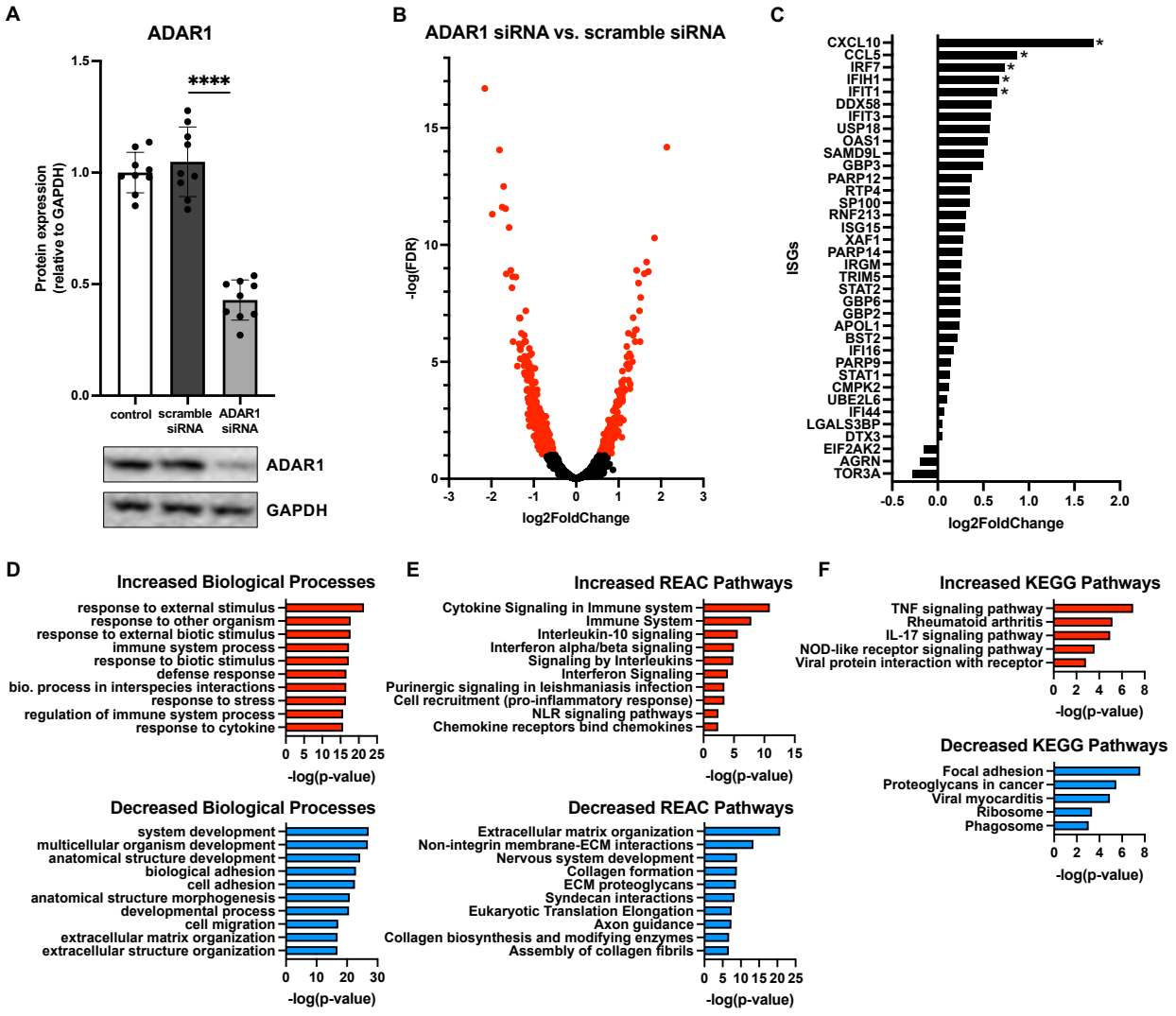


**Figure 2.1. ADAR1 knockdown increases interferon and pro-inflammatory gene expression. (A)** Immunoblot data showing knockdown of ADAR1. ****p ≤ 0.0001, one-way ANOVA, F = 104.3, DF = 26; n=9/condition. Error bars represent standard deviation (SD). **(B)**

Volcano plot of RNA-seq data for protein coding transcripts in astrocytes transfected with ADAR1 siRNA compared to scramble siRNA. Genes significantly increased/decreased in red (FDR < 0.1); n=3/condition. **(C)** Log2FoldChange of interferon stimulating genes (ISGs) and genes related to interferon signaling. *FDR < 0.1. Gene list derived from [35]. **(D-F)** Top 10 increased/decreased **(D)** GO biological processes, **(E)** REAC and **(F)** KEGG pathways with ADAR1 knockdown compared to scramble siRNA.

In line with other reports [13, 36, 38], our RNA-seq data also showed that the dsRNA sensors MDA5 (*IFIH1* gene) and retinoic acid-inducible gene I (RIG-I; *DDX58* gene) were increased and borderline increased (FDR = 0.11), respectively, following ADAR1 knockdown (**Figure 2.1C**). Increases in these transcripts translated to modestly but not significantly elevated protein levels (**Figure 2.2A and E**) that tended to correlate with downstream products of MDA5/RIG-I signaling (p = 0.02 – 0.09, **Figure A.3B**). Moreover, consistent with the key role of these proteins in dsRNA sensing and the idea that their protein levels are not as important as their activity, we found that: 1) ADAR1 knockdown resulted in an increase in dsRNA (**Figure 2.2B**); and 2) although sensors like MDA5 were diffusely expressed in cells, they tended to colocalize with ADAR1 knockdown-induced dsRNA (**Figure 2.2C**). Furthermore, these events were coupled with increases in protein markers of pro-inflammatory astrocyte activation. For example, ADAR1 knockdown resulted in increases in intracellular adhesion molecule I (ICAM-1) and tumor necrosis factor α (TNF-α) (**Figure 2.2D and 2E**). We also found increases in secreted C-X-C motif chemokine ligand 10 (CXCL10) and interferon β (IFNβ), which are downstream products of MDA5/RIG-I stimulated type I interferon signaling, in astrocyte media after ADAR1 knockdown (**Figure 2.2F**). Furthermore, although not significant, we found a variable increase (including some highly activated cells/samples) in phosphorylated interferon regulatory factor 3 (pIRF3), a transcription factor downstream of MDA5/RIG-I involved in the production of CXCL10 and IFNβ (**Figure 2.2D and E**). These pIRF3 levels correlated positively with CXCL10 secretion (**Figure A.3B**), and a transcription factor motif analysis showed that multiple IRFs were associated with the gene expression differences we observed in response to ADAR1 knockdown (**Supplementary data**). Additionally, ADAR1 knockdown resulted in a

decrease in phosphorylated nuclear factor kappa B (pNF-κB) (**Figure 2.2D and E**), which is similar to what others have reported [39], further supporting the role of IRFs in response to ADAR1 suppression. Thus, our data support the idea that, similar to other tissues, the primary response to ADAR1 knockdown in human astrocytes is type I interferon signaling driven by MDA5 and/or RIG-I binding to dsRNA.

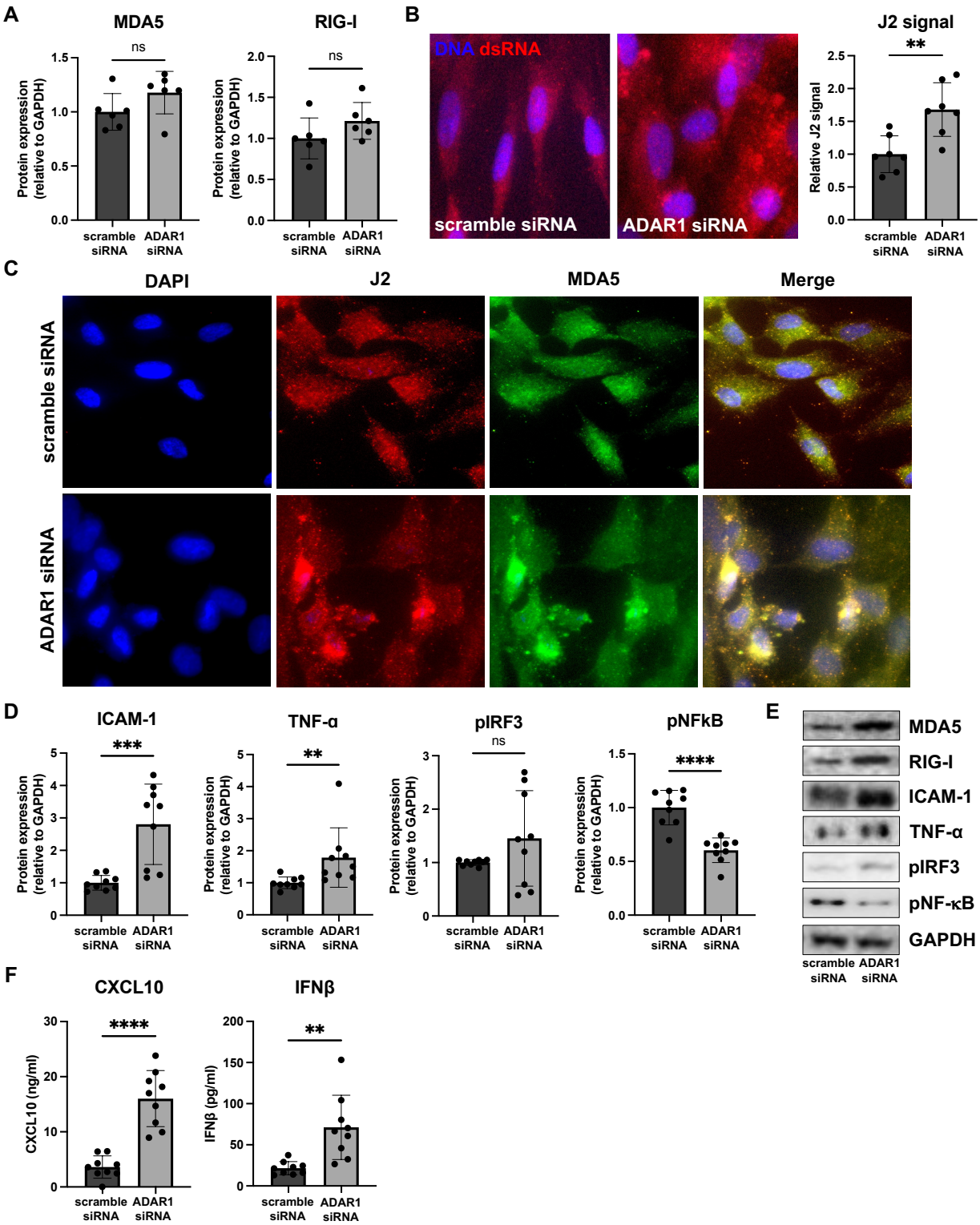


**Figure 2.2 ADAR1 knockdown results in dsRNA and dsRNA sensor increases, type I interferon signaling and pro-inflammatory protein expression. (A)** Immunoblots for MDA5 and RIG-I following ADAR1 knockdown. Unpaired t-test; n=6/condition. **(B)** Representative images and relative J2 (dsRNA antibody) immunofluorescence signal showing dsRNA

accumulation following ADAR1 knockdown. **(C)** Representative immunofluorescence images showing co-localization of dsRNA (J2) and MDA5 after transfection with ADAR1 siRNA. **(D-E)** Summary immunoblot data for ICAM-1, TNF-α, pIRF3, pNF-κB, and **(E)** representative images following ADAR1 knockdown. **(F)** Concentrations of CXCL10 and IFNβ following ADAR1 siRNA knockdown. **p ≤ 0.01, ***p ≤ 0.001, ****p ≤ 0.0001 in unpaired t-test; n=9/condition. Error bars represent SD.

To determine the potential sources of dsRNA that accumulates after ADAR1 knockdown, we examined our RNA-seq data for A-to-I RNA editing (a key function of ADAR1 and an indirect, computational estimate of dsRNA). After ADAR1 knockdown, we found a ~50% reduction in A-to-I editing (**Figure 2.3A**), and most of these editing differences occurred in TEs rather than protein-coding genes, consistent with observations of editing in general [25]. Importantly, reduced TE editing with ADAR1 knockdown was associated with increased expression of transcripts from four main types of TEs, and also with total levels of TE transcripts (**Figure 2.3B, Figure A.4A**), suggesting that ADAR1 is important for suppressing TE transcript accumulation. To determine which TE transcripts may accumulate and form dsRNA that is edited by ADAR1, we identified TE transcripts whose editing levels decreased ("Δ-edits") most with knockdown (i.e., presumably because they are usually heavily edited by ADAR1). We also examined changes in expression of these ADAR1-edited TE transcripts, and we found that many of the TE transcripts that both increased following knockdown and had high Δ-edits were SINEs, specifically Alu elements (**Figure 2.3C and D**), which are established ADAR1 targets. Moreover, several particularly likely Alu element ADAR1 targets, such as AluSx, had the potential to form highly intra-strand dsRNA structures (**Figure 2.3E**), and several of the most increased TE transcripts with ADAR1 knockdown had similarly dsRNA-prone structures (**Figure A.4B**). Additionally, a few LINEs, which are among the most abundant TEs in the human genome and have also been reported as ADAR1 targets, were increased and highly edited. Based on this observation and because Alu elements are relatively short and difficult to probe for using microscopy, we used FISH to confirm that LINE transcripts (longer and more amenable to FISH) colocalized with dsRNA immunofluorescence (**Figure 2.3F**). Together, these

data support the idea that TEs, particularly SINEs and LINEs, may be an important endogenous source of dsRNA in astrocytes, and that ADAR1 is important for reducing TE-derived dsRNA.

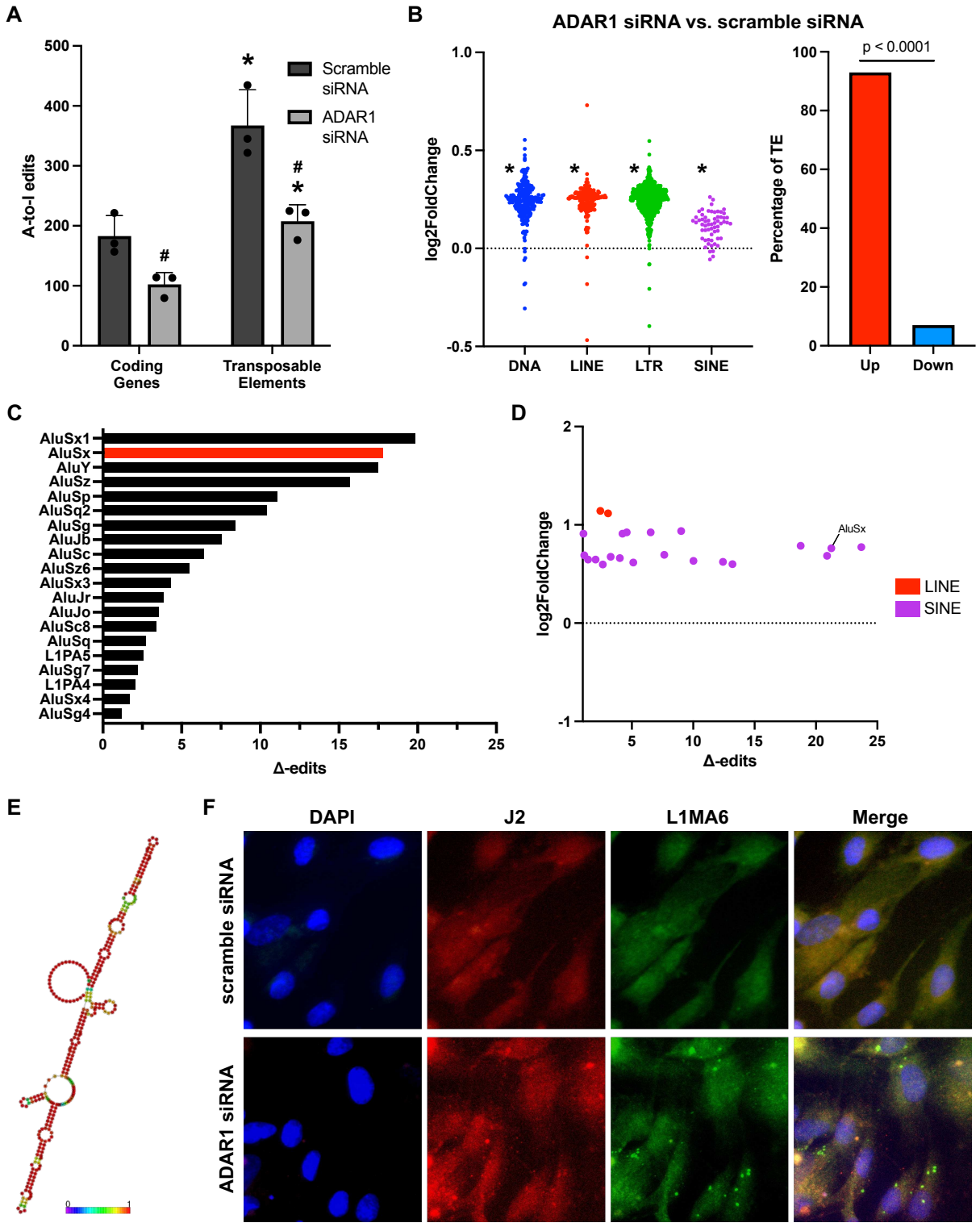

**Figure 2.3 ADAR1 knockdown increases dsRNA-prone TE transcript accumulation. (A)** Adenosine-to-inosine editing in coding genes and TEs with ADAR1 knockdown. *p ≤ 0.05 coding genes vs. TE and #p ≤ 0.05 ADAR1 siRNA vs. scramble siRNA; unpaired t-test; n=3/condition. Error bars represent SD. **(B)** Changes in TE transcript expression by major TE type (log2FoldChange) and total TEs (% increased vs. decreased). *p ≤ 0.0001; Chi-squared test vs. mean gene expression log2FoldChange. **(C)** Top 20 ∆-edited TEs (average scramble siRNA edits – average ADAR1 siRNA knockdown edits). **(D)** Scatter plot showing highly edited (Δ-edits > 1) and highly expressed (log2FoldChange) TE transcripts. **(E)** Potential RNA secondary structure of an increased, highly edited Alu element (AluSx). Red base-pairs indicate high base-pairing probabilities. **(F)** Fluorescence *in situ* hybridization images showing co-localization of dsRNA (J2) and LINE RNA after transfection with scramble siRNA or ADAR1 siRNA.

Finally, to determine if our data showing that ADAR1 knockdown in astrocytes results in innate immune sensor activation, type I interferon/pro-inflammatory signaling, and TE transcript accumulation might be clinically relevant, we conducted a secondary analysis of a published RNA-seq dataset on human brain tissue [40] (chosen specifically for data quality and carefully matched subject groups). We found a significant reduction in overall *ADAR1* gene expression in AD patients compared to healthy young adults (**Figure 2.4A**), and although there was only a trend for lower *ADAR1* gene expression in older compared to younger adults, we did find an increase in TE transcript expression in the brains of these same subjects that was exacerbated in AD vs. healthy older adult brains (**Figure 2.4B**). In addition, we found significant/borderline significant correlations among age and some dsRNA-prone TEs that were also particularly increased with ADAR1 knockdown in our *in vitro* data (**Figure A.5A and B**). We also found a negative correlation between *ADAR1* counts and overall TE transcript levels in all of these subjects (**Figure 2.4C**), consistent with the idea that ADAR1 may be an important regulator of TE-derived dsRNA. Finally, in support of the idea that these events may contribute to neuroinflammation *in vivo*, among the most increased TE transcripts in AD vs. healthy older adults and older vs. younger adults, we found 22 TE transcripts that were also identified as ADAR1 targets (TE transcripts with high number of ∆-edits) in our *in vitro* analyses (**Figure 2.4D**). These TE transcripts largely consisted of LINEs and long terminal repeats (LTRs), whereas ADAR1-edited SINEs were more common in AD vs. healthy older adult brains

(**Supplementary data).** Together, these data provide evidence of a role for ADAR1 in human brain aging and AD, and for the idea that TE-derived dsRNA may be an important, neuroinflammation-related ADAR1 substrate *in vivo*.

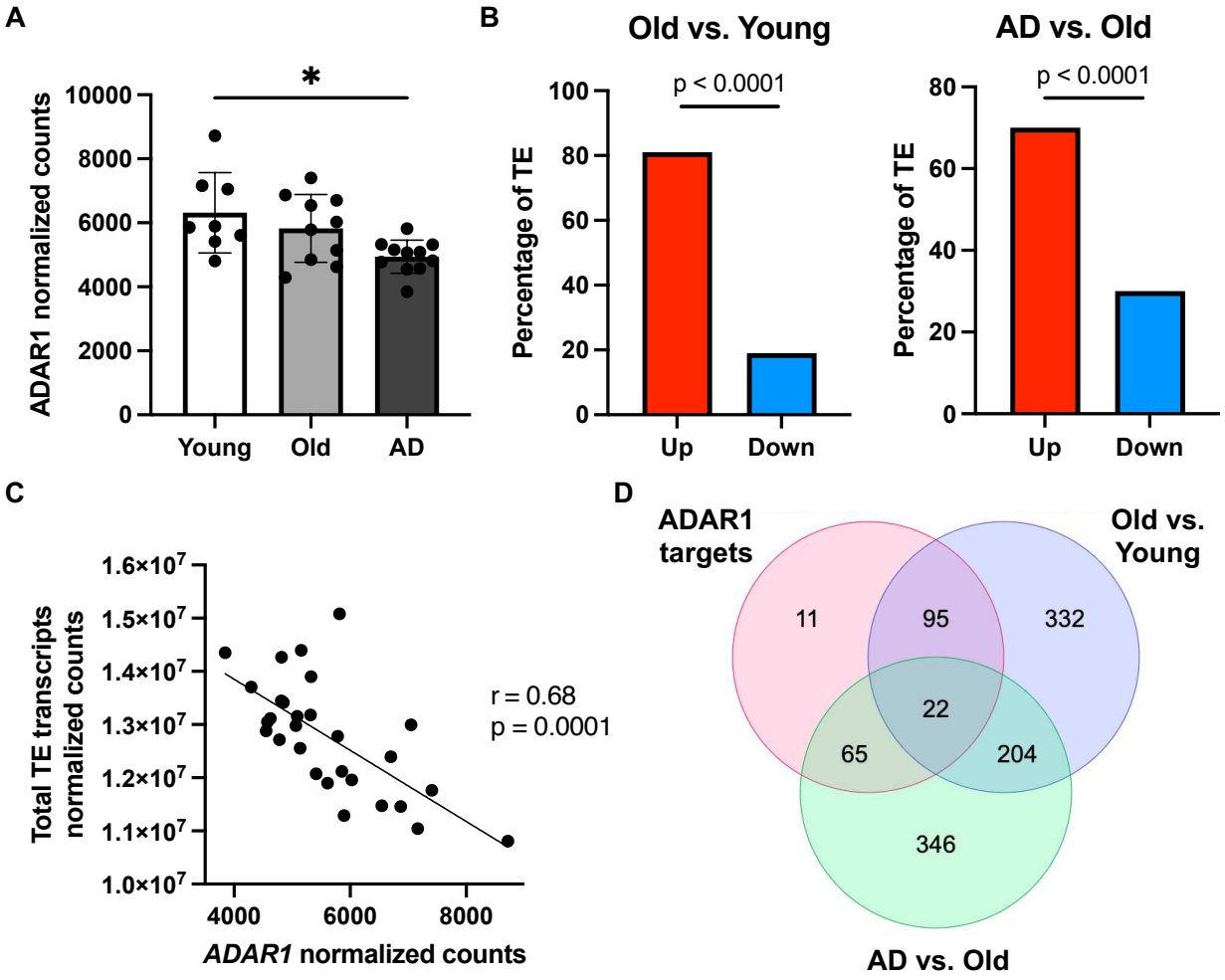


**Figure 2.4 *ADAR1* gene expression declines with age/AD are associated with TE transcript accumulation in humans**. **(A)** Changes in *ADAR1* gene expression with age and AD in postmortem brain samples from young (n=8, average age 52 years), old (n=10, average age 68 years), and Alzheimer's disease (n=12, average age 68 years) subjects, analyzed in [40]. *p ≤ 0.05, one-way ANOVA, F = 5.113, DF = 28. **(B)** Differences in TE transcript expression by major TE type in older vs. younger and AD vs. older subjects. *p ≤ 0.0001; Chi-squared test vs. mean gene expression log2FoldChange. **(C)** Negative correlation between total TE transcript levels and *ADAR1* counts in all subjects (Pearson r- and p-values). **(D)** Similar TE transcripts among potential ADAR1 targets (high Δ-edits) and increased TE transcripts (> average log2FoldChange) in older vs. younger and AD vs. older subjects.

## DISCUSSION

Pro-inflammatory signaling in glial cells is centrally involved in neuroinflammation, brain aging, and AD [1, 2, 41]. Here, we provide evidence that ADAR1 suppression causes interferon-associated pro-inflammatory signaling in human astrocytes, perhaps via TE-derived dsRNA, and that *ADAR1* gene expression is reduced while dsRNA-prone TE transcripts are increased with age and AD in the human brain. Collectively, our results suggest a potentially novel, endogenous mechanism for neuroinflammation with aging and disease, which could provide insight into future therapeutic targets.

Neuroinflammation, driven by glial cells like astrocytes, is a central mechanism of both brain aging and AD, and type I interferon signaling has been established in age- and AD-related neuroinflammation [42, 43]. Others have shown that reductions in ADAR1 may be a driver of interferon signaling in various tissues, but the transcriptomic effects of ADAR1 suppression in human astrocytes have not been extensively studied. Our data show that the accumulation of endogenous dsRNA due to ADAR1 knockdown results in increased expression of genes/pathways related to type I interferon and pro-inflammatory signaling in human astrocytes, which is consistent with previous reports in the brain and in other cell types [13, 15, 16, 38, 44]. Our data also show that ADAR1 knockdown leads to downregulation of biological processes and pathways related to extracellular matrix organization in astrocytes, events that have been linked with changes in synaptic plasticity, response to injury, and impaired blood brain barrier integrity [45-47]. We also found a downregulation of processes related to development with ADAR1 knockdown, which may reflect the connection between ADAR1 and cellular development [15, 38, 48].

Type I interferon and pro-inflammatory signaling can occur as a result of multiple upstream stimuli (e.g., injury, infection). Here, we show that type I interferon and pro-inflammatory signaling resulting from ADAR1 knockdown is likely driven by cytoplasmic dsRNA binding to MDA5 and/or RIG-I, as opposed to more generic inflammation-related pathways like

NF-κB signaling. This observation is in line with previous work showing that NF-κB is downregulated to prevent apoptosis following ADAR1 suppression, and that pro-inflammatory signaling in this context occurs through interferon regulatory factor 7 (IRF7; an additional downstream transcription factor of MDA5/RIG-I) [39]. Our findings are also consistent with studies in other tissues in which gene silencing/transgenic approaches have been used to show that ADAR1 regulates cytoplasmic dsRNA levels, and that the inflammatory response to this dsRNA occurs through the MDA5/RIG-I signaling pathway [13, 15, 36, 44]. We observed only transcript (not protein) increases in these proteins, but we found that MDA5 colocalized with dsRNA (the key event required for signaling via this pathway). Additionally, we note that our RNA-seq data show that other dsRNA sensor proteins (e.g., PKR, OAS1) were not significantly increased with ADAR1 knockdown, further supporting a specific role for MDA5/RIG-I in interferon and pro-inflammatory signaling with ADAR1 suppression. Our results are limited by our *in vitro* approach, as neuroinflammation is a physiological response that cannot be fully measured in one cell type. *In vivo*, ADAR1 mutant *Drosophila* and mouse AGS models have been used to show that dysfunctional ADAR1 results in innate immune activation in brain-like tissue and mammalian brains, respectively [16, 38, 49]. Future work using additional *in vivo* models will be important to determine if similar events may occur in brain aging and AD, but null *Adar1* knockouts are embryonically lethal [48]. As such, recent work developing mouse strains with mutations in the catalytic domains of *Adar1* that decrease dsRNA editing and stimulate interferon signaling may be particularly promising [15, 38]. However, recent data also suggest that ADAR1 downregulation can influence age-related processes like senescence independent of RNA editing [50]. Therefore, it may be necessary to develop an *in vivo* model of ADAR1 overexpression to fully investigate its protective effects.

Importantly, there are many potential triggers for neuroinflammation that involve external causes (e.g., viral infection), non-CNS processes (e.g., peripheral inflammation), and/or CNS signals in response brain aging or AD pathology (e.g., amyloid beta accumulation) [42, 51-53].

However, our data suggest a novel endogenous cause of neuroinflammation involving ADAR1 reductions and subsequent TE-derived dsRNA accumulation. These findings may be particularly important, as we and others have shown that TE transcripts increase with aging and AD [19, 21, 23] which, in combination with reduced ADAR1 activity, would support the accumulation of TE-derived dsRNA [54, 55]. Indeed, we found a global increase in total TE transcripts after ADAR1 knockdown *in vitro*, and the associated reduction in A-to-I editing occurred mostly in repetitive sequences as compared to protein coding genes, which is consistent with other reports [25]. We also identified highly expressed TE transcripts that are targets of ADAR1 (and therefore likely to form dsRNA), and these included SINEs (Alu elements) and LINEs (L1 elements). Alu and L1 elements are among the most common TEs in the human genome, and both have been shown to be edited by ADAR1 [56, 57], in line with the idea that they may be an important source of dsRNA. To confirm these findings more rigorously, future studies should leverage RNA immunoprecipitation sequencing to identify the specific TE transcripts that increase with aging/AD and bind to ADAR1 in different CNS cell types, which could provide insight into the potential to therapeutically target these events.

Rigorous characterizations of ADAR1 TE targets in the future may be particularly important, because our analyses of published RNA-seq data [40] suggest that our *in vitro* findings could be clinically relevant. We found reductions in *ADAR1* gene expression in older adult and AD patient brains, and a corresponding global increase in TE transcripts in both older adults and AD patients. In fact, higher *ADAR1* counts correlated with lower total TE transcript counts across aging and AD, supporting the idea that TEs may be an endogenous source of dsRNA that is regulated by ADAR1 in humans. Importantly, these analyses were based on bulk brain tissue containing multiple cell types, while our *in vitro* data were from homogenous astrocyte cultures. As such, it remains to be determined if astrocytes are the main cell type involved in ADAR1-related inflammatory signaling *in vivo*. However, we note that *ADAR1* counts are inversely correlated with *GFAP* counts in this dataset, suggesting a possible role for

changes in ADAR1 expression in astrocytes in the whole brain. Additionally, pro-inflammatory CNS cell activation with aging and AD is also associated with other cellular/transcriptomic processes (e.g., increased chromatin accessibility of IRFs, DNA damage, and senescence) [58-60], and it will be important to carefully design future studies on this topic to take these into account (e.g., by using multi-omics techniques to rule out other potential cell types or drivers of neuroinflammation). Finally, one key question is: What drives reductions in ADAR1 with age and/or AD? ADAR1 is reported to increase in various types of cancer [61], and cancer risk increases with age [62]. As such, it is possible that cells downregulate ADAR1 with age to prevent excessive editing that may contribute to cancer development, which would be consistent with the idea of antagonistic pleiotropy as a key mechanism of aging [63]. Therefore, before ADAR1-targeted therapeutic strategies can be advanced, long-term (e.g., lifespan) studies may be required to investigate the direct effects of ADAR1 *in vivo* on age- and AD-related neuroinflammation, as well as other health outcomes.

Collectively, our data suggest a critical role for ADAR1 in neuroinflammation via type I interferon activation in human astrocytes. Type I interferon is increasingly linked with neuroinflammation in brain aging and AD, and our findings point to a novel, upstream mechanism that may activate it (i.e., TE-derived dsRNA as a result of reduced ADAR1). The specific TE transcripts that form cytoplasmic dsRNA and activate type I interferon signaling remain unknown, but our pilot studies may serve as a foundation for future work investigating ADAR1 in brain aging and AD.

REFERENCES


1. Giovannoni, F. and F.J. Quintana, *The Role of Astrocytes in CNS Inflammation.* Trends Immunol, 2020. **41**(9): p. 805-819.
2. Colombo, E. and C. Farina, *Astrocytes: Key Regulators of Neuroinflammation.* Trends Immunol, 2016. **37**(9): p. 608-620.
3. Nedergaard, M., B. Ransom, and S.A. Goldman, *New roles for astrocytes: redefining the functional architecture of the brain.* Trends Neurosci, 2003. **26**(10): p. 523-30.
4. Burda, J.E., A.M. Bernstein, and M.V. Sofroniew, *Astrocyte roles in traumatic brain injury.* Exp Neurol, 2016. **275 Pt 3**(0 3): p. 305-315.
5. Farina, C., F. Aloisi, and E. Meinl, *Astrocytes are active players in cerebral innate immunity.* Trends Immunol, 2007. **28**(3): p. 138-45.
6. Habib, N., et al., *Disease-associated astrocytes in Alzheimer's disease and aging.* Nat Neurosci, 2020. **23**(6): p. 701-706.
7. Gantier, M.P. and B.R. Williams, *The response of mammalian cells to double-stranded RNA.* Cytokine Growth Factor Rev, 2007. **18**(5-6): p. 363-71.
8. Hogg, M., et al., *RNA editing by mammalian ADARs.* Adv Genet, 2011. **73**: p. 87-120.
9. Solomon, O., et al., *RNA editing by ADAR1 leads to context-dependent transcriptome-wide changes in RNA secondary structure.* Nat Commun, 2017. **8**(1): p. 1440.
10. George, C.X., et al., *Editing of Cellular Self-RNAs by Adenosine Deaminase ADAR1 Suppresses Innate Immune Stress Responses.* J Biol Chem, 2016. **291**(12): p. 6158-68.
11. Lamers, M.M., B.G. van den Hoogen, and B.L. Haagmans, *ADAR1: "Editor-in-Chief" of Cytoplasmic Innate Immunity.* Front Immunol, 2019. **10**: p. 1763.
12. Samuel, C.E., *Adenosine deaminase acting on RNA (ADAR1), a suppressor of double-stranded RNA-triggered innate immune responses.* J Biol Chem, 2019. **294**(5): p. 1710-1720.
13. Liddicoat, B.J., et al., *RNA editing by ADAR1 prevents MDA5 sensing of endogenous dsRNA as nonself.* Science, 2015. **349**(6252): p. 1115-20.
14. Kim, J.I., et al., *RNA editing at a limited number of sites is sufficient to prevent MDA5 activation in the mouse brain.* PLoS Genet, 2021. **17**(5): p. e1009516.
15. Guo, X., et al., *An AGS-associated mutation in ADAR1 catalytic domain results in early-onset and MDA5-dependent encephalopathy with IFN pathway activation in the brain.* J Neuroinflammation, 2022. **19**(1): p. 285.
16. Deng, P., et al., *Adar RNA editing-dependent and -independent effects are required for brain and innate immune functions in Drosophila.* Nat Commun, 2020. **11**(1): p. 1580.
17. Rice, G.I., et al., *Mutations in ADAR1 cause Aicardi-Goutières syndrome associated with a type I interferon signature.* Nat Genet, 2012. **44**(11): p. 1243-8.
18. Bourque, G., et al., *Ten things you should know about transposable elements.* Genome Biol, 2018. **19**(1): p. 199.
19. Guo, C., et al., *Tau Activates Transposable Elements in Alzheimer's Disease.* Cell Rep, 2018. **23**(10): p. 2874-2880.
20. Saleh, A., A. Macia, and A.R. Muotri, *Transposable Elements, Inflammation, and Neurological Disease.* Front Neurol, 2019. **10**: p. 894.
21. LaRocca, T.J., A.N. Cavalier, and D. Wahl, *Repetitive elements as a transcriptomic marker of aging: Evidence in multiple datasets and models.* Aging Cell, 2020. **19**(7): p. e13167.
22. Ramirez, P., et al., *Pathogenic tau accelerates aging-associated activation of transposable elements in the mouse central nervous system.* Prog Neurobiol, 2022. **208**: p. 102181.
23. Wahl, D., et al., *The reverse transcriptase inhibitor 3TC protects against age-related cognitive dysfunction.* Aging Cell, 2023.

24. Gorbunova, V., et al., *The role of retrotransposable elements in ageing and age-associated diseases.* Nature, 2021. **596**(7870): p. 43-53.
25. Porath, H.T., et al., *Massive A-to-I RNA editing is common across the Metazoa and correlates with dsRNA abundance.* Genome Biol, 2017. **18**(1): p. 185.
26. Ochoa, E., et al., *Pathogenic tau-induced transposable element-derived dsRNA drives neuroinflammation.* Sci Adv, 2023. **9**(1): p. eabq5423.
27. Chen, S., et al., *fastp: an ultra-fast all-in-one FASTQ preprocessor.* Bioinformatics, 2018. **34**(17): p. i884-i890.
28. Dobin, A., et al., *STAR: ultrafast universal RNA-seq aligner.* Bioinformatics, 2013. **29**(1): p. 15-21.
29. Love, M.I., W. Huber, and S. Anders, *Moderated estimation of fold change and dispersion for RNA-seq data with DESeq2.* Genome Biol, 2014. **15**(12): p. 550.
30. Raudvere, U., et al., *g:Profiler: a web server for functional enrichment analysis and conversions of gene lists (2019 update).* Nucleic Acids Res, 2019. **47**(W1): p. W191-w198.
31. Criscione, S.W., et al., *Transcriptional landscape of repetitive elements in normal and cancer human cells.* BMC Genomics, 2014. **15**: p. 583.
32. Zhang, F., et al., *SPRINT: an SNP-free toolkit for identifying RNA editing sites.* Bioinformatics, 2017. **33**(22): p. 3538-3548.
33. Lorenz, R., et al., *ViennaRNA Package 2.0.* Algorithms Mol Biol, 2011. **6**: p. 26.
34. LaRocca, T.J., et al., *Amyloid beta acts synergistically as a pro-inflammatory cytokine.* Neurobiol Dis, 2021. **159**: p. 105493.
35. Dhir, A., et al., *Mitochondrial double-stranded RNA triggers antiviral signalling in humans.* Nature, 2018. **560**(7717): p. 238-242.
36. Guo, X., et al., *ADAR1 RNA editing regulates endothelial cell functions via the MDA-5 RNA sensing signaling pathway.* Life Sci Alliance, 2022. **5**(3).
37. Hasel, P., et al., *Neuroinflammatory astrocyte subtypes in the mouse brain.* Nat Neurosci, 2021. **24**(10): p. 1475-1487.
38. Guo, X., et al., *Aicardi-Goutières syndrome-associated mutation at ADAR1 gene locus activates innate immune response in mouse brain.* J Neuroinflammation, 2021. **18**(1): p. 169.
39. Garcia-Gonzalez, C., et al., *ADAR1 Prevents Autoinflammatory Processes in the Heart Mediated by IRF7.* Circ Res, 2022. **131**(7): p. 580-597.
40. Nativio, R., et al., *An integrated multi-omics approach identifies epigenetic alterations associated with Alzheimer's disease.* Nat Genet, 2020. **52**(10): p. 1024-1035.
41. Matias, I., J. Morgado, and F.C.A. Gomes, *Astrocyte Heterogeneity: Impact to Brain Aging and Disease.* Front Aging Neurosci, 2019. **11**: p. 59.
42. Roy, E.R., et al., *Type I interferon response drives neuroinflammation and synapse loss in Alzheimer disease.* J Clin Invest, 2020. **130**(4): p. 1912-1930.
43. Taylor, J.M., et al., *Type-I interferon pathway in neuroinflammation and neurodegeneration: focus on Alzheimer's disease.* J Neural Transm (Vienna), 2018. **125**(5): p. 797-807.
44. Yang, S., et al., *Adenosine deaminase acting on RNA 1 limits RIG-I RNA detection and suppresses IFN production responding to viral and endogenous RNAs.* J Immunol, 2014. **193**(7): p. 3436-45.
45. Faissner, A., et al., *Contributions of astrocytes to synapse formation and maturation - Potential functions of the perisynaptic extracellular matrix.* Brain Res Rev, 2010. **63**(1-2): p. 26-38.
46. Johnson, K.M., R. Milner, and S.J. Crocker, *Extracellular matrix composition determines astrocyte responses to mechanical and inflammatory stimuli.* Neurosci Lett, 2015. **600**: p. 104-9.

47. Baeten, K.M. and K. Akassoglou, *Extracellular matrix and matrix receptors in blood-brain barrier formation and stroke.* Dev Neurobiol, 2011. **71**(11): p. 1018-39.
48. Wang, Q., et al., *Stress-induced apoptosis associated with null mutation of ADAR1 RNA editing deaminase gene.* J Biol Chem, 2004. **279**(6): p. 4952-61.
49. Inoue, M., et al., *An Aicardi-Goutières Syndrome-Causative Point Mutation in Adar1 Gene Invokes Multiorgan Inflammation and Late-Onset Encephalopathy in Mice.* J Immunol, 2021.
50. Hao, X., et al., *ADAR1 downregulation by autophagy drives senescence independently of RNA editing by enhancing p16(INK4a) levels.* Nat Cell Biol, 2022. **24**(8): p. 1202-1210.
51. Qin, L., et al., *Systemic LPS causes chronic neuroinflammation and progressive neurodegeneration.* Glia, 2007. **55**(5): p. 453-62.
52. Li, J.J., et al., *In vivo evidence for the contribution of peripheral circulating inflammatory exosomes to neuroinflammation.* J Neuroinflammation, 2018. **15**(1): p. 8.
53. Klein, R.S., et al., *Neuroinflammation During RNA Viral Infections.* Annu Rev Immunol, 2019. **37**: p. 73-95.
54. Kassiotis, G. and J.P. Stoye, *Immune responses to endogenous retroelements: taking the bad with the good.* Nat Rev Immunol, 2016. **16**(4): p. 207-19.
55. Chen, Y.G. and S. Hur, *Cellular origins of dsRNA, their recognition and consequences.* Nat Rev Mol Cell Biol, 2022. **23**(4): p. 286-301.
56. Orecchini, E., et al., *ADAR1 restricts LINE-1 retrotransposition.* Nucleic Acids Res, 2017. **45**(1): p. 155-168.
57. Ahmad, S., et al., *Breaching Self-Tolerance to Alu Duplex RNA Underlies MDA5-Mediated Inflammation.* Cell, 2018. **172**(4): p. 797-810.e13.
58. Rasa, S.M.M., et al., *Inflammaging is driven by upregulation of innate immune receptors and systemic interferon signaling and is ameliorated by dietary restriction.* Cell Rep, 2022. **39**(13): p. 111017.
59. Yu, Q., et al., *DNA-damage-induced type I interferon promotes senescence and inhibits stem cell function.* Cell Rep, 2015. **11**(5): p. 785-797.
60. Frisch, S.M. and I.P. MacFawn, *Type I interferons and related pathways in cell senescence.* Aging Cell, 2020. **19**(10): p. e13234.
61. Xu, L.D. and M. Öhman, *ADAR1 Editing and its Role in Cancer.* Genes (Basel), 2018. **10**(1).
62. Berben, L., et al., *Cancer and Aging: Two Tightly Interconnected Biological Processes.* Cancers (Basel), 2021. **13**(6).
63. Austad, S.N. and J.M. Hoffman, *Is antagonistic pleiotropy ubiquitous in aging biology?* Evol Med Public Health, 2018. **2018**(1): p. 287-294.

# CHAPTER 3 – AN AAV APPROACH TO INCREASE ADAR1 EXPRESSION IN THE BRAINS OF AGED MICE

## INTRODUCTION

Neuroinflammation, characterized by inflammatory activation in the brain and central nervous system (CNS), is a central mechanism of brain aging and Alzheimer's disease (AD) [1, 2]. While multiple events contribute to the development of neuroinflammation, one potential driver of aging- and AD-related neuroinflammation is the activation of the innate immune system in response to double-stranded RNA (dsRNA), a pathogen-associated molecular pattern (PAMP) [3, 4]. Typically associated with viral infections, dsRNA activates innate immune sensors (e.g., MDA5, RIG-I, PKR) to trigger an inflammatory response [5]. However, dsRNA may also be derived from endogenous sources [5], and the accumulation of endogenous dsRNAs is regulated by the protein adenosine deaminase acting on RNA 1 (ADAR1) [6].

ADAR1, like other ADAR enzymes, regulates dsRNA through adenosine-to-inosine (A-to-I) editing that destabilizes complimentary base pairing within dsRNA [6, 7]. This A-to-I editing is an important regulatory mechanism to prevent dsRNA accumulation and excessive inflammatory activation [8]. The homozygous knockout (KO) of the *Adar1* gene *in vivo* is embryonically lethal, and these mice show reduced A-to-I editing, increased inflammation, and apoptosis [9]. Despite the lethality of *Adar1* KO mice, animals with a mutation in the editing domain are viable but display reduced A-to-I editing, elevated neuroinflammatory markers, and cognitive deficits in adulthood [10, 11]. The inflammatory response associated with reduced or dysfunctional ADAR1 is likely mediated through RIG-I-like receptor signaling pathways, specifically melanoma differentiation-associated protein 5 (MDA5), that recognize dsRNA [7]. In fact, blocking MDA5 rescues lethality of *Adar1* KO mice and prevents neuroinflammation [11-13]. In secondary analyses of data from postmortem human brain tissue, we have found that *ADAR1* gene expression declines with aging and AD [14]. Additionally, *in vitro* studies

demonstrate that ADAR1 overexpression prevents inflammation via A-to-I editing in models of sepsis and type 1 diabetes [15, 16]. Together these data highlight a critical role for ADAR1 in preventing dsRNA-associated inflammatory activation, especially in the brain. However, whether brain-specific upregulation of ADAR1 has protective effects in brain aging remains unknown.

In this pilot study, we tested the hypothesis that ADAR1 may be protective in brain aging by injecting old mice with a CNS-specific AAV containing the *ADAR1* p110 gene (the constitutively active isoform of the enzyme). This approach was chosen because AAVs can be administered intravenously to target specific tissues/organ systems (e.g., brain) and utilize customized promoters to preferentially target specific cell types (e.g., astrocytes) [17-20]. However, we did not observe improvements in cognitive function, likely due to the absence of increased ADAR1 protein expression in the cortex or hippocampus of treated mice compared to controls. Our findings may provide insight for future studies using AAV-based overexpression approaches or exploring the role of ADAR1 in brain aging.

## METHODS

### *Animal husbandry*

Young (8 months) and old (19-21 months) male and female C57/BL6 mice were purchased from the National Institute on Aging's aged rodent colony. Mice were housed in groups of 2-3 per cage on a 12 h light/dark cycle at 22-24°C, with ad libitum access to water and food (Teklad Global irradiated 18% protein rodent diet), and routinely monitored by veterinary staff at the laboratory animal facility at Colorado State University. Body weights, food consumption, and water intake were recorded weekly. All mice were allowed to acclimatize to the facility prior to the start of the experiment, and all animal procedures were approved by Colorado State University, IACUC protocol #1441.

*AAV delivery*

The ssAAVPHP.eB vectors used in this study were produced by VectorBuilder. The custom ADAR1 ssAAVPHP.eB (ADAR1-AAV) design consisted of the p110 isoform of the *ADAR1* gene with the following specific vector design: pAAV[Exp]-CBA>hADAR[NM_001025107.3]/HA tag. The green fluorescent protein (GFP) ssAAVPHP.eB (GFP-AAV) was designed as follows: pAAV[Exp]-CBA>EGFP:WPRE. VectorBuilder determined the viral titer and sterility of both AAVs. The AAV vectors were diluted to a final concentration of $2x10^{11}$ GC/ml for injections. Mice were sedated with 3-4% isoflurane with a flow rate of 1-1.5 L and maintained under anesthesia with 1-2% isoflurane in a nose cone. Once anesthetized, mice were injected with either AAV or saline (control) into the retro-orbital sinus and monitored for any adverse effects.

*Cognitive and behavioral testing*

Before testing, the animals were familarized with the experimenter (who conducted all testing), and cognitive and behavioral testing began two weeks after injections. Equipment was cleaned with 70% ethanol to minimize scents between mice. The novel object recognition (NOR), Barnes maze, open field, and elevated plus maze (EPM) tests were performed as previously described [21, 22]. For NOR, mice were habituated to the arena for 5 min, followed by familiarization with two identifical objects (towers of Legos) placed 8 cm from each wall. After 24 h, the mice were reintroduced back to the arena, where one object was replaced with a new novel object of similar size, shape, and color (cell culture flask filled with multi-colored sand). Mice were allowed to explore the objects until they accumulated 20 s of total object exploration time or 10 min had elasped. Recognition index was calculated as the time spent exploring the novel object divided by the total object exploration time. Barnes maze was conducted on a 90

cm-diameter opaque white circular table with 20 equally spaced holes around the perimeter. Spatial cues, consisting of large triangle and square posters, were placed on the walls. The target hole with an escape box remained constant for all tests. Mice completed four trials per day where the time to enter the escape box was recorded, and once in the box, were covered for 1 min. If a mouse failed to find the target hole after 1 min, it was guided into the escape box and covered for 1 min. On the fifth day, the probe trial was conducted with the escape box removed, and the mice were allowed to explore the table for 1 min. The probe trial was recorded and analyzed with behavior cloud software (behaviorcoud.com) to measure the time spent in the target quadrant (the quarter of the table that originally contained the escape box). Anxiety was measure using the open field and EPM tests. For open field, mice were placed in the center of an open arena, whereas in the EPM test, mice were placed in the center of an apparatus consisting of two open arms and two closed arms. For both tests, mice were allowed to explore for 5 min with their movements recorded and analyzed using behavior cloud software (behaviorcoud.com).

*Grip strength testing*

Grip strength was measure using a DST-110 Digital Force Gauge (Maze Engineers), as previously described [22]. Briefly, five trials were conducted for each mouse, averaged, and force was presented relative to bodyweight.

*Animal sacrifice and tissue collection*

Mice were euthanized in a fed state four weeks after AAV injections, with all procedures conducted in the late morning. Mice were anesthetized with isoflurane, followed by cervical disolation and decaptiation. Immediately, brains were removed on ice, and the hippocampus and cortex were dissected. All tissues samples were flash-frozen on dry ice during culls and stored at -80°C for future analyses.

*Immunoblotting*

Hippocampus and cortex samples were homogenized in ice-cold RIPA buffer containing phosphatase and protease inhibitors (ThermoFisher/Roche). Protein concentration was determined using a BCA kit (ThermoFisher/Pierce). 10 ug of protein was separated by electrophoresis on 4-12% Bis-Tris gels (Bio-Rad), transferred to nitrocellulose membranes (Bio-Rad), and blocked using 5% milk in TBS-Tween for at least 1-2 h at room temperature. Membranes were incubated overnight at 4°C with ADAR1 primary antibodies (1:1000, Novus Biologicals, NBP3-05500) or GFP primary antibodies (1:1000, Novus Biologicals, NB600-308) diluted in 5% milk in TBS-Tween. This was followed by incubation of mouse or rabbit HRP-conjugated secondary antibody (1:1000, Cell Signaling, 7076s/7074s) diluted in 5% milk in TBS-Tween for 1 h at room temperature. Protein detection was performed using ECL chemiluminescent substrate (Thermo) on a FluorChem E imager (ProteinSimple). ADAR1 and GFP protein levels (ECL signal intensities) were quantified using ImageJ2 and normalized to GAPDH (1:1000, Novus Biologicals, NB100-56875).

*Statistical analyses*

GraphPad Prism software was used for ANOVAs with post-hoc t-tests for all experimental data, as well as normality testing.

RESULTS

The loss or reduction of ADAR1 is directly linked to increased inflammation [9, 10, 14, 23, 24], likely mediated through the activation of the MDA5 pathway [11, 12, 25]. However, the role of ADAR1 in the aging brain remains unexplored. To investigate this, 10 young (8 mo) and 22 old (19-21 mo) mice were injected via the retro-orbital sinus with saline, a GFP-AAV, or an

ADAR1-AAV, followed by cognitive function assessments. Unfortunately, we did not detect statistically significant differences in learning/memory in mice that received the ADAR1-AAV, as measured by NOR and Barnes maze testing (**Figure 3.1A**). However, we did observe a trend in recognition index, where the ADAR1-AAV-treated mice performed slightly better than the GFP-AAV and saline controls ($p$ = 0.1069) and appeared to perform similarly to young mice (**Figure 3.1A**). In the first cohort, mice that received the ADAR1-AAV showed modest improvements in cognitive tests (recognition index and time to reach target hole), though these data were not statistically significant ($p$ = 0.1768 and $p$ = 0.0636, respectively) (**Figure 3.1B**). However, these results were not replicated in the second cohort (**Figure 3.1C**). Also in the combined data, no significant differences were found among the older groups of mice (saline, GFP-AAV, and ADAR1-AAV) in the time taken to reach the target hole per day or in other probe trial data (e.g., the total distance explored in the target quadrant, number of errors made) (**Figure B.1B**). Additionally, we also did not detect any differences in measurements of anxiety (e.g., time spent in the center of the open field assessment, time spent in open arms vs. closed arms in the elevated plus maze) (**Figure B.1C and D**). Lastly, grip strength did not differ between treatment groups in the old mice, but the young mice did perform significantly better (**Figure B.1E**). Overall, these data suggest that the ADAR1-AAV treatment did not improve cognitive function (or other functional measurements) in aged mice.

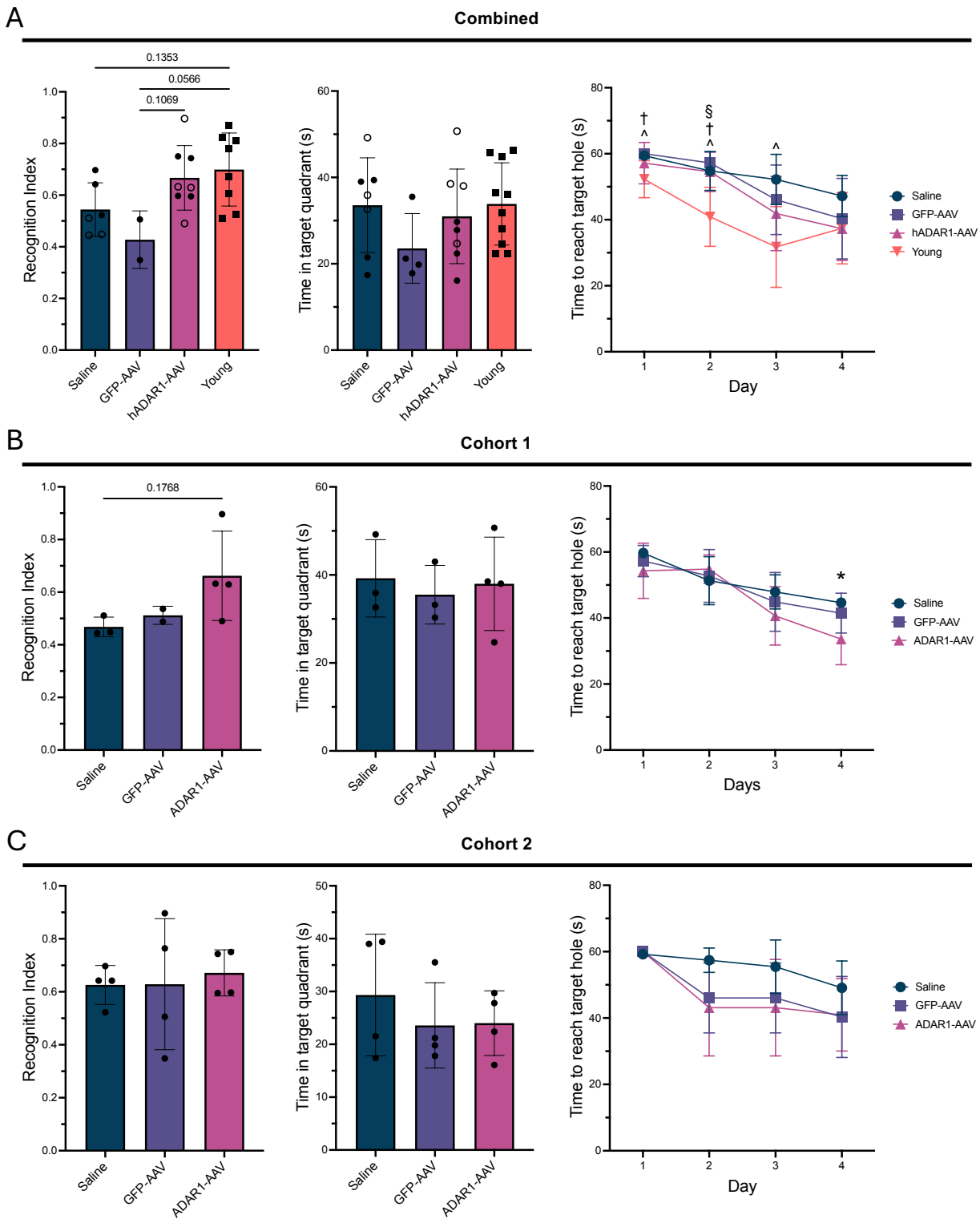


**Figure 3.1. Cognitive function analysis in aged mice treated with an ADAR1 AAV. (A)** Combined cognitive function assessments in old mice injected with an ADAR1-AAV, GFP-AAV, or saline, with young mice serving as controls. Cognitive function assessments for **(B)** cohort 1 and **(C)** cohort 2 old mice injected with an ADAR1-AAV, GFP-AAV, or saline. NOR index was quantified as the time exploring the novel object relative to the total object exploration time.

One-way ANOVA, n=2-10/condition. Spatial learning and memory assessed using the Barnes maze, measuring time spent in the target quadrant of the probe trial and time to reach the target hole per day. *$p \leq 0.05$ Day 4 vs. Day 1 for each condition, ^$p \leq 0.05$ saline vs. young, †$p \leq 0.05$ GFP-AAV vs. young, §$p \leq 0.05$ ADAR1-AAV vs. young, Two-way ANOVA; n=3-10/condition.

It is possible that we did not observe changes in cognitive function because ADAR1 expression levels in the hippocampus and cortex of the treated mice did not change. That is, we did not observe an increase in ADAR1 protein expression in these brain regions following ADAR1-AAV injection (**Figure 3.2A**). However, we were able to increase GFP expression in the mice injected with the GFP-AAV based on a similar design (**Figure 3.2B**); therefore, we believe the ADAR1-AAV should have been capable of crossing the blood brain barrier to transduce cells in the brain. Why this did not effectively happen is unclear.

One possible explanation for the lack of ADAR1 upregulation in the ADAR-AAV-treated mice may be due to the size limits of AAV constructs relative to the *ADAR1* gene. Due to the packaging (cargo) constraints of AAV vectors (~5 kb sequences), we opted to use the p110 isoform of the *ADAR1* gene instead of the full-length gene, and it is possible that ADAR1 p110 may not have been biologically effective in our model. It also is possible that counter-regulatory mechanisms may have inhibited ADAR1 upregulation, perhaps as a protective response to prevent adverse effects of increased ADAR1 expression (specifically the p110 isoform) and/or A-to-I editing, especially in the brain. This would be consistent with studies showing high amounts of ADAR1 activity in cancer and autoimmune diseases (e.g., Systemic Lupus Erythematosus) [26, 27]. In support of this idea, we were able to increase ADAR1 protein expression in primary human fibroblasts treated with the ADAR1-AAV (**Figure 3.2C**), but this approach was less effective in primary human astrocytes. In fact, the same AAVs (ADAR1 and GFP) that were used *in vivo* and in cultured fibroblasts appeared to be somewhat toxic to astrocytes. Based on this observation, we hypothesize that elevated ADAR1 expression via AAV delivery may also be toxic, potentially consistent with our results *in vivo*, but the underlying mechanism remains unknown.

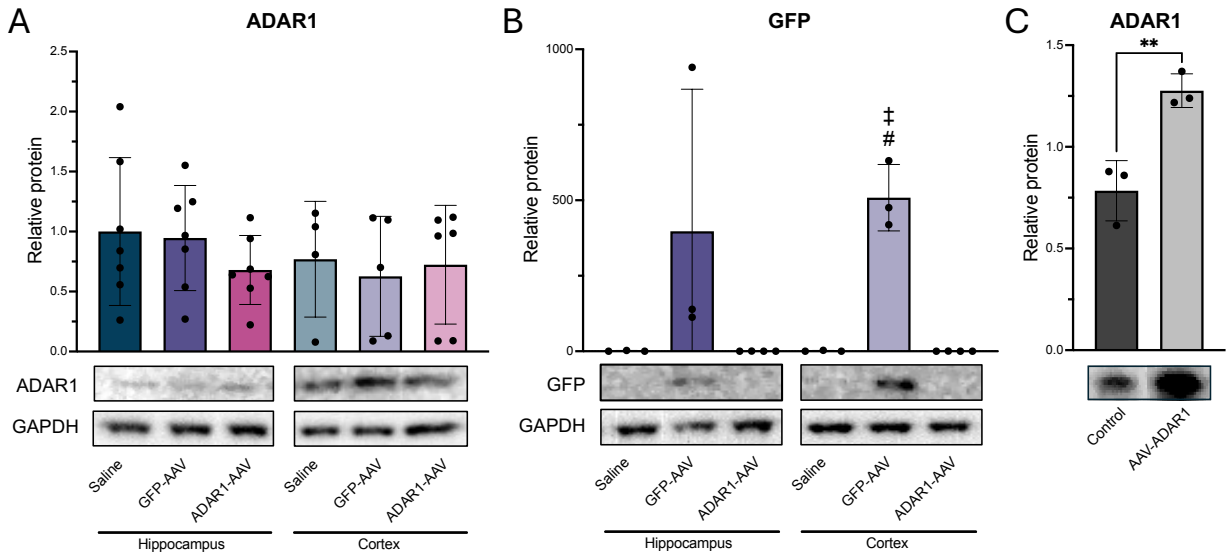


**Figure 3.2. ADAR1 and GFP expression in the brains of aged mice and primary human dermal fibroblasts treated with an ADAR1 AAV. (A)** Immunoblot data showing relative ADAR1 in the hippocampus and cortex of old mice injected with an ADAR1-AAV, GFP-AAV, or saline. **(B)** Relative GFP protein expression in the same brain regions. #$p \leq 0.0001$ Saline vs. GFP-AAV, ‡$p \leq 0.0001$ GFP-AAV vs. ADAR1-AAV, one-way ANOVA; n=3-7/condition. **(C)** Immunoblot data showing relative ADAR1 expression in primary human dermal fibroblasts treated with an ADAR1-AAV. **p ≤ 0.01, t-test; n=3/condition. All immunoblot data is normalized to GAPDH.

## DISCUSSION

Changes in ADAR1 expression and activity have been directly linked to pro-inflammatory activation [6, 7, 12, 23, 24], and there is evidence of this even occurring in the brain [10, 11, 13]. Our previous work showed that suppressing ADAR1 in human astrocytes leads to increased pro-inflammatory activation that is likely driven by endogenous dsRNAs, and we also reported that this finding may be clinically relevant in the human brain, as *ADAR1* gene expression is reduced in older adults and AD subjects [14]. However, whether ADAR1 expression can be upregulated in aging, and if this could mitigate age-related cognitive decline and neuroinflammation, has not been explored. To investigate this, in the present study we intravenously injected old mice with a brain-specific AAV encoding the human *ADAR1* p110 gene and assessed various aspects of cognitive function. Unfortunately, we did not observe improvements in cognitive function in the ADAR1-AAV-treated mice, likely due to no increase in

ADAR1 expression in the brains of these mice. Thus, at least based on our results, the potential protective role of ADAR1 against age-related cognitive decline and neuroinflammation remains unknown.

Previous research suggests that AAV transduction may be a promising method of gene therapy to enhance ADAR1 expression. Advances in AAV serotype development have enabled a targeted, at least somewhat tissue-specific approach for gene delivery. Specifically, the PHP-AAV.eB serotype crosses the blood brain barrier and preferentially targets the brain over other tissues [28]. Studies have demonstrated that the PHP-AAV.eB effectively transduces multiple brain cell types [29, 30], and when paired with the chicken β-actin (CBA) promoter, can transduce a greater number of astrocytes relative to other brain cell types [31]. However, AAV transduction in older animals (regardless of serotype) may be challenging [29]. Despite this, we successfully transduced old mice (19-21 mo) with a GFP-AAV and were able to detect GFP expression in the hippocampus and cortex (four weeks post-injection). These data support the idea that the PHP-AAV.eB may be a viable strategy for increasing gene expression in the brain.

As previously discussed, our inability to incorporate the full-length *ADAR1* gene into the AAV construct may have been limited by vector size constraints, and the shortened *ADAR1* p110 used may have not been biologically effective. Additionally, counter-regulatory mechanisms may have inhibited ADAR1 overexpression, as evidence suggests ADAR1 plays an important role in development [12, 32-34], and potentially in cancer and autoimmune disease [26, 27], alluding to potential adverse effects that enhancing ADAR1 may have. Future experiments could first confirm the successful overexpression of the full-length human *ADAR1* gene *in vitro* using alternative approaches, such as a lentiviral vector (which allows for larger transgenes to be incorporated). If effective, this lentivirus approach could be applied to young, old, and AD primary human fibroblasts to increase ADAR1 expression. Then these cells could be reprogramed into induced astrocytes (iAs) to assess the biological effects of enhanced ADAR1 expression in the context of aging and AD (as these iAs retain aging- and disease-

related characteristics [35]). Because lentiviral vectors integrate into the host genome, iAs should retain ADAR1 overexpression throughout such studies, providing a sustained increase in expression compared to other gene therapy approaches (e.g., AAVs). If these *in vitro* experiments are successful, the *in vivo* study here could be repeated using the *ADAR1*-expressing lentiviral vector delivered intranasally or via stereotactic injection. These future experiments would help to determine whether the lack of increased ADAR1 expression in our initial study was due to AAV vector design limitations or counter-regulatory mechanisms controlling ADAR1 expression. Ultimately, these studies would clarify if ADAR1 is protective against age-related cognitive decline and/or neuroinflammation.

Together, our data suggest that AAV transduction may not be an effective strategy for increasing ADAR1 in the aged brain. However, two key questions remain: 1) Was ADAR1 p110 biologically ineffective? and 2) Do compensatory mechanisms regulate ADAR1 expression, preventing its upregulation? Addressing these questions will be critical for future studies exploring ADAR1 as a potential protective mechanism against age-related cognitive decline and neuroinflammation.

REFERENCES


1. Andronie-Cioara, F.L., et al., *Molecular Mechanisms of Neuroinflammation in Aging and Alzheimer's Disease Progression.* Int J Mol Sci, 2023. **24**(3).
2. Heneka, M.T., et al., *Neuroinflammation in Alzheimer's disease.* Lancet Neurol, 2015. **14**(4): p. 388-405.
3. Saldi, T.K., et al., *Neurodegeneration, Heterochromatin, and Double-Stranded RNA.* J Exp Neurosci, 2019. **13**: p. 1179069519830697.
4. Li, D. and M. Wu, *Pattern recognition receptors in health and diseases.* Signal Transduct Target Ther, 2021. **6**(1): p. 291.
5. Chen, Y.G. and S. Hur, *Cellular origins of dsRNA, their recognition and consequences.* Nat Rev Mol Cell Biol, 2022. **23**(4): p. 286-301.
6. Samuel, C.E., *Adenosine deaminase acting on RNA (ADAR1), a suppressor of double-stranded RNA-triggered innate immune responses.* J Biol Chem, 2019. **294**(5): p. 1710-1720.
7. Rehwinkel, J. and P. Mehdipour, *ADAR1: from basic mechanisms to inhibitors.* Trends Cell Biol, 2025. **35**(1): p. 59-73.
8. Eisenberg, E. and E.Y. Levanon, *A-to-I RNA editing - immune protector and transcriptome diversifier.* Nat Rev Genet, 2018. **19**(8): p. 473-490.
9. Wang, Q., et al., *Stress-induced apoptosis associated with null mutation of ADAR1 RNA editing deaminase gene.* J Biol Chem, 2004. **279**(6): p. 4952-61.
10. Inoue, M., et al., *An Aicardi-Goutières Syndrome-Causative Point Mutation in Adar1 Gene Invokes Multiorgan Inflammation and Late-Onset Encephalopathy in Mice.* J Immunol, 2021. **207**(12): p. 3016-3027.
11. Guo, X., et al., *An AGS-associated mutation in ADAR1 catalytic domain results in early-onset and MDA5-dependent encephalopathy with IFN pathway activation in the brain.* J Neuroinflammation, 2022. **19**(1): p. 285.
12. Liddicoat, B.J., et al., *RNA editing by ADAR1 prevents MDA5 sensing of endogenous dsRNA as nonself.* Science, 2015. **349**(6252): p. 1115-20.
13. Kim, J.I., et al., *RNA editing at a limited number of sites is sufficient to prevent MDA5 activation in the mouse brain.* PLoS Genet, 2021. **17**(5): p. e1009516.
14. McEntee, C.M., A.N. Cavalier, and T.J. LaRocca, *ADAR1 suppression causes interferon signaling and transposable element transcript accumulation in human astrocytes.* Front Mol Neurosci, 2023. **16**: p. 1263369.
15. Szymczak, F., et al., *ADAR1-dependent editing regulates human β cell transcriptome diversity during inflammation.* Front Endocrinol (Lausanne), 2022. **13**: p. 1058345.
16. Shangxun, Z., et al., *ADAR1 Alleviates Inflammation in a Murine Sepsis Model via the ADAR1-miR-30a-SOCS3 Axis.* Mediators Inflamm, 2020. **2020**: p. 9607535.
17. Liu, D., et al., *Crossing the blood-brain barrier with AAV vectors.* Metab Brain Dis, 2021. **36**(1): p. 45-52.
18. Griffin, J.M., et al., *Astrocyte-selective AAV gene therapy through the endogenous GFAP promoter results in robust transduction in the rat spinal cord following injury.* Gene Ther, 2019. **26**(5): p. 198-210.
19. Massaro, G., et al., *Comparison of different promoters to improve AAV vector-mediated gene therapy for neuronopathic Gaucher disease.* Hum Mol Genet, 2024. **33**(17): p. 1467-1480.
20. Matsuzaki, Y., et al., *Optimal different adeno-associated virus capsid/promoter combinations to target specific cell types in the common marmoset cerebral cortex.* Mol Ther Methods Clin Dev, 2024. **32**(4): p. 101337.
21. Wahl, D., et al., *The reverse transcriptase inhibitor 3TC protects against age-related cognitive dysfunction.* Aging Cell, 2023. **22**(5): p. e13798.

22. Osburn, S.C., et al., *Novel effects of reverse transcriptase inhibitor supplementation in skeletal muscle of old mice.* Physiol Genomics, 2025. **57**(5): p. 308-320.
23. George, C.X., et al., *Editing of Cellular Self-RNAs by Adenosine Deaminase ADAR1 Suppresses Innate Immune Stress Responses.* J Biol Chem, 2016. **291**(12): p. 6158-68.
24. Rice, G.I., et al., *Mutations in ADAR1 cause Aicardi-Goutières syndrome associated with a type I interferon signature.* Nat Genet, 2012. **44**(11): p. 1243-8.
25. Guo, X., et al., *ADAR1 RNA editing regulates endothelial cell functions via the MDA-5 RNA sensing signaling pathway.* Life Sci Alliance, 2022. **5**(3).
26. Wang, C., et al., *Mechanisms and implications of ADAR-mediated RNA editing in cancer.* Cancer Lett, 2017. **411**: p. 27-34.
27. Roth, S.H., et al., *Increased RNA Editing May Provide a Source for Autoantigens in Systemic Lupus Erythematosus.* Cell Rep, 2018. **23**(1): p. 50-57.
28. Ling, Q., et al., *AAV-based in vivo gene therapy for neurological disorders.* Nat Rev Drug Discov, 2023. **22**(10): p. 789-806.
29. Mathiesen, S.N., et al., *CNS Transduction Benefits of AAV-PHP.eB over AAV9 Are Dependent on Administration Route and Mouse Strain.* Mol Ther Methods Clin Dev, 2020. **19**: p. 447-458.
30. Chan, K.Y., et al., *Engineered AAVs for efficient noninvasive gene delivery to the central and peripheral nervous systems.* Nat Neurosci, 2017. **20**(8): p. 1172-1179.
31. Rincon, M.Y., et al., *Widespread transduction of astrocytes and neurons in the mouse central nervous system after systemic delivery of a self-complementary AAV-PHP.B vector.* Gene Ther, 2018. **25**(2): p. 83-92.
32. Liddicoat, B.J., et al., *Adenosine-to-inosine RNA editing by ADAR1 is essential for normal murine erythropoiesis.* Exp Hematol, 2016. **44**(10): p. 947-63.
33. Ward, S.V., et al., *RNA editing enzyme adenosine deaminase is a restriction factor for controlling measles virus replication that also is required for embryogenesis.* Proc Natl Acad Sci U S A, 2011. **108**(1): p. 331-6.
34. Pestal, K., et al., *Isoforms of RNA-Editing Enzyme ADAR1 Independently Control Nucleic Acid Sensor MDA5-Driven Autoimmunity and Multi-organ Development.* Immunity, 2015. **43**(5): p. 933-44.
35. Gatto, N., et al., *Directly converted astrocytes retain the ageing features of the donor fibroblasts and elucidate the astrocytic contribution to human CNS health and disease.* Aging Cell, 2021. **20**(1): p. e13281.

# CHAPTER 4 – THE IDENTIFICATION OF TRANSPOSABLE ELEMENT-DERIVED DOUBLE-STRANDED RNAS THAT ARE MODULATED BY ADAR1 AND ACTIVATE INFLAMMATORY SIGNALING

## INTRODUCTION

Double-stranded RNA (dsRNA) is a pro-inflammatory stimulus that activates antiviral-related cellular pathways [1, 2], and has even been found to accumulate in the brains of Alzheimer's disease (AD) patients [3]. While dsRNA is commonly associated with viral infections [1], endogenous sources can also generate 'self' dsRNA [2]. One endogenous source of dsRNA involves transposable elements (TEs), non-coding DNA sequences capable of propagating throughout the genome [4, 5]. Notably, TE transcripts and the activation of dsRNA response pathways have been implicated in brain aging and AD [6-12]. For example, TE transcript expression is elevated in postmortem AD brains, and these transcripts are likely to be double-stranded [13]. Additionally, TE-derived dsRNA is elevated in *Drosophila melanogaster* models of tauopathy (a pathological hallmark of AD), and tau has been linked to increased dsRNA-related signaling in mouse models [3]. Although these data suggest that TE transcripts may contribute to dsRNA formation, these prior investigations have primarily examined TEs as a whole, and it remains unclear whether there are specific TEs or TE types (e.g., TE families or subfamilies) that are more likely to form dsRNA than others and drive dsRNA-related inflammatory signaling.

The regulation of TE-derived dsRNA is a crucial cellular process, and a key protein involved in this regulation is adenosine deaminase acting on RNA 1 (ADAR1) [14]. ADAR1 preferentially targets endogenous dsRNA and prevents its accumulation through adenosine to inosine (A-to-I) editing that destabilizes nucleotide base pairing [15, 16]. As a result, ADAR1 is essential for suppressing aberrant pro-inflammatory signaling triggered by dsRNA binding to sensor proteins, like melanoma differentiation protein 5 (MDA5) and/or protein kinase R (PKR) [16-20]. Furthermore, ADAR1 has been implicated in neurodegeneration and neurodegenerative diseases [21-24]. Previously, we demonstrated that ADAR1 suppression in primary human

astrocytes leads to the activation of pro-inflammatory signaling and accumulation of TE transcripts, some of which may form dsRNA [25]. However, the specific TE transcripts that form dsRNA and the sensor protein(s) responsible for driving inflammatory activation in this context remain unknown.

Here, we build on our previous findings by examining TE transcripts that form dsRNA and are enriched when ADAR1 is suppressed. Using a series of J2 (dsRNA antibody) RNA immunoprecipitation sequencing (RIP-seq) experiments, we identify TE transcripts that form dsRNA and accumulate when ADAR1 is knocked down. Additionally, we identify TE transcripts that bind to ADAR1 and dsRNA sensors (i.e., PKR and MDA5) by analyzing multiple existing RIP-seq datasets and comparing them with our own. Our analyses suggest that the p110 isoform of ADAR1 may play a more prominent role in regulating TE-derived dsRNA, and that many of the TE transcripts that are associated with both ADAR1 and dsRNA sensors belong to the short interspersed nuclear element (SINE) family of TEs. Furthermore, inhibiting PKR may reduce inflammatory markers, suggesting that PKR plays a vital role in the inflammatory response. Together, our findings provide insight into which TE transcripts are regulated by ADAR1 and are most likely to trigger inflammation.

## METHODS

### *Primary human astrocyte culture*

Primary human fetal astrocytes were obtained from ScienCell and cultured with standard conditions at 37 °C and 5% $CO_2$ in a humidified incubator. Cells were maintained in an astrocyte-specific medium on poly-L-lysine-coated tissue culture plates. At ~90% confluency, cells were subcultured, and experiments were conducted from passages 3-6, with no passage-associated differences observed. All cells had typical astrocyte morphology and showed >90% GFAP positivity at passage 1 (**Figure A.1**).

*siRNA transfection*

Astrocytes were transfected when 60-80% confluent using pre-designed siRNAs according to manufacturers' instructions, as previously described [25]. The ADAR1 siRNA (ThermoFisher Silencer Select, s1008, target sequence: GAGAUUCUCUCAGCCUAAAtt) and scramble siRNA (Silencer Negative Control #2 siRNA, AM4613, non-targeting sequence) were used at a final concentration of 15 nM. Briefly, lipofectamine RNAiMAX reagent (ThermoFisher, 13778-075) and siRNAs diluted in Opti-MEM Medium (ThermoFisher, 31985-070) were mixed and incubated for 5 min before further dilution in fresh astrocyte medium. After a 48 h transfection period, media was replaced with serum-free astrocyte media, with or without the drug C16 (a PKR inhibitor, Cayman Chemical), and cells were incubated for an additional 24 h. Finally, cells were rinsed with DPBS and frozen for future analyses.

*Immunoblotting*

Cells were thawed on ice and lysed using RIPA lysis buffer containing phosphatase and protease inhibitors (ThermoFisher/Roche). 5-10 ug of protein was separated by electrophoresis on 4-12% Bis Tris gels (Bio-Rad) then transferred to nitocellulose membranes (Bio-Rad). Membranes were blocked for 1 h at room temperature before overnight incubation at 4 °C with primary antibodies diluted in blocking buffer. For phosphorylated (p) proteins, 5% BSA in TBS-Tween blocking buffer was used, whereas 5% milk in TBS-Tween blocking buffer was used for all other proteins. The primary antibodies used included ADAR1 (Novus Biologicals, NBP3-05500, 1:1000), eIF2α (ABclonal, A0764, 1:1000), ICAM-1 (Novus Biologicals, NBP1-88700, 1:1000), p-eIF2α (ABclonal, AP0341, 1:1000), p-PKR (Novus Biologicals, NBP2-67426), PKR (Novus Biologicals, NBP2-37242, 1:1000), and TNF-α (ABclonal, A22227, 1:1000). Mouse and rabbit HRP-conjugated secondary antibodies (Cell Signaling, 7076s/7074s, 1:1000-1:2000) were diluted in blocking buffer and incubated for 1 h at room temperature. Proteins were detected using ECL chemiluminescent substrate (ThermoFisher) on a UVP ChemSolo Auto

Imager (Analytik Jena), and protein levels (ECL signal intensities) were normalized to GAPDH (Novus Biological, 1:2000).

RNA immunoprecipitation

J2-immunoprecipitated RNAs were isolated using the Magna RIP Kit (Signma-Aldrich, 17-700) following the manufacturer's protocol. Cells were thawed on ice and lysed in RIP lysis buffer. A 30 uL aliquot of lysate was set aside and frozen for normal RNA isolation (input RNA). The remaining cell lysates were incubated overnight on a shaker at 4 °C with J2 antibody-magnetic beads complexes. After incubation, the antibody-bead complexes and input aliquots were treated with proteinase K buffer for 30 min at 55 °C to digest proteins. Immunoprecipitated and input RNA were then isolated using a phenol-chloroform extraction. Briefly, phenol:chloroform:isoamyl alcohol was added to the samples and vortexed to mix, followed by centrifugation to separate phases. The aqueous phase was further extracted with chloroform and centrifuged again. RNA was precipitated overnight at -80 °C, pelleted, and resuspended in 10 uL of RNase-free water.

*RNA sequencing and bioinformatics*

The following libraries were sequenced on an Illumina NovaSeq6000 instrument, generating >40 million 151-bp paired-end FASTQ reads per sample: (1) abundance-based ribosomal RNA-depleted total RNA (Zymo-Seq RiboFree Total RNA Library Kit), (2) polyadenylated RNA (Universal Plus™ mRNA-seq library preparation kit with NuQuant®), (3) probed-based ribosomal RNA depleted total RNA (NEBNext® rRNA Depletion Kit v2; Zymo-Seq RiboFree Total RNA Library Kit). For all sequencing data, reads were trimmed using fastp (v.0.20.0) then aligned to the hg38 genome using STAR (v2.7.3a) with the following parameters: --outFilterScoreMinOverLread 0.4 --outFilterMatchNminOverLread 0.4 --outSAMtype BAM

Unsorted --winAnchorMultimapNmax 50 --outFilterMultimapNmax 50 [26, 27]. TEs were identified using the human RepeatMasker file (hg38) and TEtranscripts with default parameters [28]. Differential expression of genes and TE transcripts was analyzed using DESeq2 (v1.30.1) using the likelihood ratio test (LRT) with a reduced model [29], and differentially expressed genes/TE transcripts with an adjusted *p*-value (FDR) < 0.1, the starndard DESeq2 cutoff, were deemed as significant.

*RNA-seq secondary analysis*

Existing RNA-seq data used in this study are avaliable through GEO under the accession numbers GSE188937 (ADAR1 RIP), GSE108986 (PKR RIP), GSE247217 (MDA5 RIP). Bioinformatics analyses of these data were performed as described above.

*Statistical analyses*

GraphPad Prism software was used for normality testing, unpaired *t*-tests, and ANOVAs with post-hoc *t*-tests for all experimental data. Differential expression analyses were performed using DESeq2 as described above.

RESULTS

*Identifying TE-derived dsRNAs that are enriched with ADAR1 suppression*

The suppression of ADAR1 has been linked to the activation of pro-inflammatory signaling [17, 30-32], likely driven by an accumulation of dsRNA [14, 16, 18]. Our previous study suggests that these dsRNAs may arise from TE transcripts [25]. However, the specific TE transcripts that drive the inflammatory response following ADAR1 suppression remain unknown. Here, we build on our previous study by suppressing ADAR1 in primary human astrocytes and sequencing RNAs immunoprecipitated with the dsRNA antibody J2. In these cells, we achieved

a ~30% reduction in ADAR1 protein expression (**Figure 4.1A, Figure C.1E**). We then prepared multiple RNA-seq libraries of the J2 immunoprecipitated RNA (J2 RIP) to determine the most effective method for detecting changes in TE transcripts with ADAR1 knockdown. First, we generated a total RNA-seq library (version 1) using a probe-free ribosomal RNA (rRNA) depletion protocol designed to deplete the most abundant RNA (typically rRNA sequences). In the ADAR1 KD J2 RIP, we hypothesized that many immunoprecipitated RNAs would be TE transcripts and not rRNAs, based on our previous data and reports that rRNA likely is not bound by J2 [25], and the abundance of rRNAs in cellular RNA pools. However, this library preparation approach likely depleted most TE transcripts in the ADAR1 KD condition, as reflected by the global downregulation of TE transcript expression in the J2 RIP with ADAR1 KD compared to cells transfected with a scramble siRNA (transfection control; average J2 RIP TE transcript expression = -0.208, $p < 0.0001$ vs. genes) (**Figure C.1A and B**). Therefore, from the same RNA, we next generated a polyadenylated (polyA) RNA-seq library (version 2), which excludes rRNAs. In this dataset, total TE transcript expression was also reduced in the J2 RIP with ADAR1 KD compared to scramble siRNA transfected cells (average J2 RIP TE transcript expression = -0.181, $p < 0.0001$ vs. genes) (**Figure C.1C and D**). However, it is important to note that polyA RNA-seq libraries may not accurately capture changes in TE transcripts, as polyadenylation primarily targets protein-coding RNA transcripts (mRNAs). While some TE transcripts within introns may be detected by polyA RNA-seq, many TEs in intergenic regions—where a substantial proportion are located—are missed in these library preparations. Thus, we generated a total RNA library using a probe-based rRNA depletion (version 3). In this approach, we observed a global increase in TE transcripts in the J2 RIP with ADAR1 KD compared to the scramble siRNA (average TE transcript expression = 0.195, $p < 0.01$ vs. genes) (**Figure 4.1B and C**). Additionally, we identified TE transcripts that were enriched in the ADAR1 KD J2 RIP compared to Input by calculating the residual value between log2FoldChanges (log2FC) of TE transcripts in the J2 RIP and Input. This analysis identified eight significantly elevated (FDR <

0.1 in J2 RIP and Input ADAR1 siRNA vs. scramble siRNA) and enriched (residual < 0) TE transcripts in the J2 RIP (**Figure 4.1C, Table 4.1**). We also performed this analysis on transcripts from other genes/sequences, and those that were enriched in the J2 RIP with ADAR1 KD included solute carrier genes, long non-coding RNAs, and microRNAs (**Table 4.2**). Together, these data identify transcripts, from TEs and others, that form dsRNA and accumulate following ADAR1 suppression. To further this investigation, we are analyzing A-to-I editing events (a computational measure of dsRNA and activity marker for ADAR1) within TEs and other sequences (e.g., genes, microRNAs) to determine whether these transcripts are also direct targets of ADAR1, as demonstrated by our previous work [25].

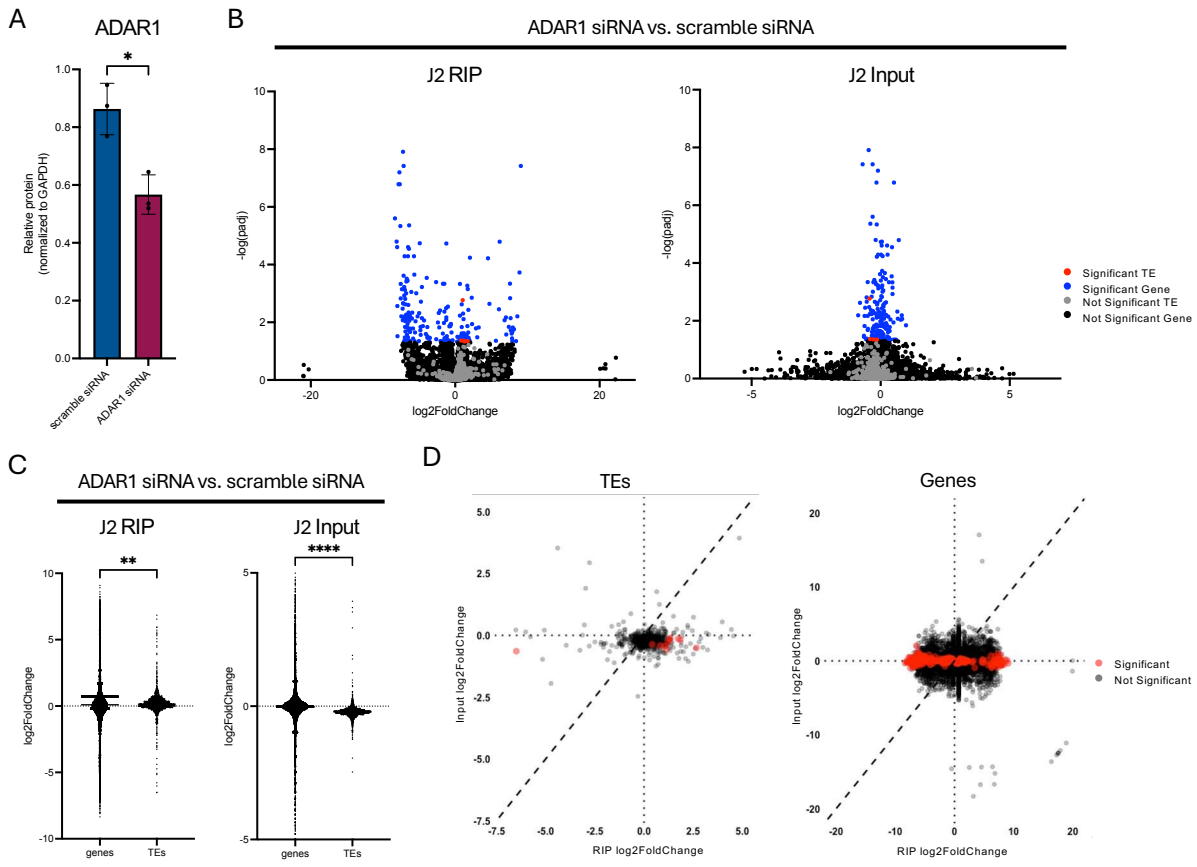


**Figure 4.1. TE transcripts enriched in J2 RIP with ADAR1 KD. (A)** Immunoblot data showing ADAR1 knockdown. *$p \leq 0.05$, unpaired *t*-test; n=3/condition. Error bars represent standard deviation (SD). **(B)** Volcano plot of J2 RIP and Input RNA-seq data showing changes in genes (black) and TE transcript (grey) expression in astrocytes transfected with the ADAR1 siRNA compared to the scramble siRNA. Significant differentially expressed genes and TE transcripts highlighted in blue and red, respectively (FDR < 0.1); n=3/group. **(C)** Median gene and TE

expression in J2 RIP and Input RNA comparing ADAR1 siRNA and scramble siRNA conditions. ** $p \leq 0.01$, **** $p \leq 0.0001$; Mann-Whitney test. **(D)** Comparison of log2FC for TE transcripts (left) and genes (right) between J2 RIP and Input samples in ADAR1 siRNA vs. scramble siRNA conditions. Red indicates transcripts that are significantly differentially expressed in both J2 RIP and Input with ADAR1 KD. Dashed line indicates J2 RIP log2FC = Input log2FC. Transcripts above the dashed line are enriched in ADAR1 KD Input, whereas those below the dashed line are enriched in ADAR1 KD J2 RIP.

**Table 4.1. TE transcripts enriched in J2 RIP with ADAR1 KD.** Log2FC and FDR were calculated using DESEq2. The residual value determined as the difference between J2 RIP log2FC and Input log2FC, and residual < 0 indicates transcripts that are enriched in the RIP.

| TE Name | Input log2FC | Input FDR | RIP log2FC | RIP FDR | Residual |
|---|---|---|---|---|---|
| HSAT5:Satellite:Satellite | -0.1752 | 0.0607 | 1.8459 | 0.0607 | -2.0211 |
| L1HS:L1:LINE | -0.2761 | 0.0442 | 1.2239 | 0.0442 | -1.4999 |
| L1M2a1:L1:LINE | -0.5645 | 0.0705 | 1.1398 | 0.0705 | -1.7043 |
| LTR18B:ERVL:LTR | -0.1390 | 0.0450 | 1.7277 | 0.0450 | -1.8667 |
| LTR26B:ERV1:LTR | -0.5062 | 0.0793 | 2.6602 | 0.0793 | -3.1665 |
| MER41C:ERV1:LTR | -0.4122 | 0.0426 | 0.8208 | 0.0426 | -1.2330 |
| MER99:hAT:DNA | -0.1663 | 0.0461 | 1.2909 | 0.0461 | -1.4572 |
| REP522:telo:Satellite | -0.1047 | 0.0739 | 1.3321 | 0.0739 | -1.4368 |

*ADAR1p110 predominately regulates TE-derived dsRNA*

To identify transcripts that bind to ADAR1 and, therefore, are likely regulated by ADAR1 through A-to-I editing, we next analyzed an existing RIP-seq dataset for transcripts bound to the ADAR1p110 and ADAR1p150 isoforms in HEK293 cells [33]. In cells transfected with the full-length, interferon inducible p150 isoform, normalized *ADAR1* counts were increased (**Figure 4.2A**), and TE transcripts were globally reduced in the ADAR1p150 RIP compared to the transfection control (MOCK, average RIP TE transcript expression = -0.647, $p < 0.0001$ vs. genes). Furthermore, only a few TE transcripts were enriched in the ADAR1p150 RIP (**Figure 4.2C, Table 4.2**), whereas many were enriched in the Input (**Figure 4.2C**). In cells transfected with the p110 ADAR1 isoform (which localizes primarily to the nucleus), normalized *ADAR1* counts were also increased (**Figure 4.2D**), and total TE transcript expression was upregulated in the ADAR1p110 RIP compared to Input (average RIP TE transcript expression = 1.116, $p < 0.0001$ vs. genes) (**Figure 4.2E**). Additionally, many TE transcripts were enriched for the ADAR1p110 RIP (**Figure 4.2F, Table 4.3**). Similar analyses conducted for other transcripts that

may be enriched in the ADAR1p150 and ADAR1p110 RIPs revealed transcripts related to zinc finger genes, but also long non-coding RNAs and microRNAs (**Table C.2 and 3**). Together, these data suggest that the ADAR1p150 isoform may not play a major role in TE-derived dsRNA regulation, but rather that TE transcripts are regulated by the ADAR1p110 isoform in the nucleus before they can potentially trigger a dsRNA-related inflammatory response in the cytoplasm. Future analyses will quantify A-to-I editing events within these transcripts to confirm ADAR1 regulation and investigate isoform-specific differences in A-to-I editing.

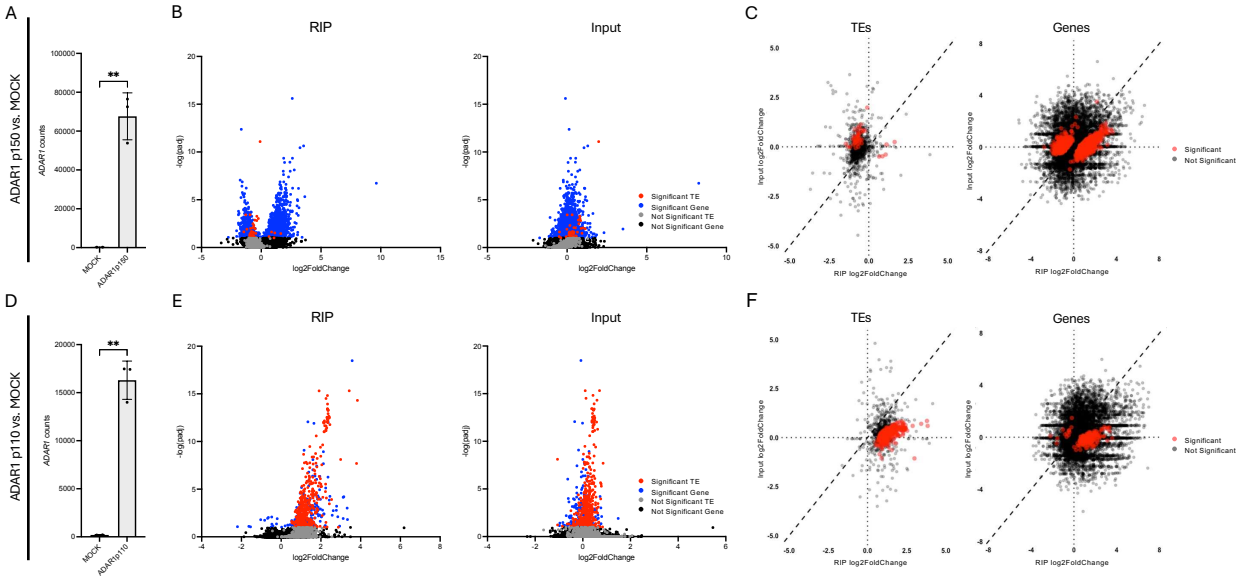


**Figure 4.2. TE transcripts enriched in ADAR1 RIP.** Normalized *ADAR1* counts in HEK293 cells transfected with **(A)** ADAR1p150 or **(D)** ADAR1p110. ** $p \leq 0.01$, unpaired *t*-test; n=3/condition. Error bars represent SD. Volcano plots of **(B)** ADAR1p150 RIP and Input RNA-seq data in HEK293 cells overexpressing ADAR1p150 compared to untransfected controls (MOCK) and **(E)** ADAR1p110 RIP and Input RNA-seq data in HEK293 cells overexpressing ADAR1p110 compared to MOCK showing changes in gene (black) and TE transcript (grey) expression. Significantly differentially expressed genes and TE transcripts highlighted in blue and red, respectively (FDR < 0.1); n=2-3/group. Comparison of log2FCs between **(C)** ADAR1p150 RIP and Input in ADAR1p150 OE vs. MOCK and **(F)** ADAR1p110 RIP and Input ADAR1p110 OE vs. MOCK of TE transcripts (left) and genes (right), with significantly differentially expressed transcripts in both RIP and input with ADAR1 isoform overexpression highlighted in red. Dashed line represents RIP log2FC = Input log2FC. Transcripts above the dashed line are enriched in ADAR1 isoform OE Input, whereas transcripts below the dashed line are enriched in ADAR1 isoform OE RIP. Original data obtained by Kleinova et al. [33].

**Table 4.2. TE transcripts enriched in ADAR1p150 RIP of HEK293 cells transfected with ADAR1p150.** Log2FC and FDR were calculated using DESEq2. The residual value determined

as the difference between ADAR1p150 RIP log2FC and Input log2FC, and residual < 0 indicates transcripts that are enriched in the RIP.

| TE Name | Input log2FC | Input FDR | RIP log2FC | RIP FDR | Residual |
|---|---|---|---|---|---|
| UCON70:UCON70:Unknown | -0.3929 | 0.0964 | 1.0700 | 0.0964 | -1.4629 |
| AluYh7:Alu:SINE | 0.2444 | 0.0343 | 1.6369 | 0.0343 | -1.3925 |
| PABL_B:ERV1:LTR | -0.4794 | 0.0237 | 0.8647 | 0.0237 | -1.3441 |
| LTR76:ERV1:LTR | -0.4945 | 0.0711 | 0.6521 | 0.0711 | -1.1466 |
| L1M2a:L1:LINE | 0.1218 | 0.0297 | 1.1268 | 0.0297 | -1.0050 |

**Table 4.3. Top 10 TE transcripts enriched in ADAR1p110 RIP of HEK293 cells transfected with ADAR1p110.** Log2FC and FDR were calculated using DESEq2. The residual value determined as the difference between ADAR1p110 RIP log2FC and Input log2FC, and residual < 0 indicates transcripts that are enriched in the RIP.

| TE Name | Input log2FC | Input FDR | RIP log2FC | RIP FDR | Residual |
|---|---|---|---|---|---|
| HSATI:Satellite:Satellite | -1.0624 | < 0.0001 | 2.9952 | < 0.0001 | -4.0576 |
| SATR2:Satellite:Satellite | 0.5966 | < 0.0001 | 3.8381 | < 0.0001 | -3.2415 |
| AluYh7:Alu:SINE | 0.8509 | < 0.0001 | 3.7936 | < 0.0001 | -2.9427 |
| SATR1:Satellite:Satellite | 0.7024 | < 0.0001 | 3.4257 | < 0.0001 | -2.7233 |
| D20S16:Satellite:Satellite | 0.5985 | 0.0985 | 2.8797 | 0.0985 | -2.2812 |
| AluYi6_4d:Alu:SINE | 0.3511 | 0.0001 | 2.5395 | 0.0001 | -2.1884 |
| LTR47A2:ERVL:LTR | -0.6462 | 0.0465 | 1.5408 | 0.0465 | -2.1870 |
| L1PA12:L1:LINE | 0.1355 | 0.0000 | 2.2585 | 0.0000 | -2.1230 |
| GSATX:centr:Satellite | -0.2980 | 0.0871 | 1.8182 | 0.0871 | -2.1161 |
| PABL_B:ERV1:LTR | 0.2152 | 0.0001 | 2.2784 | 0.0001 | -2.0632 |

*Identifying TE-derived dsRNAs that interact with MDA5, PKR, and ADAR1p110*

To identify transcripts that bind to dsRNA sensors and potentially drive inflammatory signaling, we analyzed existing RIP-seq datasets for RNAs bound to PKR and MDA5 [34, 35]. We observed that TE transcripts were globally elevated in the PKR RIP compared to Input (average RIP TE transcript expression = 0.205, $p < 0.01$ vs. genes) (**Figure 4.3A**). Similarly, in the MDA5 RIP, most TE transcripts were elevated compared to Input (average RIP TE transcript expression = 1.580, $p < 0.0001$ vs. genes) (**Figure 4.3B**). To identify TE transcripts that activate PKR and MDA5 and also are regulated by ADAR1p110, we intersected transcripts that were significantly elevated in the PKR and MDA5 RIPs (FDR < 0.1) and enriched in the ADAR1p110 RIP (residual < 0) (**Figure 4.3C**). We identified 102 TE transcripts that were common to all three datasets, most of which were SINEs, LTRs, and LINEs. The relative proportions of these TE

types were different from those in the annotated human genome (chi-square $p < 0.001$) (**Figure 4.3C and D**), suggesting that the patterns we observed reflect biologically meaningful differences (e.g., increased inflammation via dsRNA sensors). A similar pattern was observed for TE transcripts bound to MDA5 and ADAR1p110 (**Figure 4.3D**). Interestingly, only a few TE transcripts were only common to PKR and ADAR1p110, and these were mostly SINEs. In contrast, TE transcripts bound to dsRNA sensors but not ADAR1p110 consisted largely of LTRs (**Figure 4.3D**). Among the TE transcripts that were enriched in the ADAR1 KD J2 RIP (**Table 4.1**), HSAT5 (Satellite) and L1HS (LINE1) overlapped with transcripts identified in the PKR, MDA5, and ADAR1p110 RIPs. However, neither HSAT5 nor L1HS formed secondary RNA structures indicative of intra-stranded dsRNA, as predicted by RNA folding algorithms (**Figure 4.3E**). This suggests that if these TE transcripts form dsRNA, its likely through inter-stranded annealing of two transcripts transcribed from opposite strands (e.g., sense/antisense binding), consistent with the repetitive nature of TEs throughout the genome [36]. Collectively, these data suggest that SINE transcripts are the primary TE family regulated by ADAR1p110 and are drivers of inflammatory signaling, aligning with previous reports [37, 38]. While PKR and MDA5 may also be activated by LTRs, this TE family does not appear to be regulated by ADAR1p110. Additionally, LTRs were enriched in the ADAR1 KD J2 RIP (not SINEs), suggesting that TE-derived dsRNA accumulation following ADAR1 suppression may be driven by mechanisms other than ADAR1 editing. To expand on these studies, we are conducting fluorescence *in situ* hybridization (FISH) for L1HS transcripts—a TE with a long enough sequence to develop FISH probes for—in ADAR1 knocked down astrocytes.

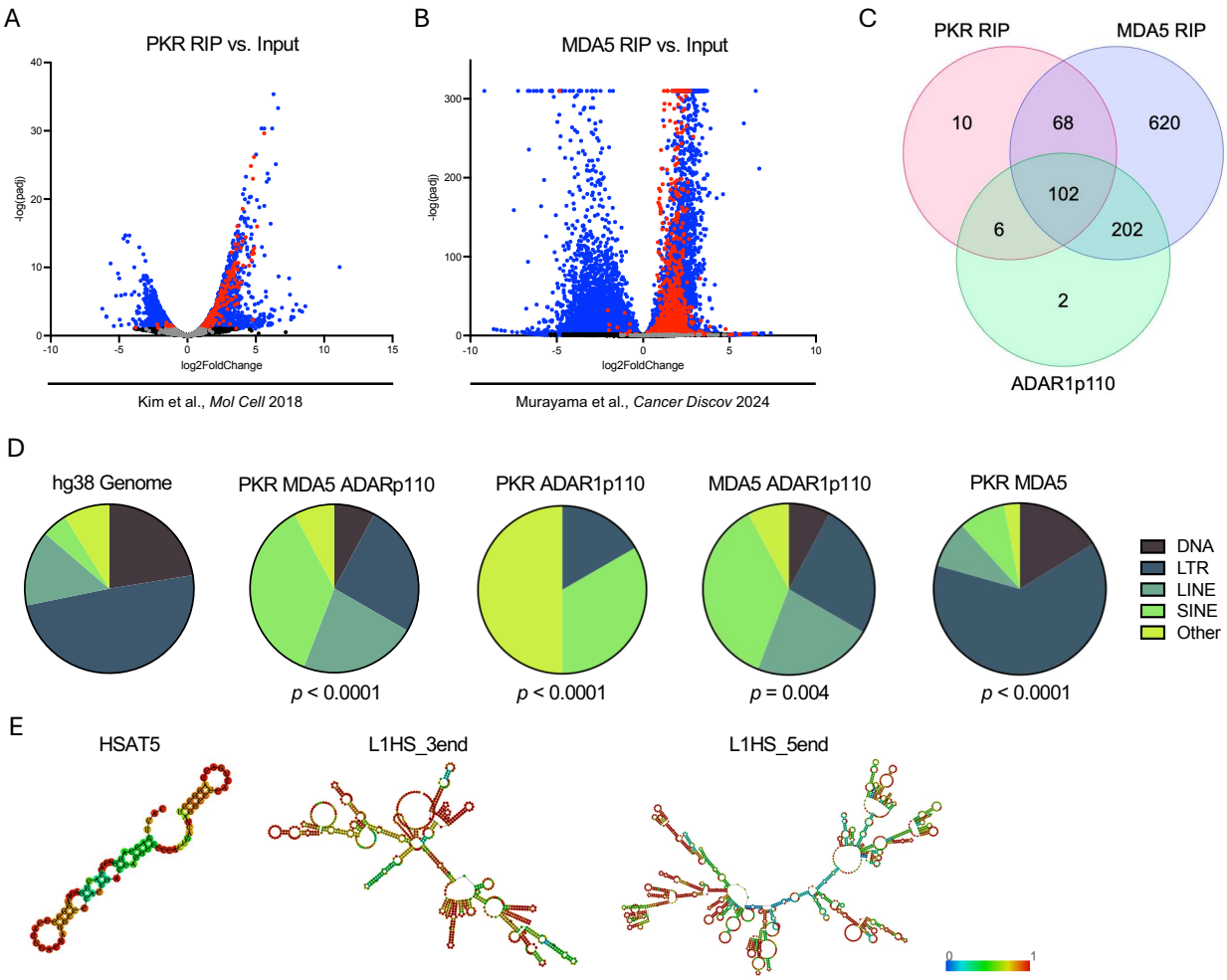


**Figure 4.3. TE transcripts bound to dsRNA sensors and regulated by ADAR1p110.** Volcano plots of **(A)** PKR RIP and Input RNA-seq data in HeLa cells and **(B)** MDA5 RIP and Input RNA-seq data in H446 cells showing changes in gene (black) and TE transcript (grey) expression. Original data obtained by Kim et al. [34] and Murayama et al. [35]. Significantly differentially expressed genes and TE transcripts highlighted in blue and red, respectively (FDR < 0.1); n=1-3/group. **(C)** Venn diagram illustrating the overlap of increased/enriched TE transcripts (FDR < 0.1) between PKR RIP, MDA5 RIP, and ADAR1p110 RIP. **(D)** TE type composition of overlapping TE transcripts across conditions, showing differences in the proportions of TE families compared to the hg38 genome. $p < 0.0001$, chi-square. **(E)** Predicted RNA secondary structures of HSAT5 and L1HS (TE transcripts enriched with ADAR1 KD J2 RIP and present in PKR, MDA5, ADAR1p110 overlap). Red base pairs indicate high likelihood of nucleotide binding.

*PKR inhibition reduced inflammatory markers with ADAR1 suppression*

Mechanistic studies modulating ADAR1 expression suggest that the inflammatory response is driven by dsRNA binding to the dsRNA sensor MDA5 [17, 18, 20]. However, other dsRNA sensor proteins may also contribute inflammation in the context of ADAR1 suppression

[2]. For instance, PKR, a key inflammatory protein implicated in aging and AD, also binds to dsRNA to trigger an inflammatory response [20, 39, 40], and it has been reported that PKR may act downstream in MDA5 signaling [41], suggesting that the MDA5-driven inflammatory response could be dependent on PKR activation. To investigate the role of PKR in ADAR1-related inflammation, we co-treated ADAR1 knockdown astrocytes with the PKR inhibitor C16 to block PKR activation. Although not statistically significant, we observed a reduction in ADAR1p110 expression in cells that were transfected with the ADAR1 siRNA, which was maintained in cells co-treated with C16 (**Figure 4.4A**). Similarly, the expression of the cytoplasmic, interferon-inducible ADAR1p150 isoform was reduced with ADAR1 KD and further reduced with C16 (**Figure 4.4B**). Interestingly, ICAM-1 expression (an astrocyte inflammatory marker) did not increase with ADAR1 KD, as in our previous data [25]. However, C16 treatment attenuated ICAM-1 expression in scramble siRNA transfected cells and appeared to reduce its expression in cells transfected with the ADAR1 siRNA (**Figure 4.4C**). A similar trend was observed for TNF-α expression (a pro-inflammatory cytokine), with a significant reduction in ADAR1 KD cells co-treated with C16 (**Figure 4.4D**). Although not significant, activated PKR (p-PKR) appeared to be reduced with C16 co-treatment (**Figure 4.4E**), suggesting that the reduction in inflammatory markers (e.g., ICAM-1, TNF-α) with C16 treatment may result from inhibiting PKR signaling. However, we did not detect any differences in p-eIF2α expression (**Figure 4.4F**), a downstream effector of PKR signaling. To further this investigation, we are increasing the sample size per condition to determine whether the observed trends are statistically significant. Additionally, we are investigating proteins involved in the MDA5 signaling pathway to determine whether C16 modulates MDA5-related signaling.

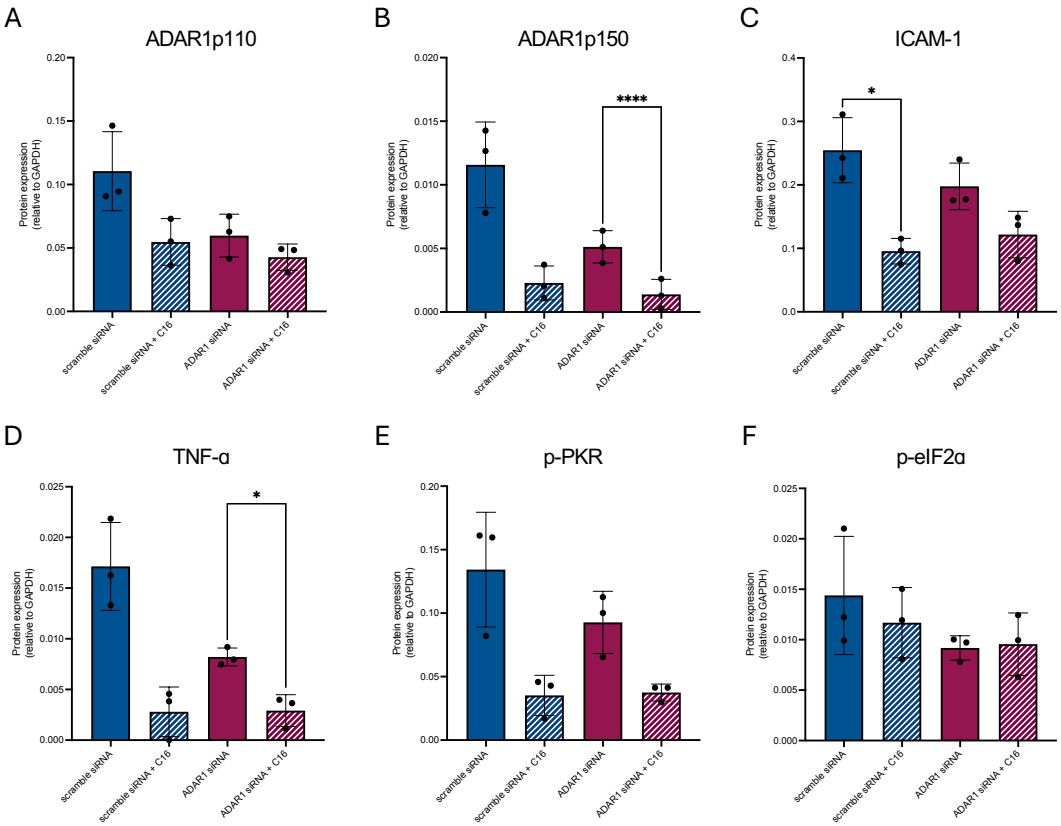


**Figure 4.4. C16 attenuates inflammation by inhibiting PKR signaling.** Immunoblot data showing relative protein expression of **(A)** ADAR1p110, **(B)** ADAR1p150, **(C)** ICAM1, **(D)** TNF-α, **(E)** p-PKR, and **(F)** p-eIF2α in astrocytes transfected with ADAR1 siRNA or scramble siRNA and cotreated with the compound C16 (PKR inhibitor). *$p \leq 0.05$, **$p \leq 0.01$, ***$p \leq 0.001$, ****$p \leq 0.0001$; one-way ANOVA with multiple testing; n=2-3/condition. Error bars represent SD.

## DISCUSSION

Reduced expression of ADAR1 and the subsequent accumulation of TE-derived dsRNA may contribute to pro-inflammatory signaling pathway activation observed in aging and AD [25]. In our study, we identified TE transcripts that form dsRNA in human astrocytes following ADAR1 knockdown and assessed whether these transcripts are specifically regulated by ADAR1 and bind to dsRNA sensors (i.e., PKR and MDA5). Additionally, we explored the potential role of PKR activation in mediating the inflammatory response when ADAR1 is suppressed. Collectively, our data highlight specific TE transcripts that may drive dsRNA-mediated inflammation, offering potential therapeutic targets to alleviate inflammation associated with aging and/or AD.

Evidence of elevated dsRNA and TE transcripts has been found in the brains of older adults and individuals with AD [3, 9, 13, 42], potentially linked to altered gene expression of *ADAR1* [25], a key regulator of endogenous dsRNA [14]. Emerging studies indicate that some TE transcripts may form dsRNA [3], and our previous work demonstrated that TE transcripts—some of which likely form dsRNA—accumulate following ADAR1 suppression [25]. Building on these findings, we performed J2 RIP-seq studies to further examine TE-derived dsRNA when ADAR1 is suppressed. This analysis revealed eight TEs significantly enriched in the J2 RIP of ADAR1-suppressed astrocytes, suggesting these TE transcripts are strong candidates for dsRNA formation. While many of these TE transcripts have not yet been directly implicated in dsRNA formation, L1M2a and MER41 elements have been associated with dsRNA-related inflammation [43-45]. Others, including HSAT5 and REP522, have been linked to cancer [46-49], and elevated A-to-I RNA editing (a marker of ADAR1 activity) is frequently observed in tumors and cancer cells [50, 51]. Notably, HSAT5 has also been associated with senescence [52], and additional TE-derived dsRNAs, such as endogenous retroviruses (a subfamily of LTRs), accumulate in senescence cells [53]. Importantly, L1HS, a LINE1 element, is the only autonomously active TE in the human genome [54], capable of retrotransposing and generating new genomic insertions. Due to the widespread copy number of L1HS, we suspect that this TE transcript may form inter-stranded dsRNA through complimentary base pairing between two transcripts (e.g., two L1HS transcripts or one L1HS and another TE transcript), similar to reports of inter-stranded dsRNA formation between SINE transcripts [55].

ADAR1 is comprised of two isoforms: the nuclear p110 and the cytoplasmic, interferon inducible p150 [19], and both isoforms participate in A-to-I editing [56]. Previous studies suggest that ADAR1p150 plays a more prominent role in the regulation of inflammation, as evidenced by the fact that simultaneous knockout (KO) of dsRNA sensors and ADAR1p150 attenuates the inflammatory response [20, 33, 57]. Additionally, some evidence suggests that ADAR1p150 exhibits higher A-to-I editing compared to ADAR1p110 [17, 56]. However, our data suggest that

ADAR1p110 is primarily most responsible for regulating TE-derived dsRNA, specifically. We detected a greater enrichment of TE transcripts in the ADAR1p110 RIP compared to the ADAR1p150 RIP. TE transcripts that were highly enriched in the ADAR1p110 RIP included Alu elements (SINEs), ERV1 (LTRs), and L1 (LINEs), aligning with previous reports of A-to-I editing of these elements [38, 58-60]. These findings suggest that ADAR1p110 may regulate TE-derived dsRNA within the nucleus, preventing its accumulation and potential recognition by cytoplasmic dsRNA sensors that trigger inflammation. This would be consistent with the idea that TEs are tonically transcribed at some low level, and that ADAR1p110 is an important "surveyor" of these transcripts. Although ADAR1p150 may still play a crucial role in regulating inflammation triggered by other substrates (e.g., long non-coding RNAs, microRNAs, Z-RNAs) in the cytoplasm [58, 61, 62], our data indicate that ADAR1p150 is unlikely to bind to TE-derived dsRNA. Interestingly, Adar1p110 KO mice do not exhibit the dsRNA-specific inflammatory response observed in full-length Adar1 and Adar1p150 KO models [17]. This would suggest that TE-derived dsRNA regulated by ADARp110 in the nucleus does not trigger an inflammatory response in the cytoplasm, where interactions with dsRNA sensors likely occur. Therefore, the precise mechanisms by which ADAR1 KO or suppression leads to inflammation, potentially via TE-derived dsRNA, remains unclear. Additionally, is it possible that aging- or AD-related cellular dysfunction (e.g., reduced ADAR1, increased nuclear permeability) may lead to an increase in the accumulation of TE-derived dsRNA in the cytoplasm, thus triggering inflammatory pathways.

The inflammatory response resulting from the ADAR1 suppression is likely driven by the activation of dsRNA sensors, and our data specifically point to TE-derived dsRNA binding to MDA5 and PKR. KO and genetic mutation studies have shown that inflammation caused by ADAR1 KO or editing-deficient ADAR1 can be rescued by the simultaneous KO of MDA5 [17, 18, 30]. However, other studies suggest that PKR KO may attenuate the effects of ADAR1p150-specific KOs [20]. Additionally, PKR may act downstream of MDA5 activation [41]. Here, we identified TE transcripts bound to PKR and MDA5 and examined their overlap with TE

transcripts that also bind to ADAR1p110. These shared TE transcripts primarily consisted of SINEs, LTRs, and LINEs—transcripts previously reported to undergo A-to-I editing by ADAR1 and to activate MDA5 [38, 58-60]. Among these TE transcripts, only two, HSAT5 and L1HS, were enriched when ADAR1 was suppressed. Neither formed predicted secondary RNA structures, but as discussed above, prior literature supports the possibility that these TE transcripts could form inter-stranded dsRNA [54, 55]. While our findings highlight TE-derived dsRNAs that are common substrates of PKR, MDA5, ADAR1p110, a key limitation of our analysis is that the RIP-seq experiments for each protein were performed in different cell types. Thus, cell-type-specific differences may influence TE transcript expression and impact which of these transcripts bind to dsRNA sensors, such as MDA5 or PKR, and ADAR1.

In addition to identifying TE-derived dsRNAs that activate PKR and/or MDA5, we also found that the PKR inhibitor C16 appeared to reduce siRNA transfection-related inflammatory markers, though our study was not sufficiently powered to detect statistical significance in many of our markers. Although others support a role for MDA5 activation with accumulating dsRNAs, the downstream pro-inflammatory signaling may be dependent on indirect PKR activation. To support this idea, previous studies have shown that in the absence of PKR, IRF3 (a transcription factor in the MDA5 pathway) fails to translocate to the nucleus, thereby preventing inflammation [41]. However, whether C16 modulates MDA5-related signaling by inhibiting PKR remains incompletely understood.

Collectively, our findings suggest that TE transcripts with a higher likelihood of forming dsRNA are regulated by ADAR1 and can trigger an inflammatory response through the activation of MDA5 and PKR. TE-derived dsRNA may serve as a potential mechanism driving inflammation in brain aging and AD, highlighting potential biomarkers and/or therapeutic targets in these contexts.

REFERENCES


1. de Faria, I.J., et al., *dsRNA sensing during viral infection: lessons from plants, worms, insects, and mammals.* J Interferon Cytokine Res, 2013. **33**(5): p. 239-53.
2. Chen, Y.G. and S. Hur, *Cellular origins of dsRNA, their recognition and consequences.* Nat Rev Mol Cell Biol, 2022. **23**(4): p. 286-301.
3. Ochoa, E., et al., *Pathogenic tau-induced transposable element-derived dsRNA drives neuroinflammation.* Sci Adv, 2023. **9**(1): p. eabq5423.
4. Porath, H.T., et al., *Massive A-to-I RNA editing is common across the Metazoa and correlates with dsRNA abundance.* Genome Biol, 2017. **18**(1): p. 185.
5. Cordaux, R. and M.A. Batzer, *The impact of retrotransposons on human genome evolution.* Nat Rev Genet, 2009. **10**(10): p. 691-703.
6. Heinrich, M.J., et al., *Endogenous double-stranded Alu RNA elements stimulate IFN-responses in relapsing remitting multiple sclerosis.* J Autoimmun, 2019. **100**: p. 40-51.
7. Saleh, A., A. Macia, and A.R. Muotri, *Transposable Elements, Inflammation, and Neurological Disease.* Front Neurol, 2019. **10**: p. 894.
8. Polesskaya, O., et al., *The role of Alu-derived RNAs in Alzheimer's and other neurodegenerative conditions.* Med Hypotheses, 2018. **115**: p. 29-34.
9. Wahl, D., et al., *The reverse transcriptase inhibitor 3TC protects against age-related cognitive dysfunction.* Aging Cell, 2023. **22**(5): p. e13798.
10. Ramirez, P., et al., *Pathogenic tau accelerates aging-associated activation of transposable elements in the mouse central nervous system.* Prog Neurobiol, 2022. **208**: p. 102181.
11. Morel, M., et al., *PKR, the double stranded RNA-dependent protein kinase as a critical target in Alzheimer's disease.* J Cell Mol Med, 2009. **13**(8a): p. 1476-88.
12. de Rivero Vaccari, J.P., et al., *RIG-1 receptor expression in the pathology of Alzheimer's disease.* J Neuroinflammation, 2014. **11**: p. 67.
13. Saldi, T.K., et al., *Neurodegeneration, Heterochromatin, and Double-Stranded RNA.* J Exp Neurosci, 2019. **13**: p. 1179069519830697.
14. Samuel, C.E., *Adenosine deaminase acting on RNA (ADAR1), a suppressor of double-stranded RNA-triggered innate immune responses.* J Biol Chem, 2019. **294**(5): p. 1710-1720.
15. Eisenberg, E. and E.Y. Levanon, *A-to-I RNA editing - immune protector and transcriptome diversifier.* Nat Rev Genet, 2018. **19**(8): p. 473-490.
16. George, C.X., et al., *Editing of Cellular Self-RNAs by Adenosine Deaminase ADAR1 Suppresses Innate Immune Stress Responses.* J Biol Chem, 2016. **291**(12): p. 6158-68.
17. Kim, J.I., et al., *RNA editing at a limited number of sites is sufficient to prevent MDA5 activation in the mouse brain.* PLoS Genet, 2021. **17**(5): p. e1009516.
18. Liddicoat, B.J., et al., *RNA editing by ADAR1 prevents MDA5 sensing of endogenous dsRNA as nonself.* Science, 2015. **349**(6252): p. 1115-20.
19. Rehwinkel, J. and P. Mehdipour, *ADAR1: from basic mechanisms to inhibitors.* Trends Cell Biol, 2025. **35**(1): p. 59-73.
20. Hu, S.B., et al., *ADAR1p150 prevents MDA5 and PKR activation via distinct mechanisms to avert fatal autoinflammation.* Mol Cell, 2023. **83**(21): p. 3869-3884.e7.
21. Deng, P., et al., *Adar RNA editing-dependent and -independent effects are required for brain and innate immune functions in Drosophila.* Nat Commun, 2020. **11**(1): p. 1580.
22. Wang, H., et al., *ADAR1 Suppresses the Activation of Cytosolic RNA-Sensing Signaling Pathways to Protect the Liver from Ischemia/Reperfusion Injury.* Sci Rep, 2016. **6**: p. 20248.
23. Pozdyshev, D.V., et al., *Differential Analysis of A-to-I mRNA Edited Sites in Parkinson's Disease.* Genes (Basel), 2021. **13**(1).

24. Cheng, L., et al., *A Wonderful Journey: The Diverse Roles of Adenosine Deaminase Action on RNA 1 (ADAR1) in Central Nervous System Diseases.* CNS Neurosci Ther, 2025. **31**(1): p. e70208.
25. McEntee, C.M., A.N. Cavalier, and T.J. LaRocca, *ADAR1 suppression causes interferon signaling and transposable element transcript accumulation in human astrocytes.* Front Mol Neurosci, 2023. **16**: p. 1263369.
26. Dobin, A., et al., *STAR: ultrafast universal RNA-seq aligner.* Bioinformatics, 2013. **29**(1): p. 15-21.
27. Chen, S., et al., *fastp: an ultra-fast all-in-one FASTQ preprocessor.* Bioinformatics, 2018. **34**(17): p. i884-i890.
28. Jin, Y., et al., *TEtranscripts: a package for including transposable elements in differential expression analysis of RNA-seq datasets.* Bioinformatics, 2015. **31**(22): p. 3593-9.
29. Love, M.I., W. Huber, and S. Anders, *Moderated estimation of fold change and dispersion for RNA-seq data with DESeq2.* Genome Biol, 2014. **15**(12): p. 550.
30. Guo, X., et al., *An AGS-associated mutation in ADAR1 catalytic domain results in early-onset and MDA5-dependent encephalopathy with IFN pathway activation in the brain.* J Neuroinflammation, 2022. **19**(1): p. 285.
31. Inoue, M., et al., *An Aicardi-Goutières Syndrome-Causative Point Mutation in Adar1 Gene Invokes Multiorgan Inflammation and Late-Onset Encephalopathy in Mice.* J Immunol, 2021. **207**(12): p. 3016-3027.
32. Rice, G.I., et al., *Mutations in ADAR1 cause Aicardi-Goutières syndrome associated with a type I interferon signature.* Nat Genet, 2012. **44**(11): p. 1243-8.
33. Kleinova, R., et al., *The ADAR1 editome reveals drivers of editing-specificity for ADAR1-isoforms.* Nucleic Acids Res, 2023. **51**(9): p. 4191-4207.
34. Kim, Y., et al., *PKR Senses Nuclear and Mitochondrial Signals by Interacting with Endogenous Double-Stranded RNAs.* Mol Cell, 2018. **71**(6): p. 1051-1063.e6.
35. Murayama, T., et al., *Targeting DHX9 Triggers Tumor-Intrinsic Interferon Response and Replication Stress in Small Cell Lung Cancer.* Cancer Discov, 2024. **14**(3): p. 468-491.
36. Hayward, A. and C. Gilbert, *Transposable elements.* Curr Biol, 2022. **32**(17): p. R904-r909.
37. Riedmann, E.M., et al., *Specificity of ADAR-mediated RNA editing in newly identified targets.* Rna, 2008. **14**(6): p. 1110-8.
38. Ahmad, S., et al., *Breaching Self-Tolerance to Alu Duplex RNA Underlies MDA5-Mediated Inflammation.* Cell, 2018. **172**(4): p. 797-810.e13.
39. Gal-Ben-Ari, S., et al., *PKR: A Kinase to Remember.* Front Mol Neurosci, 2018. **11**: p. 480.
40. García, M.A., E.F. Meurs, and M. Esteban, *The dsRNA protein kinase PKR: virus and cell control.* Biochimie, 2007. **89**(6-7): p. 799-811.
41. Pham, A.M., et al., *PKR Transduces MDA5-Dependent Signals for Type I IFN Induction.* PLoS Pathog, 2016. **12**(3): p. e1005489.
42. Feng, Y., et al., *Widespread transposable element dysregulation in human aging brains with Alzheimer's disease.* Alzheimers Dement, 2024. **20**(11): p. 7495-7517.
43. Schmid, C.D. and P. Bucher, *MER41 repeat sequences contain inducible STAT1 binding sites.* PLoS One, 2010. **5**(7): p. e11425.
44. Nataf, S., J. Uriagereka, and A. Benitez-Burraco, *The Promoter Regions of Intellectual Disability-Associated Genes Are Uniquely Enriched in LTR Sequences of the MER41 Primate-Specific Endogenous Retrovirus: An Evolutionary Connection Between Immunity and Cognition.* Front Genet, 2019. **10**: p. 321.
45. Buttler, C.A., et al., *An intronic LINE-1 regulates IFNAR1 expression in human immune cells.* Mob DNA, 2023. **14**(1): p. 20.

46. Kaczkowski, B., et al., *Transcriptome Analysis of Recurrently Deregulated Genes across Multiple Cancers Identifies New Pan-Cancer Biomarkers.* Cancer Res, 2016. **76**(2): p. 216-26.
47. Yandım, C. and G. Karakülah, *Dysregulated expression of repetitive DNA in ER+/HER2- breast cancer.* Cancer Genet, 2019. **239**: p. 36-45.
48. Köse, S.N., et al., *Expressions of the satellite repeat HSAT5 and transposable elements are implicated in disease progression and survival in glioma.* Turk J Biol, 2024. **48**(4): p. 242-256.
49. Horie, M., et al., *Integrative CAGE and DNA Methylation Profiling Identify Epigenetically Regulated Genes in NSCLC.* Mol Cancer Res, 2017. **15**(10): p. 1354-1365.
50. Zhang, Y., et al., *Advances in A-to-I RNA editing in cancer.* Mol Cancer, 2024. **23**(1): p. 280.
51. Paz, N., et al., *Altered adenosine-to-inosine RNA editing in human cancer.* Genome Res, 2007. **17**(11): p. 1586-95.
52. KarakÜlah, G. and C. Yandim, *Signature changes in the expressions of protein-coding genes, lncRNAs, and repeat elements in early and late cellular senescence.* Turk J Biol, 2020. **44**(6): p. 356-370.
53. Di Giorgio, E., et al., *Transcription of endogenous retroviruses in senescent cells contributes to the accumulation of double-stranded RNAs that trigger an anti-viral response that reinforces senescence.* Cell Death Dis, 2024. **15**(2): p. 157.
54. Campitelli, L.F., et al., *Reconstruction of full-length LINE-1 progenitors from ancestral genomes.* Genetics, 2022. **221**(3).
55. Masson, E., et al., *Alu insertion-mediated dsRNA structure formation with pre-existing Alu elements as a disease-causing mechanism.* Am J Hum Genet, 2024. **111**(10): p. 2176-2189.
56. Sun, T., et al., *Decoupling expression and editing preferences of ADAR1 p150 and p110 isoforms.* Proc Natl Acad Sci U S A, 2021. **118**(12).
57. Pestal, K., et al., *Isoforms of RNA-Editing Enzyme ADAR1 Independently Control Nucleic Acid Sensor MDA5-Driven Autoimmunity and Multi-organ Development.* Immunity, 2015. **43**(5): p. 933-44.
58. de Reuver, R., et al., *ADAR1 interaction with Z-RNA promotes editing of endogenous double-stranded RNA and prevents MDA5-dependent immune activation.* Cell Rep, 2021. **36**(6): p. 109500.
59. Mannion, N.M., et al., *The RNA-editing enzyme ADAR1 controls innate immune responses to RNA.* Cell Rep, 2014. **9**(4): p. 1482-94.
60. Chung, H., et al., *Human ADAR1 Prevents Endogenous RNA from Triggering Translational Shutdown.* Cell, 2018. **172**(4): p. 811-824.e14.
61. Nishikura, K., *A-to-I editing of coding and non-coding RNAs by ADARs.* Nat Rev Mol Cell Biol, 2016. **17**(2): p. 83-96.
62. Kudriavskii, V.V., et al., *RNA Editing by ADAR Adenosine Deaminases in the Cell Models of CAG Repeat Expansion Diseases: Significant Effect of Differentiation from Stem Cells into Brain Organoids in the Absence of Substantial Influence of CAG Repeats on the Level of Editing.* Biochemistry (Mosc), 2024. **89**(8): p. 1474-1489.

# CHAPTER 5 – SINGLE-CELL TRANSCRIPTOME PATTERNS OF TRANSPOSABLE ELEMENTS IN ALZHEIMER'S DISEASE[2]

## INTRODUCTION

Alzheimer's disease (AD) is a complex neurodegenerative disease involving many cell type-specific changes in in the brain. Recent studies of AD patients and AD transgenic mouse models have leveraged single-cell/nucleus RNA-sequencing (sc/snRNA-seq) to understand the role of cell-specific transcriptome changes with AD [1, 2]. However, none of these analyses have examined transposable elements (TEs), despite growing evidence of a role for TE transcripts in multiple neurodegenerative diseases [3-5].

TEs make up ~half of the human genome and are a type of mobile DNA element that can propagate throughout the genome [6]. They are classified broadly as transposons or retrotransposons, depending on how they move (transpose) from one genomic location to another. Transposons operate through a 'cut-and-paste' mechanism involving DNA intermediates, whereas retrotransposons utilize a 'copy-and-paste' mechanism involving RNA intermediates [6]. Typically, TEs are epigenetically suppressed (e.g., via heterochromatin), which prevents their expression/activity, but aging and disease are associated with increased TE accessibility and expression [7, 8]. In AD, TE transcripts, especially from retrotransposons, are reported to increase with tau pathology and cognitive impairment, and they have been linked with neuroinflammation (potentially due to the activation of immune response pathways by transposition intermediates) [9-13]. However, which specific cells in the brain drive AD-related changes in TE transcript expression remains unknown.

[2]McEntee CM, LaRocca TJ. Single-Cell Transcriptome Patterns of Transposable Elements in Alzheimer's Disease. Mol Neurobiol. 2025 Jun 19. doi: 10.1007/s12035-025-05140-9. Epub ahead of print. PMID: 40537665.

Here, we analyzed benchmark snRNA-seq AD datasets to evaluate cell type-specific differences in TE transcripts with AD. In total, we studied 143,951 prefrontal cortex cells [14, 15], and we found that: (1) increases in TE transcripts with AD pathology/diagnosis occur broadly in most cell types of the brain; (2) the greatest TE increases occur in retrotransposon transcripts from excitatory neurons; and (3) TEs are likely transcriptionally accessible due to chromatin differences in AD. Together, our data provide new insight into AD-related TE dysregulation, which may be helpful in current efforts to target TEs in neurodegeneration.

## METHODS

### *RNA-seq datasets and availability*

The primary RNA-seq data used in this study are available on the Synapse server (synapse.org) under the accession numbers: syn18485175 (Mathys et al., 2019 [14]; snRNA-seq), syn22079621 (Morabito et al., 2021 [15]; snRNA-seq), syn3388564 (ROSMAP [16]; bulk RNA-seq). Other bulk RNA-seq datasets can be found on the Gene Expression Omnibus (GEO) via the accession numbers: GSE125050 (Srinivasan et al., 2020 [17]) and GSE255902 (Parra Bravo et al., 2024 [18]).

### *snRNA-seq bioinformatics analyses*

snRNA gene and TE transcripts were analyzed using the soloTE program, an established pipeline for evaluating TEs in sc/snRNA-seq data, as reported elsewhere [19, 20]. Briefly, reads were aligned to the hg38 human genome using STARsolo (v2.7.3a) with default parameters except for the following, as suggested in the soloTE manual: --winAnchorMultimapNmax 100 --outFilterNultimapNmax 100 --outSAMmultiNmax 1 --outSAMattributes CB UB GN [21]. According to 10x Genomics library preparations reported in the original studies, the following barcode whitelists were used for alignments: 737K-august-

2016.txt (Mathys et al.), 3M-february-2018.txt (Morabito et al.). The soloTE pipeline (v1.08) with default parameters was used to identify TE transcripts with the hg38 Repeatmasker file and generate counts for genes and TE transcripts [19]. Count matrices containing gene and TE transcript counts were processed with Seurat (v5.1.0) using standard workflows [22, 23]. For each subject dataset, cells with less than 200 and more than 2500 features were removed (to remove potential empty droplets and doublets), and the remaining cells were used for downstream analyses. Cells/counts were normalized and scaled according to default parameters, and the top 2000 highly variable features were identified. Individual subject datasets were integrated using IntegrateLayers(method = CCAIntegration) and joined together. The top 30 PCs were used to find the nearest neighbors in the integrated dataset, and the data were clustered using a resolution of 0.8. Cluster-specific differentially expressed genes and TE transcripts were identified with FindAllMarkers(), and cell types were annotated manually and confirmed with the scType program (v1.0). For manual annotation, differentially expressed genes/TEs per cluster were identified using FindAllMarkers() and compared to previously established marker genes [14]. For scType annotation, cell type scores were generated using positive and negative cell markers from the integrated dataset compared to the scType brain database [24]. The two methods of annotation were compared before finalizing cell type calls for each cluster. Lastly, cell type identification was further confirmed by comparing annotated cell barcodes from the original studies to those in our analyses. Both snRNA-seq datasets were analyzed independently in order to confirm similar findings in different datasets, and because subjects in each original study were selected based on different criteria (Aβ pathology in Mathys et al., clinical diagnosis in Morabito et al.).

*snRNA-seq pseudobulk differential expression analyses*

Differentially expressed genes and TE transcripts were identified using pseudobulk approaches with the DESeq2 program (v1.38.3) [25]. Briefly, the annotated datasets were aggregated by subject for each cell type, and individual cell types were isolated into their own count matrices. Genes and TE transcripts were separated, and DESeq2 was used to evaluate differential expression for each. The primary/larger dataset in these analyses (Mathys et al.) was age- and sex-matched, and the second dataset (Morabito et al.) was age-matched but not balanced for sex. Moreover, neither of these original studies corrected for age/sex in their analyses (perhaps because of the potential for introducing more noise/error in the case of Morabito et al.'s small subject numbers). Therefore, to perform analyses as similar as possible to those reported in the original data, differential expression of genes/TE transcripts were not corrected for these variables. For our analyses, count matrices were filtered to retain genes and TE transcripts with one count in at least 70% of all samples. After filtering, differential gene expression was performed with the following arguments: test = "LRT", reduced = ~1, useT = TRUE, minmu = 1e-6, minReplicatesForReplace = Inf, according to recommendations from the DESeq2 manual. TE transcripts were normalized to sample-specific size factors (based on gene counts) prior to estimating dispersions. The likelihood ratio test to determine differentially expressed TE transcripts was also used with the following arguments: reduced = ~1, minmu = 1e-6. Differentially expressed genes/TEs between conditions with an adjusted *p*-value (FDR) < 0.1 were considered significant.

*snRNA-seq pseudobulk WGCNA*

To relate cell type TE transcript levels to clinical traits, normalized count matrices containing only TEs were used in a pseudobulk unsigned weighted gene co-expression network analysis (WGCNA) using the WGCNA program (v1.72-5) [26]. Briefly, normalized snRNA-seq counts were aggregated and separated by individual cell types. For each cell type, power was

determined as the value just below the peak of the soft threshold curve, networks were constructed with a minModuleSize = 200, and the modules were correlated to subject traits, all of which were previously reported in the original study (Mathys et al.). Individual TE transcript-trait correlations with a *p*-value < 0.05 were considered significant and were used to calculate average correlation coefficients by cell type.

*snATAC-seq/TE intersection*

Processed differentially accessible chromatin regions (DARs), as reported by Morabito et al. [15], were intersected with the hg38 RepeatMasker file using BEDTools Intersect Intervals to identify TEs within transcriptomically chromatin-accessible regions [27]. As reported by Morabito et al., DARs with a $\log_2$foldchange > 0 (AD vs. C) were considered 'more accessible', whereas regions with a $\log_2$foldchange < 0 (AD vs. C) were considered 'less accessible'. The number of overlaps between TEs and DARs was counted and normalized to TE copy number.

*Bulk RNA-seq bioinformatics, differential expression analyses, and gene ontology*

Bulk RNA-seq reads were aligned to the hg38 genome using STAR (v2.7.10b) with default parameters except for the following: --outFilterScoreMinOverLread 0.4 --outFilterMatchNminOverLread 0.4 --outFilterMultimapNmax 50 --winAnchorMultimapNmax 50 [28], as suggested in the TEtranscripts manual. TE transcripts were identified using the hg38 RepeatMasker file and TEtranscripts program (v2.1.4) with default settings [29]. Differentially expressed genes and TE transcripts were analyzed using DESeq2 (v1.38.3), and genes/TE transcripts with an adjusted *p*-value (FDR) < 0.05 were considered significant [25]. These significantly differentially expressed genes were correlated to total TE transcript counts for all 90 subjects, and genes that met a Bonferroni-corrected *p*-value ($-\log_{10}$(*p*-value) > 10) were used for standard Gene Ontology (GO) analysis with the g:Profiler program [30].

*Statistical analysis*

Statistical analysis details can be found in all figure legends and methods. Seurat was used for clustering of snRNA-seq data, and DESeq2 was used for all differential expression analyses, as described above. GraphPad Prism was used for Mann-Whitney and Kruskal Wallis tests after normality testing, and JMP was used for correlation analyses with Bonferroni correction.

RESULTS

*AD-related TE transcript increases are broad and most pronounced in neurons*

To identify which cell type(s) may drive TE transcript expression in AD, we first re-analyzed a benchmark AD snRNA-seq dataset, generated by Mathys et al. [14], using the soloTE pipeline. As reported in the original study, this dataset is based on prefrontal cortex samples from 48 subjects, including 24 with no/low AD pathology and 24 with high AD pathology [14]. After aligning and processing the snRNA-seq data, we annotated 64,760 cells and identified cell types/clusters similar to those reported in the original study (**Figure 5.1A**, **Supplementary Table S2**) [14]. These cells/clusters differentially expressed the same cell type markers originally reported [14], and we confirmed their identification using the scType algorithm (**Figure 5.1B**). Additionally, we compared barcodes/cell identifications from our analysis to those originally reported [14], and we found >80% overlap. We did identify a cluster of neurons that expressed excitatory neuron markers but did not meet the scType requirements (i.e., match the reference brain database) to be classified as such or share barcodes with cells originally reported as excitatory neurons (<25%). This cluster was at least in part defined by differences in

TE expression, suggesting its presence was likely due to differences in analysis pipelines (e.g., different aligners combined with including TE transcripts in QC/clustering) [14]. Therefore, we kept this cluster (EX2) separate from other neuronal subtypes.

Next, to identify changes in TE transcripts associated with high AD pathology across all cell types, we performed pseudobulk differential gene and TE transcript expression analyses across cell types. We found a global increase in total TE transcripts across most cell types in high compared to no pathology subjects (**Figure 5.1C**), which was driven by many significantly differentially expressed individual TE transcripts with AD in multiple cell types, except in the END (endothelial cell) cluster (**Figure D.1**). Additionally, we found that the astrocyte (AST), excitatory neuron (EX), and EX2 clusters had the greatest numbers of individual significantly increased TE transcripts in high pathology subjects (179, 868, and 198, respectively) (**Figure D.1**), and this trend was consistent across all major TE types (**Figure 5.1C and D**).

A pseudobulk network analysis (WGCNA) of the snRNA-seq data revealed strong positive correlations ($p < 0.05$) between subject clinical data (e.g., clinical cognitive diagnosis, overall AD pathology score) and TE transcripts in the EX and EX2 clusters, modest correlations with TEs in the AST cluster, and only negative/low correlations with TEs in other clusters (e.g., oligodendrocytes [OD], **Figure 5.1E, Figure D.2**). Among the TE transcripts that were positively related to clinical AD characteristics in the AST, EX, and EX2 clusters, we found 32 common to all three cell types. 75% of these common TE transcripts were long interspersed nuclear elements (LINEs) (**Figures 5.1F, Supplemental Table D.1**), a type of retrotransposon that remains active in the human genome [31], can stimulate inflammation [32], and has been implicated in neurodegeneration (**Figures D.2 and 5.1F**) [13, 33]. LINEs are also the only TEs that encode for their own proteins; however, these proteins only aid in their propagation throughout the genome and do not serve other biological functions [34]. This TE type was also commonly increased in EX and EX2 clusters, whereas TEs specifically enriched in each cell type were largely long terminal repeats (LTRs), another type of retrotransposon implicated in

aging, AD and inflammation (**Figure 5.1F**) [4, 35]. Lastly, we found that total normalized counts from LINEs and short interspersed nuclear elements (SINEs, also retrotransposons) were increased in the EX cluster in AD compared to not cognitively impaired (NCI) subjects (**Figure 5.1G**). We also found that this trend was consistent for all major TE types in the EX2 cluster, but the increase in normalized retrotransposon counts from AD subjects was absent in the inhibitory neurons (IN) cluster (**Figures D.3A and B**). Interestingly, we noted a bimodal pattern of total normalized counts for all TE types in the EX cluster of NCI subjects, and those with higher TE transcript levels tended to have higher pathology, although this trend was not statistically significant (**Figure D.3C**).

Finally, to provide insight into potential mechanisms underlying AD-associated increases in TE transcripts, especially in neurons, we evaluated correlations among differentially expressed genes (DEGs) associated with high pathology and total TE transcript counts in the EX cluster. Gene ontology (GO) analyses of DEGs that were positively related to TE levels showed enrichment for GO molecular function terms reflecting epigenetic modifications and chromatin maintenance (**Figure 5.1H**), whereas DEGs that were negatively related to TE transcript levels were associated with mitochondrial function in EX (**Figure D.4**). Together, these data show that TE transcripts are broadly elevated in most cell types of the brain, that increased retrotransposon/LINE expression in excitatory neurons is most closely related to AD pathology, and that these increases are associated with epigenetic and mitochondrial changes, both of which are established contributors to AD.

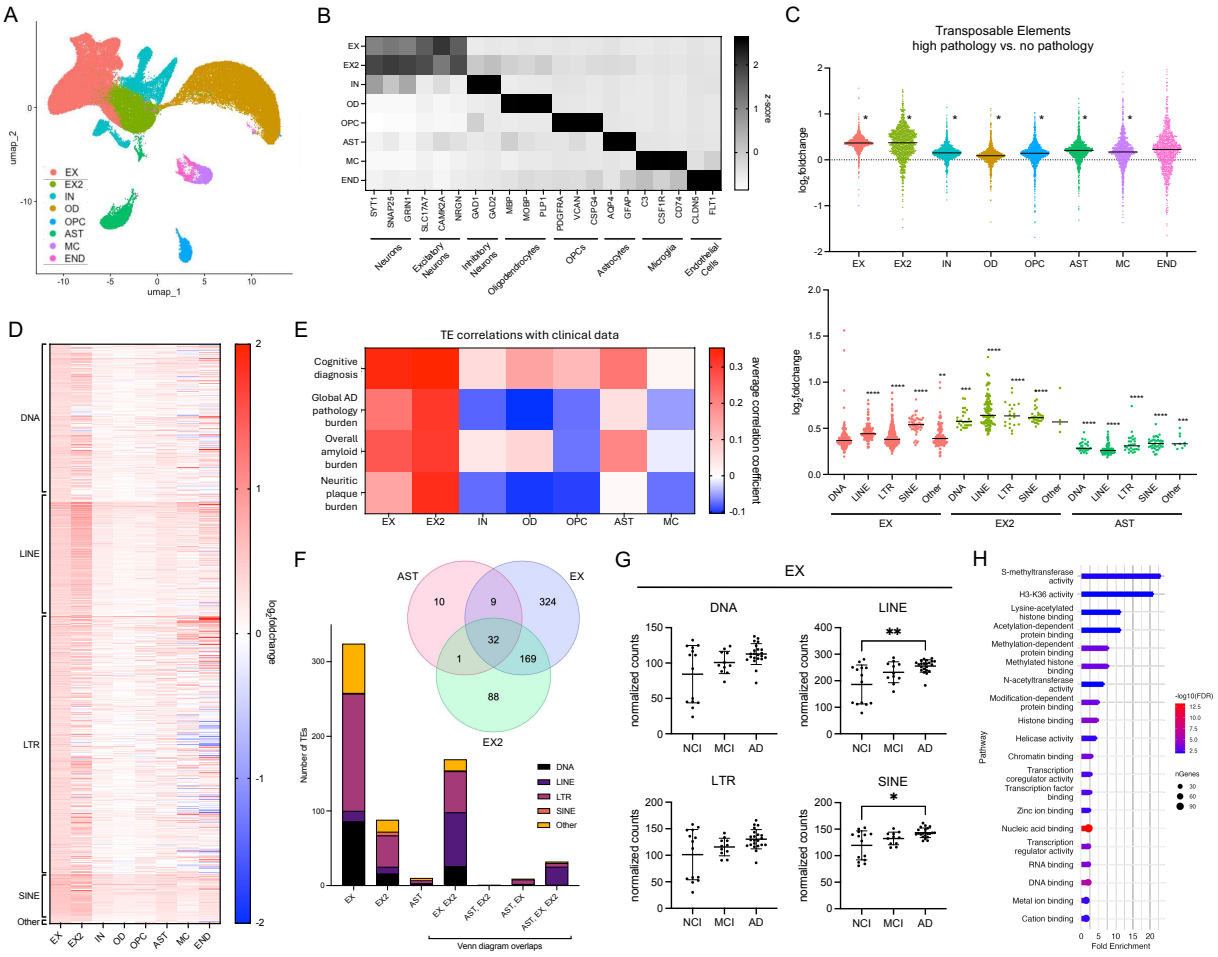


**Figure 5.1. TE transcripts increase in most cell types of the AD brain. (A)** UMAP projection of all annotated cells; EX = excitatory neurons, OD = oligodendrocytes, EX2 = excitatory neurons 2, AST = astrocytes, IN = inhibitory neurons, OPC = oligodendrocyte progenitor cell, MC = microglia, END = endothelial cells. **(B)** Relative (*z*-scored) expression of cell marker genes for each cell type identified [14]. **(C)** Cell type increases in median TE transcript expression (black bars; vs. median gene expression) in high pathology vs. no pathology subjects (top; **p* ≤ 0.0001; Mann-Whitney test) and by major TE type for EX, EX2, and AST clusters (bottom; ***p* ≤ 0.01, ****p* ≤ 0.001, *****p* ≤ 0.0001; Mann-Whitney test). **(D)** Heatmap showing $log_2$foldchanges of all significant TE transcripts (FDR < 0.1) by cell and TE type. **(E)** WGCNA showing TE transcript correlations with subject clinical data by cell type. **(F)** Venn diagram of TEs among those most associated with clinical data in AST, EX, and EX2 clusters, and (bar graph) the number of TEs by type in each Venn diagram overlap. **(G)** Total normalized counts of TEs by type in the EX cluster in non-cognitively impaired (NCI), mild cognitive impairment (MCI) and AD subjects. Data represented as means ± SD. **p* ≤ 0.05, ***p* ≤ 0.01; Kruskal-Wallis test. (**H**) Gene Ontology (GO) analysis of high pathology vs. no pathology differentially expressed genes within the EX cluster correlating with total TE transcript counts in all subjects.

*Increased chromatin accessibility in AD is associated with cell type-specific TE transcript increases*

Given our findings above and to address a potential mechanism underlying AD-related increases in TE transcripts among cell types, we re-analyzed a second AD snRNA-seq dataset and compared our TE transcript expression data to the authors' publicly available single nucleus assay for transposase-accessible chromatin sequencing (snATAC-seq) data on the same samples [15]. As previously reported by Morabito et al., this dataset is based on prefrontal cortex samples from 11 late-stage AD and 7 control subjects [15]. We analyzed 79,191 cells and identified cell types/clusters similar to those originally reported (**Figure 5.2A, Supplementary Table S3)** [15], and as above, we annotated clusters according to the same cell markers and with scType (**Figure 5.2B**) [14], and cross-checked our annotated barcodes with those in the original study [15]. Similarly to our analyses of the Mathys dataset above, although manual annotation and scType identified the IN2 cluster as inhibitory neurons (**Figure 5.2B**), its cell barcodes did not match annotated inhibitory neurons as originally reported [15], so for consistency we again kept this cluster separate from other neuronal subtypes.

In this second dataset, we again found a broad increase in TE transcripts in most cell types in AD vs. healthy controls, although this trend was absent in the IN2 cluster (**Figure 5.2C**). However, consistent with the idea that TEs are broadly/randomly dysregulated across the genome and among different subjects with AD (i.e., no specific individual TEs consistently increased more than others) [7, 11, 36], we did not observe increases in individual TE transcripts identical to those in the Mathys dataset (**Figure D.5**). Importantly though, when we examined TE occurrences in differentially accessible chromatin regions (DARs) in AD vs. controls and controlled for TE copy number (the number of times a TE appears throughout the genome), we found that TEs were generally enriched in 'more accessible' regions of chromatin (**Figure 5.2D**). This increase was most obvious in the EX, OD, and microglial cell (MC) clusters, and opposite in the IN cluster (**Figures 5.2D and D.6**). Moreover, on average, all major TE

types, except for SINEs, were both more transcriptionally accessible (accessibility ratio > 1) and increased in relative expression with AD (**Figure 5.2E**), although these two metrics were not strongly correlated, suggesting that post-transcriptional events (e.g., degradation) could influence TE transcript levels [37]. Despite this, we found that a highly significant number (>70%) of 'more accessible' TEs had a positive $log_2$foldchange in transcript levels in all cell types (**Figure 5.2F**), and this finding was consistent for all TE types in the EX cluster, except for SINEs (**Figure 5.2F**), and similar in other cell types (**Figure D.7**). Collectively, these data suggest the AD-related increase in TE transcripts in most cell types may be a result of changes in chromatin accessibility.

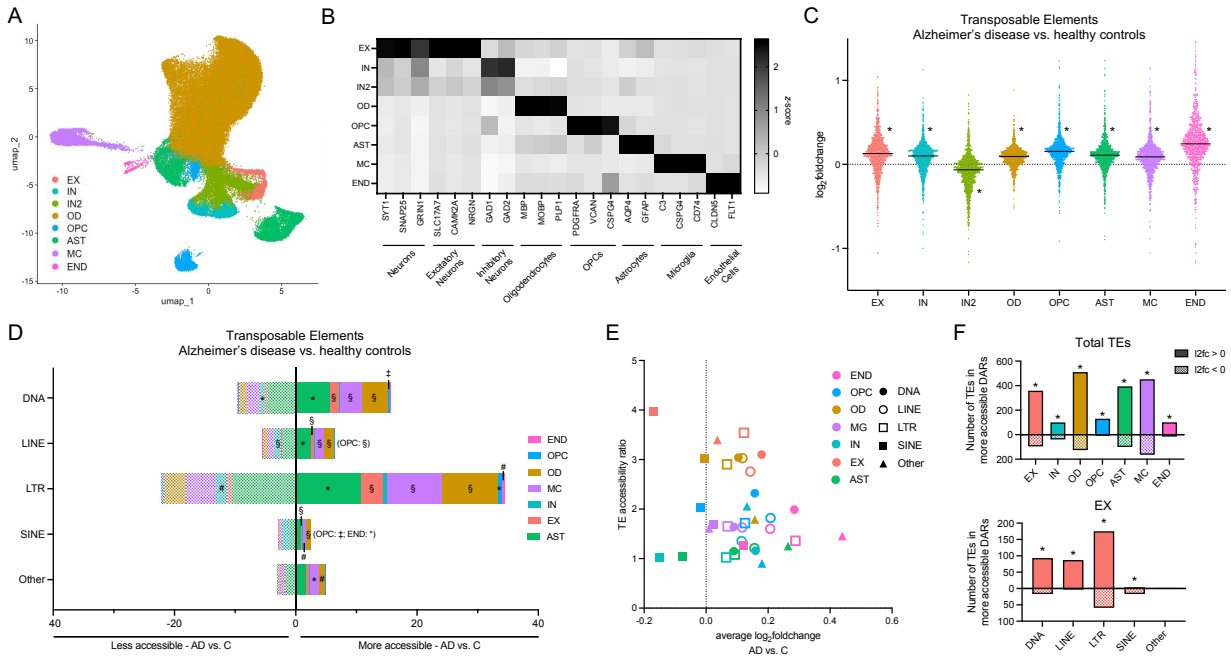


**Figure 5.2. AD-related TE transcript accumulation is associated with increased chromatin accessibility. (A)** UMAP projection of all annotated cells (as in Figure 1A, except IN2 = inhibitory neuron 2). **(B)** Relative (*z*-scored) expression of cell marker genes by cell type [14]. **(C)** Cell type increases in median TE transcript levels (black bars, vs. median gene expression) in AD patients vs. healthy controls (C, **p* ≤ 0.0001; Mann-Whitney test). **(D)** Number of TEs (normalized to copy number) within differentially accessible chromatin regions (DAR; AD vs. C) by major TE type for each cell type. *p < 0.05, #p < 0.01, ‡p < 0.001, §p < 0.0001; Mann-Whitney test. **(E)** TE accessibility ratio (average number of TEs in 'more accessible' regions [DAR $log_2$foldchange > 0, AD vs. C] to average number of TEs in 'less accessible' regions [DAR $log_2$foldchange < 0, AD vs. C]) compared to average transcript expression $log_2$foldchange by major TE type and cell type. **(F)** Total number of TEs in 'more accessible' chromatin regions (accessibility ratio > 1) and their relative transcript levels for all cell types, and the same analysis for EX TEs by major type. *p < 0.0001; Chi-square test.

*Commonly dysregulated TE transcripts by cell type*

To identify TE transcripts commonly increased with AD, we examined those that were most increased in relative expression for each cell type in both datasets. We identified 200-300 TE transcripts that were increased in both datasets within each cell type, and these overlaps were most significant in the AST, END, and OD clusters (**Figure 5.3A**). A majority of these shared TE transcripts, regardless of significance, were LTRs (**Figure 5.3A**), potentially consistent with the greater number of LTR subfamilies compared to other TEs [38] and/or the fact that LTRs may act as tissue-specific promoters, driving cell type differentiation [39]. However, there was no obvious pattern in increased TE transcripts across all cell types (again consistent with the idea of random/broad dysregulation of TEs in AD)—although four LINEs (HAL1, L1M4, L1M4b, L1ME1) were particularly enriched in all cell types from both datasets (**Figure 5.3B and D.8A**), and L1M4b counts correlated with AD pathology and cognitive diagnosis (**Figure D.8B-E**). This observation was interesting, because while most TEs do not have established biological functions, certain LINEs (the most commonly increased TE type in both datasets) have the ability to autonomously propagate throughout the genome [34], and the protein machinery they code for can be 'hijacked' by other, non-autonomous TEs [40, 41]. Many TE transcripts/types (mostly LTRs) appeared to be more cell type-specific (**Figure 5.3B and Supplementary Table S4**). Overall, these data are consistent with our finding that LINE transcripts may be particularly increased with AD pathology, but also with our and others' reports that TE dysregulation with AD may be 'generic' (i.e., affecting most/all TEs) and at least somewhat random [7, 9-11, 13, 42].

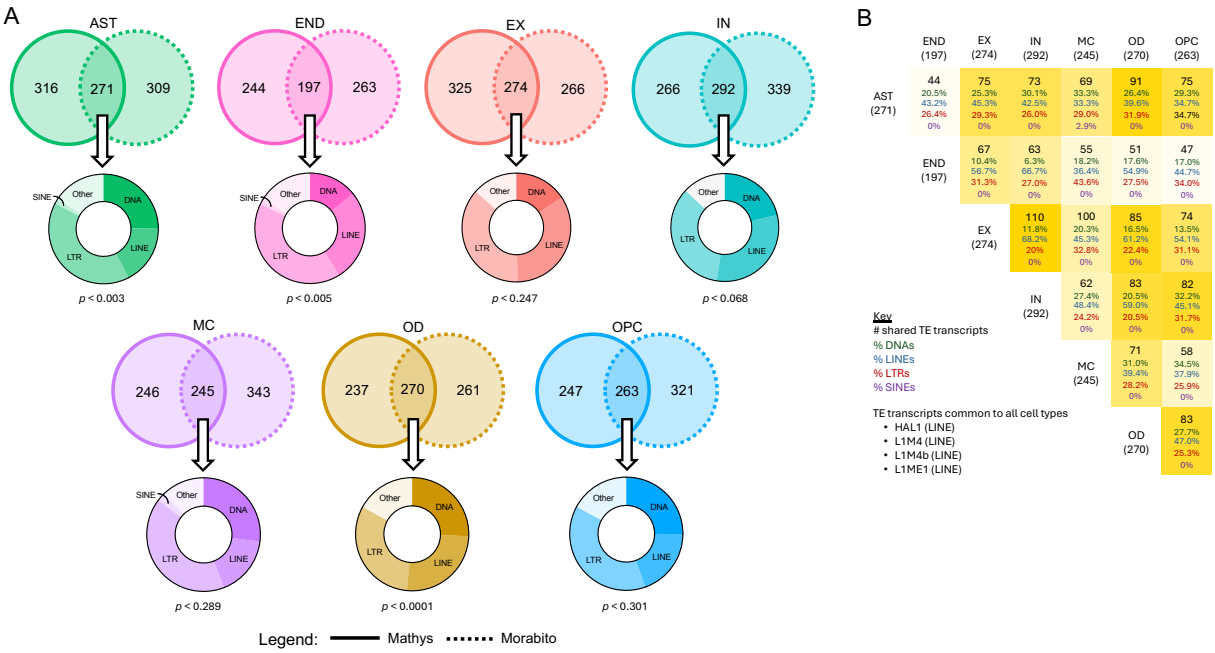


**Figure 5.3. TE transcripts commonly increased in each cell type. (A)** Overlaps of increased TE transcripts (>average TE $\log_2$foldchange) by cell type in both datasets, and TE transcripts by major type within each overlap. *p* values represent the significance of the hypergeometric overlap. **(B)** Venn diagram showing increased TEs shared among all cell types in both datasets.

*Neuron- and tau-related TE transcript increases with AD in bulk RNA-seq data*

To further confirm our snRNA-seq analyses, we examined TEs in bulk brain RNA-seq data from prefrontal cortex samples of 90 subjects from the ROSMAP study (30 AD patients, 30 MCI subjects, and 30 healthy controls [NCI], all age- and sex-matched). Differential expression analyses showed broad increases in overall TE transcript expression in AD and MCI subjects compared to healthy controls (**Figure 5.4A, Figure D.9A**), consistent with our findings above and what we and others have previously reported [9-11]. Additionally, we observed an increase in total TE transcripts in AD compared to MCI subjects (**Figure 5.4A**). To identify which cell types might be associated with these TE transcript patterns in this bulk sequencing dataset, we examined correlations among DEGs in AD subjects and total TE transcript counts in all subjects, then used significantly correlated DEGs for GO analysis (**Figure 5.4B**). This analysis resulted in GO cellular compartment terms relating to neuronal function (**Figure 5.4B**), despite the fact that glial/inflammatory signaling signatures were highly in increased DEGs

(Supplementary Table S5)—further suggesting that neurons are closely associated with TE transcript increases in AD. We also observed a similar trend in a fluorescence-activated cell sorted (FACS) bulk RNA-seq dataset on AD and healthy control brain tissue [17], wherein TE transcript expression was greater in neurons compared to glia and endothelial cells in AD (**Figure 5.4C, Figure D.9B**), and we found strong overlap in dysregulated/increased TE profiles among all of these datasets (**Figure D.10A**).

Finally, as suggested by our single-cell analyses of 'high-pathology' subjects in the Mathys dataset and also reported by others (although in model organisms and mice), pathological tau could contribute to TE transcript increases in neurons [9, 43]. To test this idea specifically in human/excitatory neurons, we analyzed changes in TE transcripts in an RNA-seq dataset on iPSC-derived excitatory neurons expressing 4R Tau (control) and 4R Tau with the P301S *MAPT* mutation (*MAPT*-neurons) [18]. While TE transcript levels were unchanged in *MAPT*-neurons (*MAPT* mutation vs. control), their expression was higher in cells stimulated with tau fibrils (*MAPT* mutation + tau fibrils vs. *MAPT* mutation) (**Figure 5.4D, Figure D.9C**). A similar effect was present in *MAPT*-neurons treated with tau compared to control cells *(MAPT* mutation + tau fibrils vs. control + tau fibrils) (**Figure 5.4D, Figure D.9C**). Lastly, we observed the largest increase in TE transcript expression in the *MAPT*-neurons with tau fibrils vs. unstimulated *MAPT*-neurons (**Figure 5.4D**), further suggesting a connection between tau/AD pathology and TE transcript expression in neurons. The overlaps in TE profiles among these datasets and our snRNA-seq and bulk RNA-seq analyses were less pronounced, perhaps because TE increases were more modest in these cells (**Figures D.10B and C**). However, together with our single-cell analyses, these bulk brain and cell RNA-seq analyses further point to neurons as key drivers of TE transcript increases with AD, and to tau/pathology as a potential mechanism underlying these events.

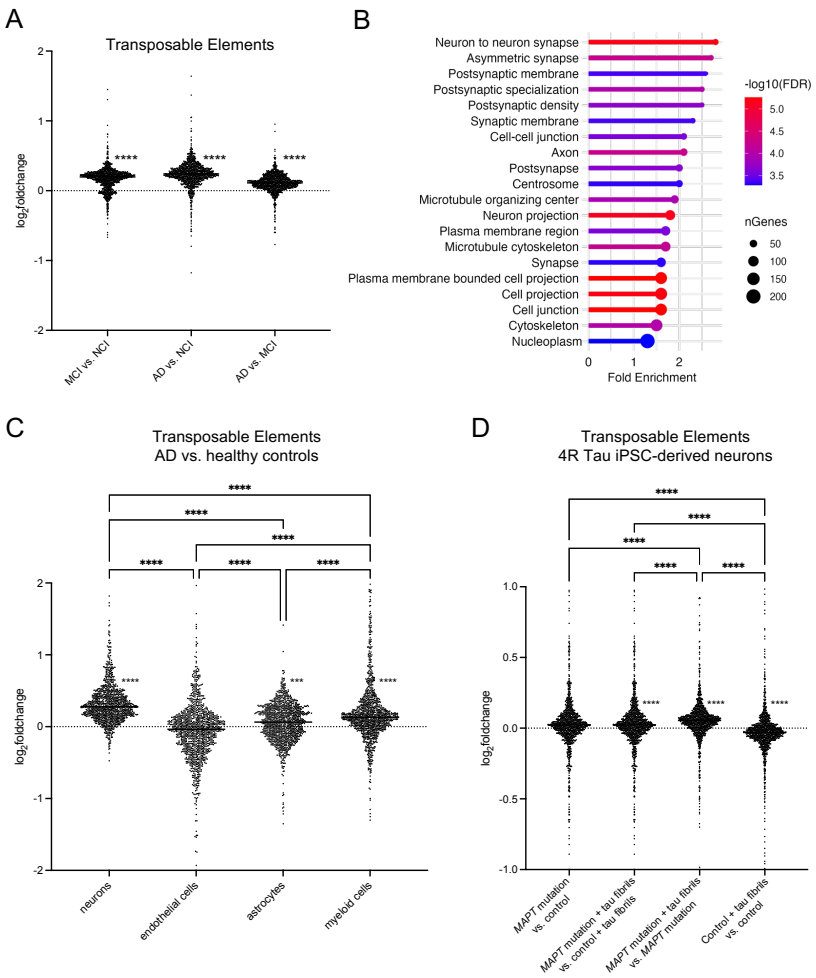


**Figure 5.4. TE transcript increases with AD in bulk RNA-seq data are neuron- and tau-related. (A)** Increases in median total TE transcript levels (vs. median gene expression) in MCI vs. NCI, AD vs. NCI, and AD vs. MCI (n = 30/group). ****$p \leq 0.0001$; Mann-Whitney test. Original data obtained by the ROSMAP consortium (Bennett et al. [16]). **(B)** Gene Ontology (GO) analysis of AD vs. NCI differentially expressed genes correlating with total TE transcript counts in all subjects. **(C)** Increases in TE transcripts (vs. median gene expression) in bulk RNA-seq data on FACS-isolated cells in AD vs. healthy controls. ***$p \leq 0.001$, ****$p \leq 0.0001$; Mann-Whitney test. Comparisons between median expression (AD vs. healthy controls) between cell types, #$p \leq 0.0001$ vs. astrocytes, ‡$p \leq 0.0001$ vs. endothelial cells, §$p \leq 0.0001$ vs. myeloid cells, Kruskal-Wallis test. Original data obtained by Srinivason et al. [17], **(D)** Increases in TE transcripts (vs. median gene expression) in 4R Tau iPSC-derived neurons with/without *MAPT* mutation and with/without tau fibrils. ***$p \leq 0.001$, ****$p \leq 0.0001$; Mann-Whitney test. #$p \leq 0.0001$ vs. (*MAPT* mutation vs. control), ‡$p \leq 0.0001$ vs. (*MAPT* mutation + tau fibrils vs. control + tau fibrils), Kruskal-Wallis test. Original data obtained by Parra Bravo et al. [18].

## DISCUSSION

Growing evidence implicates TEs in the pathogenesis of AD and other neurodegenerative diseases. However, it is unknown which cell types contribute most to TE transcript dysregulation in AD. Our key finding, using benchmark snRNA-seq datasets, is that TE transcripts are elevated in all cell types with AD, but that retrotransposons (e.g., LINEs) are the most increased TEs with AD pathology, specifically in excitatory neurons. We also show that these cell type patterns of increased TE transcript expression are associated with greater TE chromatin accessibility. Finally, we confirm our snRNA-seq findings by showing that AD-related increases in TE transcripts in bulk RNA-seq datasets track with neuronal gene expression signatures, and that tau accumulation in neurons could underlie these events, which is consistent with prior reports. These findings may be useful for others studying cellular contributions to AD, and they also are clinically relevant, as efforts to target TEs therapeutically have prompted related clinical trials (e.g., NCT04552795, NCT04500847) [44-47].

We and others have shown that TE transcripts (including active and potentially deleterious LINEs and LTRs) increase with AD and other neurodegenerative diseases [9-13, 48, 49], as well as in normal aging and age-related diseases in other tissues [7, 8, 42, 50, 51]. Other lines of evidence also implicate SINE/Alu TEs in neurodegeneration [52-55]. However, the brain is a heterogeneous mix of cells, all of which may play a role in AD [56], and studies to date have been based on bulk brain qPCR and/or RNA-seq data. Our single-cell analyses suggest that all cell types contribute to AD-related TE dysregulation, and that excitatory neurons may be key drivers in the increase of retrotransposon TE transcripts. We confirmed this finding by showing TE transcript expression is correlated with gene expression signatures related to neurons in bulk RNA-seq data, and in an AD FACS/bulk RNA-seq dataset, we also found that neurons had higher TE transcripts levels compared to other CNS cells. We were unable to distinguish between neuronal subtypes in these bulk datasets, and we note that FACS-isolated glia in this latter study were sorted using reactive markers such as GFAP and CD11b (which could reflect

reactive rather than homeostatic glial cell populations). However, on balance, our data suggest an important role for neurons in TE changes with AD. The exact reason for this finding is unclear, but neurons may be more susceptible than other cell types to AD-related increases in TE transcripts due to increased activity/expression of TEs during development and neuronal differentiation [57-60]. For example, TEs serve as binding sites for transcription factors specific to glutamatergic neuronal progenitors that aid in differentiation [61]. Also, in contrast to most other cell types in the brain, neurons are post-mitotic, so it is possible that they are unable to diffuse genomic damage/changes that accumulate with aging and AD. Multiple lines of evidence also indicate that neurons may inappropriately re-enter the cell cycle/de-differentiate in AD [62-64], which could partly explain our observations as well. Still, it remains unknown whether TE transcript increases occur in healthy adult neurons during aging more than other cell types, if these increases precede AD pathology, and/or if pathology exacerbates their expression. Future studies leveraging single-cell data on the human brain across the aging spectrum are needed to provide insight—but appropriately large datasets of this kind are currently lacking.

Importantly, genomic and epigenomic dysregulation are established mechanisms of age-related neurodegenerative diseases, including AD [65-68]. Significant epigenetic changes have been found in circulation and the brains of AD patients [69-74], and we and others have reported a link between epigenetic dysregulation and TE transcript expression in aging and age-related diseases [36, 75], supporting a potential mechanism for increased TE transcript expression. In this study, we found that upregulated DEGs that correlated to TE transcript expression were related to chromatin maintenance within excitatory neurons. We then used a second dataset with snATAC-seq data to show that transcriptionally enriched TEs in AD reside largely in chromatin-accessible regions of the genome. We did not observe this trend for SINEs, which often reside closer to or more frequently within genes than other TEs types [76], suggesting alternative mechanisms for their enrichment in AD, such as read-through transcription. We also found that more accessible TEs are present in excitatory neurons,

oligodendrocytes, and microglia compared to other cell types. TEs by nature are located throughout the genome, and we did not identify accessible TEs at specific genomic loci, although recent data suggest widespread dysregulation of TEs at specific sites that are associated with AD pathology and colocalize with AD risk loci [77]. Additionally, many processes contribute to genome accessibility (e.g., DNA methylation, histone modifications), and their potential role in our observations is unknown.

One possible mechanism connecting TE transcript expression and chromatin accessibility specifically involves pathological tau, a hallmark of AD that accumulates most in neurons [78]. For example, tau alters gene/TE expression in *Drosophila* AD models [79, 80], likely by changing the chromatin landscape, which results in increased TE transcript expression [12, 81]. Consistent with this idea, here we found that TE transcript levels were greatest in excitatory neurons from 'high-pathology' subjects, and that tau treatment of excitatory iPSC-derived neurons was associated with similar effects. Still, it is unclear if aging-related increases in TE transcripts precede tau pathology, and alternative explanations for our findings could include genomic damage accumulation from the absence of mitosis-associated chromatin reorganization and/or other related events in post-mitotic neurons [82], as noted above. To address these and other questions regarding epigenetics and TEs in the AD brain, future studies could utilize single-cell bisulfite (methylation) or targeted chromatin immunoprecipitation sequencing, perhaps alongside single-cell transcriptomics and/or even spatial transcriptomics (i.e., to determine if pathology and specific epigenetic differences co-localize).

Interestingly, our data show that TE transcripts are increased in all brain cell types with AD, yet it remains unknown which specific TEs are the most deleterious in this context. In both datasets we analyzed, we found broad TE increases in all cell types, consistent with the idea of random/genome-wide TE dysregulation, and this effect could contribute to AD via multiple processes. Indeed, LTRs and LINEs were most elevated with AD, and these TE types have been associated with several neurodegenerative diseases [13, 33]. TE transcripts in general

have also been associated with neuroinflammation [4, 5, 11, 12], likely due to their 'virus-like' DNA/RNA signatures, which can stimulate pro-inflammatory signaling pathways [6, 83]. Specifically, TE transcripts may form both double-stranded RNA and/or cDNA [8, 84], both of which can stimulate antiviral sensors like MDA5/PKR and cGAS-STING, respectively [85-88]. However, it is unknown if the activation of these anti-viral pathways and the TE transcripts that stimulate them are cell type-specific in the brain and with AD, and snRNA-seq datasets are not ideal for investigating these events involving largely cytosolic signaling pathways, as they are based on transcripts isolated from nuclei. Additionally, TE transcript propagation has been associated with DNA damage [4, 6, 8], and DNA damage is elevated in aged/AD neurons [89, 90], which can contribute to neurodegeneration [91, 92], although the specific subtypes of TEs and their role in neuronal DNA damage in AD has yet to be investigated. These remain open questions in research on TEs and neurodegeneration, and in this regard, an important consideration for future studies could be to integrate locus-specific TE analyses that might identify specific TEs or chromatin regions of interest.

Key limitations of our study are related to its secondary, retrospective analysis nature. For example, we observed differences in TE transcript expression patterns between snRNA-seq datasets, meaning we could not determine if specific TEs might be the most related to cell type expression differences. This could have been due to the nature of TE dysregulation, as noted above, or to differences in library preparation/sequencing and subject selection criteria between datasets (e.g., Mathys et al. selected subjects based on Aβ pathology, whereas Morabito et al. focused on clinical diagnosis). Cellular compositions also differed between datasets, with Mathys et al. originally reporting more neurons in their dataset and Morabito et al. reporting more oligodendrocytes [14, 15], and it is possible that sampling different subregions of the brain (e.g., within the prefrontal cortex) contributed to these disparities. Current efforts using regional scRNA-seq, spatial transcriptomics, or large multi-regional bulk RNA-seq studies in mice and humans have the potential to address such complex compositional and transcriptomic

differences across such regions of the brain [93-97], including in TE transcript expression. Finally, we chose to analyze the datasets in this study separately for reasons outlined above, but future analyses could leverage the growing number of snRNA-seq datasets on AD and use a meta-analysis approach in which multiple datasets are integrated. With greater numbers of cells per cluster, this approach could also allow for subcluster analyses (e.g., to identify specific excitatory neuron types with greater TE dysregulation), which we did not perform here. These may represent important research directions for understanding TE dynamics in AD with more detail.

*Conclusions*

Collectively, our data show a broad increase in TE transcripts across most cell types in the AD brain, with the greatest increases occurring in retrotransposons from excitatory neurons. TE transcripts are reported to increase in the AD brain in bulk RNA-seq analyses, but our data are the first to show the same trend in individual cell types linked to AD. We also show that TE transcript increases intersect with transcriptionally accessible regions of the genome in AD, which may be a mechanism underlying their increased expression. The precise connection between epigenetic regulation of TE transcripts and their expression on the single-cell level in AD remains to be determined, but our study may serve as a foundation for future work investigating TE transcripts in AD sc/snRNA-seq data.

REFERENCES


1. Jin, W., et al., *Comprehensive review on single-cell RNA sequencing: A new frontier in Alzheimer's disease research.* Ageing Res Rev, 2024. **100**: p. 102454.
2. Ding, Y., et al., *Single-Cell Sequencing Technology and Its Application in the Study of Central Nervous System Diseases.* Cell Biochem Biophys, 2024. **82**(2): p. 329-342.
3. Tam, O.H., L.W. Ostrow, and M. Gale Hammell, *Diseases of the nERVous system: retrotransposon activity in neurodegenerative disease.* Mob DNA, 2019. **10**: p. 32.
4. Saleh, A., A. Macia, and A.R. Muotri, *Transposable Elements, Inflammation, and Neurological Disease.* Front Neurol, 2019. **10**: p. 894.
5. Jönsson, M.E., et al., *Transposable Elements: A Common Feature of Neurodevelopmental and Neurodegenerative Disorders.* Trends Genet, 2020. **36**(8): p. 610-623.
6. Bourque, G., et al., *Ten things you should know about transposable elements.* Genome Biol, 2018. **19**(1): p. 199.
7. LaRocca, T.J., A.N. Cavalier, and D. Wahl, *Repetitive elements as a transcriptomic marker of aging: Evidence in multiple datasets and models.* Aging Cell, 2020. **19**(7): p. e13167.
8. Gorbunova, V., et al., *The role of retrotransposable elements in ageing and age-associated diseases.* Nature, 2021. **596**(7870): p. 43-53.
9. Guo, C., et al., *Tau Activates Transposable Elements in Alzheimer's Disease.* Cell Rep, 2018. **23**(10): p. 2874-2880.
10. Sun, W., et al., *Pathogenic tau-induced piRNA depletion promotes neuronal death through transposable element dysregulation in neurodegenerative tauopathies.* Nat Neurosci, 2018. **21**(8): p. 1038-1048.
11. Wahl, D., et al., *The reverse transcriptase inhibitor 3TC protects against age-related cognitive dysfunction.* Aging Cell, 2023. **22**(5): p. e13798.
12. Ochoa, E., et al., *Pathogenic tau-induced transposable element-derived dsRNA drives neuroinflammation.* Sci Adv, 2023. **9**(1): p. eabq5423.
13. Macciardi, F., et al., *A retrotransposon storm marks clinical phenoconversion to late-onset Alzheimer's disease.* Geroscience, 2022. **44**(3): p. 1525-1550.
14. Mathys, H., et al., *Single-cell transcriptomic analysis of Alzheimer's disease.* Nature, 2019. **570**(7761): p. 332-337.
15. Morabito, S., et al., *Single-nucleus chromatin accessibility and transcriptomic characterization of Alzheimer's disease.* Nat Genet, 2021. **53**(8): p. 1143-1155.
16. Bennett, D.A., et al., *Religious Orders Study and Rush Memory and Aging Project.* J Alzheimers Dis, 2018. **64**(s1): p. S161-s189.
17. Srinivasan, K., et al., *Alzheimer's Patient Microglia Exhibit Enhanced Aging and Unique Transcriptional Activation.* Cell Rep, 2020. **31**(13): p. 107843.
18. Parra Bravo, C., et al., *Human iPSC 4R tauopathy model uncovers modifiers of tau propagation.* Cell, 2024. **187**(10): p. 2446-2464.e22.
19. Rodríguez-Quiroz, R. and B. Valdebenito-Maturana, *SoloTE for improved analysis of transposable elements in single-cell RNA-Seq data using locus-specific expression.* Commun Biol, 2022. **5**(1): p. 1063.
20. Valdebenito-Maturana, B., *Transposable Elements are differentially activated in cell lineages during the developing murine submandibular gland.* bioRxiv, 2023: p. 2023.04.01.535217.
21. Kaminow, B., D. Yunusov, and A. Dobin, *STARsolo: accurate, fast and versatile mapping/quantification of single-cell and single-nucleus RNA-seq data.* bioRxiv, 2021: p. 2021.05.05.442755.

22. Hao, Y., et al., *Dictionary learning for integrative, multimodal and scalable single-cell analysis.* Nat Biotechnol, 2024. **42**(2): p. 293-304.
23. Satija, R., et al., *Spatial reconstruction of single-cell gene expression data.* Nat Biotechnol, 2015. **33**(5): p. 495-502.
24. Ianevski, A., A.K. Giri, and T. Aittokallio, *Fully-automated and ultra-fast cell-type identification using specific marker combinations from single-cell transcriptomic data.* Nat Commun, 2022. **13**(1): p. 1246.
25. Love, M.I., W. Huber, and S. Anders, *Moderated estimation of fold change and dispersion for RNA-seq data with DESeq2.* Genome Biol, 2014. **15**(12): p. 550.
26. Langfelder, P. and S. Horvath, *WGCNA: an R package for weighted correlation network analysis.* BMC Bioinformatics, 2008. **9**: p. 559.
27. Quinlan, A.R. and I.M. Hall, *BEDTools: a flexible suite of utilities for comparing genomic features.* Bioinformatics, 2010. **26**(6): p. 841-2.
28. Dobin, A., et al., *STAR: ultrafast universal RNA-seq aligner.* Bioinformatics, 2013. **29**(1): p. 15-21.
29. Jin, Y., et al., *TEtranscripts: a package for including transposable elements in differential expression analysis of RNA-seq datasets.* Bioinformatics, 2015. **31**(22): p. 3593-9.
30. Raudvere, U., et al., *g:Profiler: a web server for functional enrichment analysis and conversions of gene lists (2019 update).* Nucleic Acids Res, 2019. **47**(W1): p. W191-w198.
31. Beck, C.R., et al., *LINE-1 retrotransposition activity in human genomes.* Cell, 2010. **141**(7): p. 1159-70.
32. De Cecco, M., et al., *L1 drives IFN in senescent cells and promotes age-associated inflammation.* Nature, 2019. **566**(7742): p. 73-78.
33. Floreani, L., et al., *Analysis of LINE1 Retrotransposons in Huntington's Disease.* Front Cell Neurosci, 2021. **15**: p. 743797.
34. Thomas, C.A., A.C. Paquola, and A.R. Muotri, *LINE-1 retrotransposition in the nervous system.* Annu Rev Cell Dev Biol, 2012. **28**: p. 555-73.
35. Dhillon, P., et al., *Increased levels of endogenous retroviruses trigger fibroinflammation and play a role in kidney disease development.* Nat Commun, 2023. **14**(1): p. 559.
36. Smith, M.E., et al., *Repetitive element transcript accumulation is associated with inflammaging in humans.* Geroscience, 2024. **46**(6): p. 5663-5679.
37. Warkocki, Z., *An update on post-transcriptional regulation of retrotransposons.* FEBS Lett, 2023. **597**(3): p. 380-406.
38. Smit, A.F., *The origin of interspersed repeats in the human genome.* Curr Opin Genet Dev, 1996. **6**(6): p. 743-8.
39. Thompson, P.J., T.S. Macfarlan, and M.C. Lorincz, *Long Terminal Repeats: From Parasitic Elements to Building Blocks of the Transcriptional Regulatory Repertoire.* Mol Cell, 2016. **62**(5): p. 766-76.
40. Dewannieux, M., C. Esnault, and T. Heidmann, *LINE-mediated retrotransposition of marked Alu sequences.* Nat Genet, 2003. **35**(1): p. 41-8.
41. Wallace, N., et al., *LINE-1 ORF1 protein enhances Alu SINE retrotransposition.* Gene, 2008. **419**(1-2): p. 1-6.
42. De Cecco, M., et al., *Transposable elements become active and mobile in the genomes of aging mammalian somatic tissues.* Aging (Albany NY), 2013. **5**(12): p. 867-83.
43. Ramirez, P., et al., *Pathogenic tau accelerates aging-associated activation of transposable elements in the mouse central nervous system.* Prog Neurobiol, 2022. **208**: p. 102181.
44. Sullivan, A.C., et al., *A pilot study to investigate the safety and feasibility of antiretroviral therapy for Alzheimer's disease (ART-AD).* medRxiv, 2024.

45. De Francesco, D., et al., *Associations between plasma nucleoside reverse transcriptase inhibitors concentrations and cognitive function in people with HIV.* PLoS One, 2021. **16**(7): p. e0253861.
46. Obiabo, Y.O., O.A. Ogunrin, and A.S. Ogun, *Effects of highly active antiretroviral therapy on cognitive functions in severely immune-compromised HIV-seropositive patients.* J Neurol Sci, 2012. **313**(1-2): p. 115-22.
47. Simon, M., et al., *LINE1 Derepression in Aged Wild-Type and SIRT6-Deficient Mice Drives Inflammation.* Cell Metab, 2019. **29**(4): p. 871-885.e5.
48. Saldi, T.K., et al., *Neurodegeneration, Heterochromatin, and Double-Stranded RNA.* J Exp Neurosci, 2019. **13**: p. 1179069519830697.
49. Frost, B. and J. Dubnau, *The Role of Retrotransposons and Endogenous Retroviruses in Age-Dependent Neurodegenerative Disorders.* Annu Rev Neurosci, 2024. **47**(1): p. 123-143.
50. Andrenacci, D., V. Cavaliere, and G. Lattanzi, *The role of transposable elements activity in aging and their possible involvement in laminopathic diseases.* Ageing Res Rev, 2020. **57**: p. 100995.
51. Liu, X., et al., *Resurrection of endogenous retroviruses during aging reinforces senescence.* Cell, 2023. **186**(2): p. 287-304.e26.
52. Larsen, P.A., et al., *The Alu neurodegeneration hypothesis: A primate-specific mechanism for neuronal transcription noise, mitochondrial dysfunction, and manifestation of neurodegenerative disease.* Alzheimers Dement, 2017. **13**(7): p. 828-838.
53. Larsen, P.A., et al., *Warning SINEs: Alu elements, evolution of the human brain, and the spectrum of neurological disease.* Chromosome Res, 2018. **26**(1-2): p. 93-111.
54. Cheng, Y., et al., *Increased Alu RNA processing in Alzheimer brains is linked to gene expression changes.* EMBO Rep, 2021. **22**(5): p. e52255.
55. Polesskaya, O., et al., *The role of Alu-derived RNAs in Alzheimer's and other neurodegenerative conditions.* Med Hypotheses, 2018. **115**: p. 29-34.
56. Murdock, M.H. and L.H. Tsai, *Insights into Alzheimer's disease from single-cell genomic approaches.* Nat Neurosci, 2023. **26**(2): p. 181-195.
57. Garza, R., et al., *LINE-1 retrotransposons drive human neuronal transcriptome complexity and functional diversification.* Sci Adv, 2023. **9**(44): p. eadh9543.
58. Mustafin, R.N. and E.K. Khusnutdinova, *Involvement of transposable elements in neurogenesis.* Vavilovskii Zhurnal Genet Selektsii, 2020. **24**(2): p. 209-218.
59. Sasaki, T., et al., *Possible involvement of SINEs in mammalian-specific brain formation.* Proc Natl Acad Sci U S A, 2008. **105**(11): p. 4220-5.
60. Patoori, S., et al., *Young transposable elements rewired gene regulatory networks in human and chimpanzee hippocampal intermediate progenitors.* Development, 2022. **149**(19).
61. Sekine, K., M. Onoguchi, and M. Hamada, *Transposons contribute to the acquisition of cell type-specific cis-elements in the brain.* Commun Biol, 2023. **6**(1): p. 631.
62. Frost, B., *Alzheimer's disease and related tauopathies: disorders of disrupted neuronal identity.* Trends Neurosci, 2023. **46**(10): p. 797-813.
63. Seward, M.E., et al., *Amyloid-β signals through tau to drive ectopic neuronal cell cycle re-entry in Alzheimer's disease.* J Cell Sci, 2013. **126**(Pt 5): p. 1278-86.
64. Mertens, J., et al., *Age-dependent instability of mature neuronal fate in induced neurons from Alzheimer's patients.* Cell Stem Cell, 2021. **28**(9): p. 1533-1548.e6.
65. Gao, X., et al., *Epigenetics in Alzheimer's Disease.* Front Aging Neurosci, 2022. **14**: p. 911635.
66. Martinez-Feduchi, P., P. Jin, and B. Yao, *Epigenetic modifications of DNA and RNA in Alzheimer's disease.* Front Mol Neurosci, 2024. **17**: p. 1398026.

67. Nativio, R., et al., *An integrated multi-omics approach identifies epigenetic alterations associated with Alzheimer's disease.* Nat Genet, 2020. **52**(10): p. 1024-1035.
68. Frost, B., *Alzheimer's disease: An acquired neurodegenerative laminopathy.* Nucleus, 2016. **7**(3): p. 275-83.
69. Sun, Y., et al., *Identification of candidate DNA methylation biomarkers related to Alzheimer's disease risk by integrating genome and blood methylome data.* Transl Psychiatry, 2023. **13**(1): p. 387.
70. Smith, R.G., et al., *A meta-analysis of epigenome-wide association studies in Alzheimer's disease highlights novel differentially methylated loci across cortex.* Nat Commun, 2021. **12**(1): p. 3517.
71. Zhang, W., et al., *Distinct CSF biomarker-associated DNA methylation in Alzheimer's disease and cognitively normal subjects.* Alzheimers Res Ther, 2023. **15**(1): p. 78.
72. Santana, D.A., M.A.C. Smith, and E.S. Chen, *Histone Modifications in Alzheimer's Disease.* Genes (Basel), 2023. **14**(2).
73. Qin, Y., et al., *Novel histone post-translational modifications in Alzheimer's disease: current advances and implications.* Clin Epigenetics, 2024. **16**(1): p. 39.
74. Park, J., et al., *The role of histone modifications: from neurodevelopment to neurodiseases.* Signal Transduct Target Ther, 2022. **7**(1): p. 217.
75. Lindehell, H., Y.B. Schwartz, and J. Larsson, *Methylation of lysine 36 on histone H3 is required to control transposon activities in somatic cells.* Life Sci Alliance, 2023. **6**(8).
76. Zhang, X.O., H. Pratt, and Z. Weng, *Investigating the Potential Roles of SINEs in the Human Genome.* Annu Rev Genomics Hum Genet, 2021. **22**: p. 199-218.
77. Feng, Y., et al., *Widespread transposable element dysregulation in human aging brains with Alzheimer's disease.* Alzheimers Dement, 2024.
78. Iqbal, K., et al., *Tau pathology in Alzheimer disease and other tauopathies.* Biochim Biophys Acta, 2005. **1739**(2-3): p. 198-210.
79. Mangleburg, C.G., et al., *Integrated analysis of the aging brain transcriptome and proteome in tauopathy.* Mol Neurodegener, 2020. **15**(1): p. 56.
80. Wu, T., et al., *Tau polarizes an aging transcriptional signature to excitatory neurons and glia.* Elife, 2023. **12**.
81. Frost, B., et al., *Tau promotes neurodegeneration through global chromatin relaxation.* Nat Neurosci, 2014. **17**(3): p. 357-66.
82. Ramos-Alonso, L., et al., *Mitotic chromosome condensation resets chromatin to safeguard transcriptional homeostasis during interphase.* Proc Natl Acad Sci U S A, 2023. **120**(4): p. e2210593120.
83. Hayward, A. and C. Gilbert, *Transposable elements.* Curr Biol, 2022. **32**(17): p. R904-r909.
84. Sadeq, S., et al., *Endogenous Double-Stranded RNA.* Noncoding RNA, 2021. **7**(1).
85. Chen, Y.G. and S. Hur, *Cellular origins of dsRNA, their recognition and consequences.* Nat Rev Mol Cell Biol, 2022. **23**(4): p. 286-301.
86. Lemaire, P.A., et al., *Mechanism of PKR Activation by dsRNA.* J Mol Biol, 2008. **381**(2): p. 351-60.
87. Ou, L., et al., *The cGAS-STING Pathway: A Promising Immunotherapy Target.* Front Immunol, 2021. **12**: p. 795048.
88. Rehwinkel, J. and M.U. Gack, *RIG-I-like receptors: their regulation and roles in RNA sensing.* Nat Rev Immunol, 2020. **20**(9): p. 537-551.
89. Asada-Utsugi, M. and M. Urushitani, *Tau beyond Tangles: DNA Damage Response and Cytoskeletal Protein Crosstalk on Neurodegeneration.* Int J Mol Sci, 2024. **25**(14).
90. Chen, J., et al., *DNA damage and cell cycle events implicate cerebellar dentate nucleus neurons as targets of Alzheimer's disease.* Mol Neurodegener, 2010. **5**: p. 60.

91. Konopka, A. and J.D. Atkin, *The Role of DNA Damage in Neural Plasticity in Physiology and Neurodegeneration.* Front Cell Neurosci, 2022. **16**: p. 836885.
92. Stavgiannoudaki, I., E. Goulielmaki, and G.A. Garinis, *Broken strands, broken minds: Exploring the nexus of DNA damage and neurodegeneration.* DNA Repair (Amst), 2024. **140**: p. 103699.
93. Mathys, H., et al., *Single-cell multiregion dissection of Alzheimer's disease.* Nature, 2024. **632**(8026): p. 858-868.
94. Li, X.W., et al., *SCAD-Brain: a public database of single cell RNA-seq data in human and mouse brains with Alzheimer's disease.* Front Aging Neurosci, 2023. **15**: p. 1157792.
95. Yao, Z., et al., *A high-resolution transcriptomic and spatial atlas of cell types in the whole mouse brain.* bioRxiv, 2023.
96. Patel, H., R.J.B. Dobson, and S.J. Newhouse, *A Meta-Analysis of Alzheimer's Disease Brain Transcriptomic Data.* J Alzheimers Dis, 2019. **68**(4): p. 1635-1656.
97. Sun, N., et al., *Single-nucleus multiregion transcriptomic analysis of brain vasculature in Alzheimer's disease.* Nat Neurosci, 2023. **26**(6): p. 970-982.

# CHAPTER 6 – ADAR1 vs. CHROMATIN ACCESSIBILITY: WHICH DRIVES TRANSPOSABLE ELEMENT TRANSCRIPT ACCUMULATION IN AGING AND AD?

## INTRODUCTION

This dissertation explores transposable element (TE) transcript accumulation as a potential mechanism of neuroinflammation with aging and Alzheimer's disease (AD), and the findings suggest that the up- and/or downstream dysregulation of TE transcripts may underlie their accumulation and negative consequences. Specifically, I identified ADAR1 as a key regulator of TE-derived double-stranded RNA (dsRNA) and the subsequent inflammatory response. Additionally, I demonstrated that TE transcript accumulation (likely driven by changes in chromatin accessibility) occurs across all cell types in the AD brain, with a potential greatest effect in excitatory neurons. However, it is unclear which mechanism (reduced ADAR1 vs. increased chromatin accessibility) drives most of the changes in TE transcript accumulation with aging and AD. Together, my findings suggest two key questions for future investigation:

1. Are there pharmacological or nutraceutical compounds that may activate ADAR1 to prevent age- and AD-related TE transcript accumulation and neuroinflammation?
2. Do age-related changes in TE transcript expression and accessibility occur in all cell types, and are these changes in any one cell type key to the development of AD?

I would hypothesize that existing compounds may increase ADAR1 activity to reduce dsRNA accumulation and mitigate neuroinflammation in aging and AD. Additionally, I would hypothesize that TE transcripts are increased across all cell types with aging due to changes in ADAR1 expression and/or chromatin accessibility. Lastly, I would hypothesize that these age-related changes in TE transcripts precede AD, and this may be largely driven by excitatory neurons. In addition to the above, it is possible that my hypotheses could occur in tandem and synergistically contribute to inflammation. Based on what I observed in my dissertation data, I might suggest future studies to address these questions through the following aims:

**Aim 1: Identify activators of ADAR1 activity that reduce TE transcript accumulation and neuroinflammation with aging and AD.** I would a) perform a high-throughput screen (HTS) using an *in vitro,* cell-free model to identify pharmacological and/or nutraceutical compounds that activate ADAR1 by measuring reductions in accumulating dsRNA. To determine the effects of the compounds identified in Aim 1a on age- and AD-related TE transcript accumulation and neuroinflammation, the ADAR1 activator would be tested in the following: b) reprogrammed astrocytes and neurons (iAstrocytes [iAs] and iNeurons [iNs], respectively) from young, old, and AD human fibroblasts; and c) young and old C57BL/6 mice. It is possible that changes in chromatin accessibility drive TE transcript accumulation in these models of aging and AD. To test this, I would d) generate chromatin profiling sequencing data (ATAC-seq) on the young, old, and AD iAs/iNs and prefrontal cortex from young and old mice that were treated/untreated with the ADAR1 activator.

**Aim 2: Determine if age-associated changes in TE transcript accumulation and accessibility precede AD in all cell types of the brain.** I would: a) generate single-nucleus RNA sequencing (snRNA-seq) and single-nucleus assay for transposase accessible chromatin sequencing (snATAC-seq) data from young, old, and AD prefrontal cortex samples; b) analyze and compare cell type-specific changes in TE transcript accumulation as a result of aging and AD; and c) determine if changes in TE accessibility by cell type drive TE transcript accumulation by intersecting accessible chromatin regions with locus-specific TE expression with aging and/or AD or d) if changes in TE transcript accumulation may be associated with cell type-specific changes in *ADAR1* expression with aging and/or AD.

GENERAL APPROACH

To determine whether reduced ADAR1 activity or increased chromatin accessibility drive TE transcript accumulation in aging and AD, I have developed two independent, yet complementary aims. In Aim 1, I would conduct a HTS of ~900 CNS-penetrant compounds (including some FDA-approved drugs) to identify potential ADAR1 activators. Using a fluorescence-based dsRNA assay, I would assess reductions in accumulating dsRNA in a cell-free *in vitro* model. ADAR1-activating compounds would then be tested in iAs and iNs reprogrammed from young, old, and AD human dermal fibroblasts to evaluate the effects of the ADAR1 activator on ADAR1 activity, dsRNA accumulation, and neuroinflammation. In parallel, the identified compound would also be administered to young and old mice to determine its impact on cognitive function and the same molecular outcomes (as above) in the brain. Additionally, I would generate and analyze ATAC-seq data from these models to examine whether chromatin accessibility contributes to TE-derived dsRNA accumulation and if these RNAs are regulated by ADAR1. In Aim 2, I would generate and analyze single-nucleus sequencing data (snRNA-seq and snATAC-seq) from NIH NeuroBioBank prefrontal cortex samples of healthy younger and older adults as well as AD patients to investigate cell type-specific changes in chromatin accessibility and TE transcript accumulation with aging and AD, and to identify if these age-related changes precede AD. Additionally, I would assess if TE transcript accumulation and/or accessibility correlates with *ADAR1* expression in all or specific cell types with aging and/or AD. Together, these aims would provide critical insight into the upstream and downstream regulation of TE transcripts in aging and AD.

AIM 1: IDENTIFY ACTIVATORS OF ADAR1 ACTIVITY THAT REDUCE TE TRANSCRIPT ACCUMULATION AND NEUROINFLAMAMTION WITH AGING AND AD.

*Rationale*

Knockout and suppression studies, both *in vitro* and *in vivo,* have proven ADAR1 to be an integral protein involved in the regulation of dsRNA-related inflammation [1-9], associated with neuroinflammatory activation [10-14], and it may even regulate TE-derived dsRNAs [15, 16]. My data suggest that ADAR1 expression declines with aging/AD, coinciding with an increase in TE transcripts that may form dsRNA, a potential pro-inflammatory stimulus (Chapter 2) [17]. Given that neuroinflammation is a key component of aging and AD [18-20], compounds that increase ADAR1 activity could be promising therapeutics for mitigating neuroinflammation in aging and AD. Preliminary data I generated based on secondary analyses of RNA-seq data on mouse liver overexpressing full length (FL) ADAR1 show modest reductions in TE transcript expression, but this effect was greater in mice overexpressing the ADAR1 p110 isoform (**Figure 6.1A, B**). The p110 isoform localizes to the nucleus [21], and this may suggest that ADAR1 regulates TE transcript expression before these transcripts enter the cytoplasm, where they can bind innate immune sensors. Additionally, most A-to-I editing (ADAR1 function that regulates endogenous dsRNAs) of TE transcripts occurs within SINEs (**Figure 6.1C**), aligning with my findings and those of others (Chapter 2) [15, 17]. Together, these data suggest that enhancing ADAR1 activity could reduce the accumulation of endogenous, TE-derived dsRNAs, and may prevent pro-inflammatory activation with aging and/or AD. Therefore, as described below, I would propose to identify ADAR1 activators that could be used to reduce neuroinflammation in these contexts.

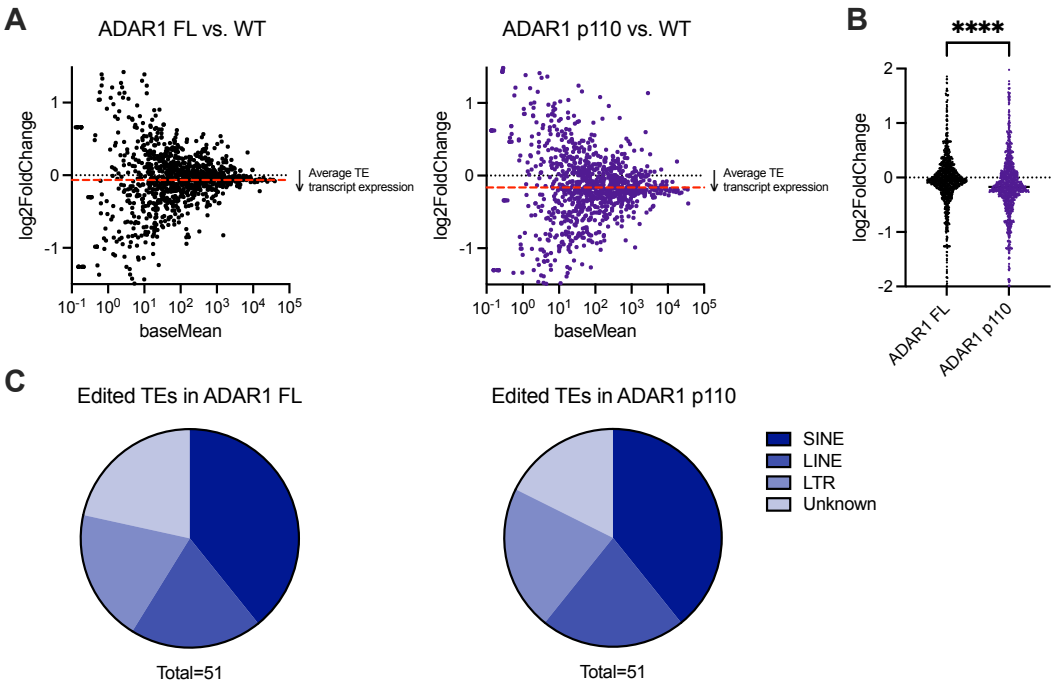


**Figure 6.1. Overexpression of ADAR1 reduces TE transcript expression and increases A-to-I editing of TE transcripts.** (A) MA plot showing reduced total TE transcript expression in mouse liver overexpressing the FL (black) and p110 isoform (purple) of ADAR1 compared to wild type. Red dashed line indicates shift in average TE transcript log2FoldChange relative to wild type. (B) The reduction in average TE transcript expression is greater with p110 isoform overexpression compared to FL ADAR1. ****$p \leq 0.0001$; Mann-Whitney test. (C) TE transcripts by type showing increased A-to-I editing when ADAR1 is overexpressed (FL and p110 isoform) in mouse liver. Original data obtained by Mendez Ruiz et al. [22].

*Experimental design and analyses*

To identify activators of ADAR1, I would perform a HTS in an *in vitro,* cell-free model to assess ADAR1-mediated regulation of dsRNA. Briefly, a synthetic dsRNA (designed with a string of adenosines flanked by a 5' uracil and 3' guanine, as preferred by ADAR1 [23]) would be incubated with purified recombinant ADAR1 protein. A-to-I editing of the synthetic dsRNA would be confirmed using Sanger sequencing [24], and the presence of dsRNA (an indirect measurement of ADAR1 activity) would be detected by a fluorescence-based dsRNA detection kit (Revvity, 64RNAPEG). This kit employs a dual-antibody fluorescence resonance energy transfer (FRET) system that emits fluorescence (665 nm) when both antibodies bind dsRNA, and the signal intensity is proportional to dsRNA levels. This *in vitro* model would be screened

against the CNS-Penetrant Compound Library (MedChemExpress, HY-L028), which includes over 900 bioactive compounds, some FDA-approved, with demonstrated preclinical and clinical research. The levels of dsRNA (fluorescence) would be measured at 24 h, 48 h, and 72 h post-treatment to identify potential ADAR1 activators. Following HTS, the most promising ADAR1 activator would be tested in iAs and iNs derived from young, old, and AD biobanked human dermal fibroblasts (CNS cell models that retain aging and disease-related characteristics [25, 26]). Treated cells would be compared to untreated age- and disease-matched controls. In these cells, I would generate RNA-seq data to analyze A-to-I editing (using SPRINT [27]) and changes in TE transcript expression (using TEtranscripts [28]), following methods described in Chapter 2 and prior studies [17, 29]. Additionally, I would quantify markers of astrocyte- and neuron-related neuroinflammation (e.g., ICAM-1, GFAP, C3, S100β, NfL), the dsRNA response pathway (e.g., MDA5, RIG-I, MAVS, IRF3, NFκB), and pro-inflammatory cytokines (e.g., IL-6, TNF-α, IFN-β, IL-1β) through immunoblotting and ELISAs. To evaluate the *in vivo* efficacy of the ADAR1 activator, I would perform a pilot study in young (8 mo) and old (19 mo) mice. Given that the screened compounds are CNS-penetrant, the compound would be administered via intraperitoneal (IP) injection, intravenous injection, or delivered orally, depending on prior evidence. Four weeks post treatment, I would measure cognitive function using the novel object recognition test, which I and others in our lab have conducted [30-32]. In this test, cognitive function is quantified as recognition index (the time mice spend with a new object relative to the total exploration time of the new object and a familiar object). After cognitive function testing, mice would be euthanized using a combination of isoflurane, cardiac puncture/blood collection, and decapitation. Cortical tissue, an area of the brain critical for learning/memory and declines with aging, would be collected to: 1) generate RNA-seq data to analyze A-to-I editing activity and TE transcript expression as above; 2) quantify dsRNA using the fluorescence-based assay; and, 3) measure cell-type specific markers of neuroinflammation and the dsRNA signaling pathway (as described above and including microglial-specific markers like IBA1 and CD68).

Additionally, I would assess neuroinflammatory cytokines (e.g., IL-6, TNF-α, IL-1β, IFN$\gamma$, IL-12, IL-18) and dsRNA-related type I interferons (e.g., IFN-α, IFN-β) in circulation using ELISAs. Finally, in addition to altered ADAR1 activity, age- and AD-related chromatin remodeling may also drive TE transcript dysregulation. To investigate this, I would generate and analyze bulk ATAC-seq data on the iAs, iNs, and cortical tissue using Bowtie2/MACS2 [33-35] and integrate TE loci to identify transcriptionally accessible TEs and determine if transcripts from these accessible TEs are modulated by ADAR1 activity.

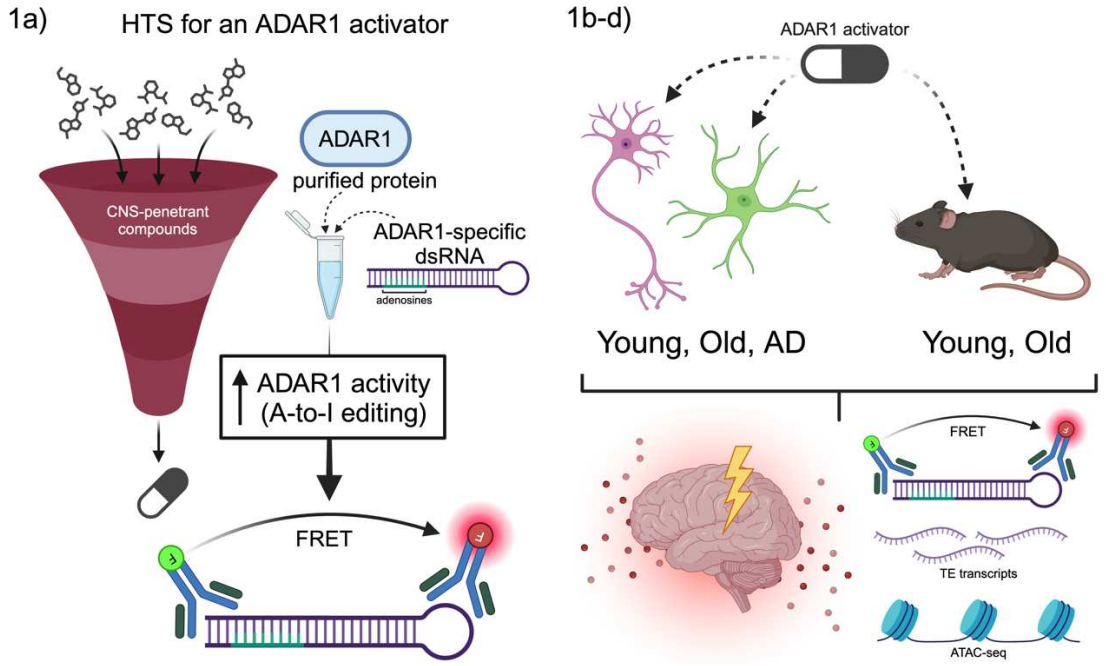


**Figure 6.2. Diagram of Aim 1.** In Aim 1a, a HTS using an *in vitro,* cell-free model would identify ADAR1 activators from a library of CNS-penetrant compounds. The selected compound is expected to enhance ADAR1 activity (A-to-I editing), leading to a reduction in dsRNA accumulation (quantified by a reduction in dsRNA-antibody FRET assay). The compound would be tested in cell models of aging/AD and old mice to determine its effects on markers of neuroinflammation and accumulating dsRNA. Lastly, chromatin accessibility would be analyzed in these models to determine its role as an upstream mechanism of TE transcript accumulation and assess whether increased ADAR1 activity can mitigate the pro-inflammatory response.

*Expected results and interpretation*

I would anticipate identifying at least one compound that increases ADAR1 activity, as indicated by a reduction in accumulating dsRNA in the *in vitro,* cell-free model. In aged and AD-derived iAs and iNs, I would expect treatment with the ADAR1 activator to reduce dsRNA

accumulation (by increasing A-to-I editing), decrease TE transcript accumulation, and attenuate pro-inflammatory signaling. Similarly, I would expect that the ADAR1 activator would produce the same effects in old mice, in addition to reducing neuroinflammatory markers in the brain and circulation while mitigating cognitive decline. Lastly, I would expect to observe age- and AD-related differences in chromatin accessibility in the iAs, iNs, and aged mouse cortex; however, I do not anticipate that the ADAR1 activator would directly alter chromatin accessibility. Rather, despite these increases in chromatin accessibility with aging and AD, the ADAR1 activator would be expected to reduce the amount of dsRNA coming from these accessible regions and the associated inflammatory response in all models.

*Potential problems and alternative strategies*

It is possible that the fluorescence-based dsRNA assay may not accurately detect changes in dsRNA accumulation in the screening model. If this occurs, alternative dsRNA detection methods, such as dsRNA ELISAs or custom single molecule FRET with fluorescently labeled nucleotides in the synthetic dsRNA, can be explored. Additionally, if the CNS-penetrant compound library does not contain an effective ADAR1 activator, other libraries with a broader range of compounds from MedChemExpress (e.g., Bioactive Compound Library, FDA-Approved Drug Library) can be explored. A custom library containing compounds related to dsRNA binding and regulation and/or programs aimed at identifying molecules that may interact with ADAR1 domains (e.g., dsRNA binding domains) could also be considered. If there are challenges treating the iAs/iNs with the ADAR1 activator (e.g., toxicity to reprogrammed cells), similar experiments can be conducted in fibroblasts (cells that iAs/iNs are reprogrammed from), as these cells also retain aging and AD features [36, 37]. If the ADAR1 activator does not effectively cross the blood brain barrier in aged mice, the compound could be administered directly into the brain via stereotaxic injection. It is possible that the ADAR1 activator may have off-target effects, and to determine if this is true, the compound could be tested in ADAR1-

knockout cells. Furthermore, if the ADAR1 activator reduces dsRNA levels but not specifically TE transcripts, alternative sources of endogenous dsRNA (e.g., mitochondrial-derived dsRNA) can be investigated using the RNA-seq data. Lastly, I do not anticipate issues generating or analyzing the RNA-seq or ATAC-seq data, as our lab has extensive experience with these techniques.

## AIM 2: DETERMINE IF AGE-ASSOCIATED CHANGES IN TE TRANSCRIPT ACCUMULATION AND ACCESSIBILITY PRECEDE AD IN ALL CELL TYPES OF THE BRAIN

*Rationale*

Our lab and others have shown that TE transcripts are elevated with aging and AD in bulk RNA-seq and NanoString data [30, 38-43]. My data suggest that AD-related increases in TE transcripts occur in all brain cell types, with the most pronounced effects in excitatory neurons, and these increases may be driven by changes in chromatin accessibility (Chapter 5) [44]. Consistent with my data, other studies have reported links between chromatin accessibility and TE transcript expression in bulk RNA-seq and targeted TE analyses [42, 45-48]. However, in my data, I was unable to determine if aging-related changes in TE transcripts may precede the increases of these transcripts seen in AD, and if AD may further exacerbate the accumulation of TE transcripts with aging. Given that age is the greatest risk factor for AD and increases in TE transcripts with normal aging precede AD [38, 49], this distinction is crucial. Additionally, I was unable to directly compare changes in chromatin accessibility with TE transcript expression at specific loci across all cell types in the AD brain, and it remains unknown whether specific TE loci play a critical role in brain aging. The retrospective nature of my analyses (which relied on existing, publicly available snRNA-seq and snATAC-seq datasets) limited the scope of questions that could be addressed. Still, these data suggest that it is possible that aging-related changes of TE transcripts in one or multiple brain cell types increase prior to AD—possibly excitatory neurons—before the onset of AD and that these changes may

result from dysregulated control of these transcripts, such as changing chromatin accessibility. Even if TE transcript dysregulation occurs broadly across cell types, it remains unclear whether one specific cell type plays a predominant role in triggering the initial pro-inflammatory response associated with aging, thereby increasing the risk for AD. Therefore, I would propose to examine TE transcript expression across all brain cell types with aging and AD and identify whether specific TE loci are linked with changes in chromatin accessibility across all brain cell types in the aging and AD brain.

*Experimental design and analyses*

To investigate whether age-related changes in TE transcript expression and accessibility occur across all brain cell types and precede AD, I would generate snRNA-seq and snATAC-seq data from NIH NeuroBioBank prefrontal cortex samples of younger (~40 years old), older (~85 years old), and AD (old age-matched) human subjects (n=5M/5F per group, **Supplemental Table C.1**). To ensure simultaneous analysis of TE transcript expression and chromatin accessibility from the same nuclei, I would follow the 10x Chromium Next GEM Single Cell Multiome ATAC + Gene Expression protocol (10x Genomics, CG000338), as described by Guyer et al. [49]. Briefly, nuclei would be isolated from a cortical tissue sample, and a transposase would bind to open chromatin regions. The nuclei would then be barcoded and partitioned on a Chromium Next GEM Chip J before constructing snRNA and snATAC libraries that are sequenced on an Illumina platform with paired-end sequencing. For data analysis, TE transcript expression (focusing on specific loci) would be analyzed using STARsolo [50], soloTE [51], Seurat [52, 53], and DESeq2 [54], as in Chapter 5 [55]. Chromatin accessibility and peak calling would be analyzed using Signac in addition to the above programs [52]. TE transcripts that are both accessible and elevated with aging—and remain accessible and elevated in AD—may indicate aging-associated TE transcripts that precede AD. However, chromatin accessibility may not be the only mechanism regulating TE transcript accumulation. To assess whether

differences in *ADAR1* expression contribute to. Next, I would integrate the snRNA and snATAC datasets using Seurat to determine whether changes to the chromatin landscape are driving locus-specific TE transcript accumulation across all cell types with aging and AD [53]. TE transcripts that are both accessible and elevated with aging–-and remain accessible and elevated in AD–-may indicate aging-associated TE transcripts that precede AD. However, chromatin accessibility may not be the only mechanism regulating TE transcript accumulation. To assess whether differences in *ADAR1* expression contribute to TE transcript changes in aging and AD, I would examine correlations between *ADAR1* counts and total TE transcript counts. Additionally, I would run a principal component analysis to determine if these changes are specifically associated with aging and/or AD.

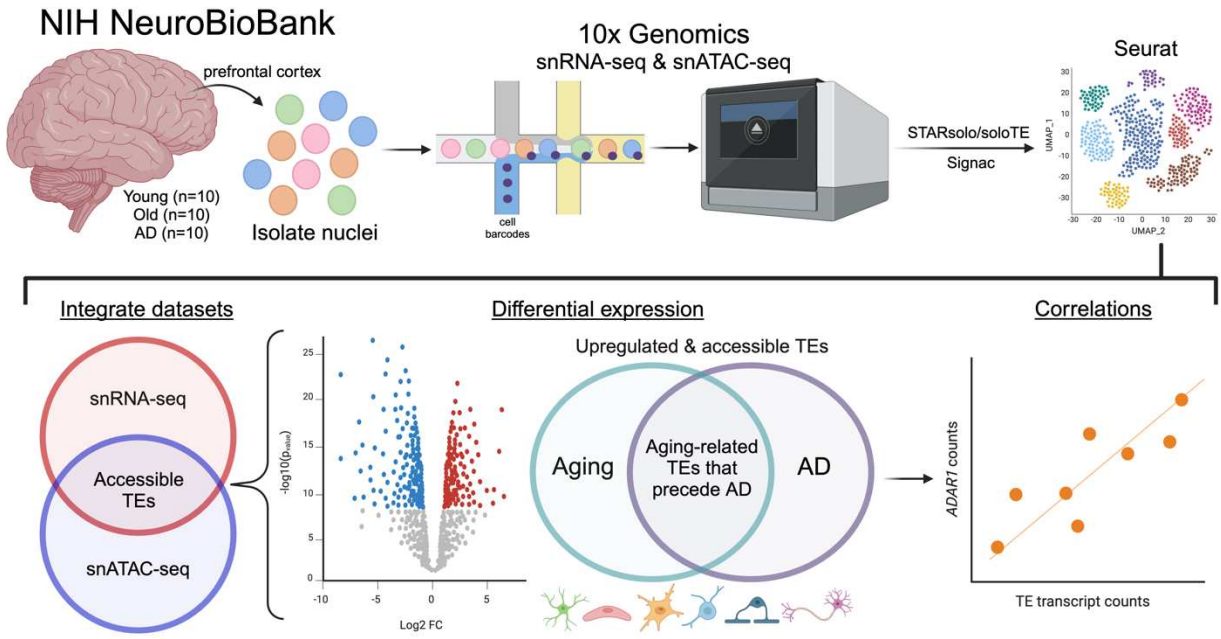


**Figure 6.3. Diagram of Aim 2.** Nuclei would be isolated from the prefrontal cortex of young, old, and AD subjects from the NIH NeuroBioBank, followed by the generation of snRNA-seq/snATAC-seq libraries. These datasets would be integrated to identify TE transcripts with increased expression and chromatin accessibility in aging and AD. Lastly, *ADAR1* expression and TE transcripts would be examined to investigate potential downstream mechanisms of TE transcript regulation.

*Expected results and interpretation*

I would anticipate that locus-specific TE transcripts elevated in aging and AD will be located in chromatin-accessible regions of the brain across all cell types. However, this effect is likely more pronounced in excitatory neurons, consistent with my previous findings (Chapter 5) [44], in both aging and AD. Additionally, I would expect a substantial overlap between TE transcripts that are unregulated and accessible in aging and those exhibiting the same pattern in AD across all cell types. Lastly, I would predict that *ADAR1* expression correlates with TE transcript accumulation and/or accessibility in both aging and AD, with a potentially stronger correlation in neurons, given that A-to-I editing is more prevalent in neurons than other cell types [56].

*Potential problems and alternative strategies*

It is possible that generating snRNA-seq and snATAC-seq libraries from the same nuclei could result in low sequencing depth. If this occurs, an alternative approach would be to prepare libraries from separate subsections of the prefrontal cortex samples for each sequencing method, though this would mean sequencing different nuclei between snRNA-seq and snATAC-seq. I do not anticipate any challenges in aligning and processing the snRNA-seq data, as I have experience analyzing such datasets (Chapter 5) [44]. However, processing snATAC-seq data, particularly for TEs, may be more complex. Currently, soloTE has not been applied to analyze TEs in snATAC-seq data, and if this proves ineffective, an alternative approach would be to intersect processed snATAC-seq data with the human RepeatMasker (TE annotation file) to assess TE accessibility, as I have previously done (Chapter 5) [44]. Additionally, it is possible that TE transcripts that are upregulated and accessible with aging do not exhibit the same pattern in AD. If so, this would support the idea that changes in TE transcripts with AD are disease-specific rather than an exacerbation of aging. Finally, if *ADAR1* expression does not

correlate with total TE transcript levels, this would suggest that ADAR1 may not be a key downstream mechanism of TE transcript regulation.

## FUTURE DIRECTIONS

If successful, these experiments will generate valuable insights into the mechanisms driving TE transcript accumulation (ADAR1 vs. chromatin accessibility). Specifically, these studies will identify potential novel activators of ADAR1 activity that could mitigate neuroinflammation and cognitive decline associated with aging and/or AD, while also determining whether cell-type-specific changes in TE accessibility and expression with aging precede AD. If my hypotheses are correct, future studies could investigate the effects of the ADAR1 activator in AD transgenic models (e.g., rTg4510 and/or hTau mice) or other preclinical models (e.g., canine cognitive decline). Additionally, aging-associated accessible TE transcripts that precede AD could be examined in other tissues to assess whether changes in these transcripts are brain specific.

REFERENCES


1. Eisenberg, E. and E.Y. Levanon, *A-to-I RNA editing - immune protector and transcriptome diversifier.* Nat Rev Genet, 2018. **19**(8): p. 473-490.
2. George, C.X., et al., *Editing of Cellular Self-RNAs by Adenosine Deaminase ADAR1 Suppresses Innate Immune Stress Responses.* J Biol Chem, 2016. **291**(12): p. 6158-68.
3. Liddicoat, B.J., et al., *RNA editing by ADAR1 prevents MDA5 sensing of endogenous dsRNA as nonself.* Science, 2015. **349**(6252): p. 1115-20.
4. Hu, S.B., et al., *ADAR1p150 prevents MDA5 and PKR activation via distinct mechanisms to avert fatal autoinflammation.* Mol Cell, 2023. **83**(21): p. 3869-3884.e7.
5. Rehwinkel, J. and P. Mehdipour, *ADAR1: from basic mechanisms to inhibitors.* Trends Cell Biol, 2025. **35**(1): p. 59-73.
6. Rice, G.I., et al., *Mutations in ADAR1 cause Aicardi-Goutières syndrome associated with a type I interferon signature.* Nat Genet, 2012. **44**(11): p. 1243-8.
7. Yang, S., et al., *Adenosine deaminase acting on RNA 1 limits RIG-I RNA detection and suppresses IFN production responding to viral and endogenous RNAs.* J Immunol, 2014. **193**(7): p. 3436-45.
8. Wang, H., et al., *ADAR1 Suppresses the Activation of Cytosolic RNA-Sensing Signaling Pathways to Protect the Liver from Ischemia/Reperfusion Injury.* Sci Rep, 2016. **6**: p. 20248.
9. Pujantell, M., et al., *RNA editing by ADAR1 regulates innate and antiviral immune functions in primary macrophages.* Sci Rep, 2017. **7**(1): p. 13339.
10. Deng, P., et al., *Adar RNA editing-dependent and -independent effects are required for brain and innate immune functions in Drosophila.* Nat Commun, 2020. **11**(1): p. 1580.
11. Guo, X., et al., *An AGS-associated mutation in ADAR1 catalytic domain results in early-onset and MDA5-dependent encephalopathy with IFN pathway activation in the brain.* J Neuroinflammation, 2022. **19**(1): p. 285.
12. Kim, J.I., et al., *RNA editing at a limited number of sites is sufficient to prevent MDA5 activation in the mouse brain.* PLoS Genet, 2021. **17**(5): p. e1009516.
13. Inoue, M., et al., *An Aicardi-Goutières Syndrome-Causative Point Mutation in Adar1 Gene Invokes Multiorgan Inflammation and Late-Onset Encephalopathy in Mice.* J Immunol, 2021. **207**(12): p. 3016-3027.
14. Guo, X., et al., *Aicardi-Goutières syndrome-associated mutation at ADAR1 gene locus activates innate immune response in mouse brain.* J Neuroinflammation, 2021. **18**(1): p. 169.
15. Ahmad, S., et al., *Breaching Self-Tolerance to Alu Duplex RNA Underlies MDA5-Mediated Inflammation.* Cell, 2018. **172**(4): p. 797-810.e13.
16. Orecchini, E., et al., *ADAR1 restricts LINE-1 retrotransposition.* Nucleic Acids Res, 2017. **45**(1): p. 155-168.
17. McEntee, C.M., A.N. Cavalier, and T.J. LaRocca, *ADAR1 suppression causes interferon signaling and transposable element transcript accumulation in human astrocytes.* Front Mol Neurosci, 2023. **16**: p. 1263369.
18. Heneka, M.T., et al., *Neuroinflammation in Alzheimer's disease.* Lancet Neurol, 2015. **14**(4): p. 388-405.
19. DiSabato, D.J., N. Quan, and J.P. Godbout, *Neuroinflammation: the devil is in the details.* J Neurochem, 2016. **139 Suppl 2**(Suppl 2): p. 136-153.
20. Andronie-Cioara, F.L., et al., *Molecular Mechanisms of Neuroinflammation in Aging and Alzheimer's Disease Progression.* Int J Mol Sci, 2023. **24**(3).
21. Savva, Y.A., L.E. Rieder, and R.A. Reenan, *The ADAR protein family.* Genome Biol, 2012. **13**(12): p. 252.

22. Mendez Ruiz, S., et al., *Over-expression of ADAR1 in mice does not initiate or accelerate cancer formation in vivo.* NAR Cancer, 2023. **5**(2): p. zcad023.
23. Eggington, J.M., T. Greene, and B.L. Bass, *Predicting sites of ADAR editing in double-stranded RNA.* Nat Commun, 2011. **2**: p. 319.
24. Fishman, A. and A.T. Lamm, *Obstacles in quantifying A-to-I RNA editing by Sanger sequencing.* Methods Enzymol, 2025. **710**: p. 285-302.
25. Gatto, N., et al., *Directly converted astrocytes retain the ageing features of the donor fibroblasts and elucidate the astrocytic contribution to human CNS health and disease.* Aging Cell, 2021. **20**(1): p. e13281.
26. Mertens, J., et al., *Age-dependent instability of mature neuronal fate in induced neurons from Alzheimer's patients.* Cell Stem Cell, 2021. **28**(9): p. 1533-1548.e6.
27. Zhang, F., et al., *SPRINT: an SNP-free toolkit for identifying RNA editing sites.* Bioinformatics, 2017. **33**(22): p. 3538-3548.
28. Jin, Y., et al., *TEtranscripts: a package for including transposable elements in differential expression analysis of RNA-seq datasets.* Bioinformatics, 2015. **31**(22): p. 3593-9.
29. LaRocca, T.J., et al., *TDP-43 knockdown causes innate immune activation via protein kinase R in astrocytes.* Neurobiol Dis, 2019. **132**: p. 104514.
30. Wahl, D., et al., *The reverse transcriptase inhibitor 3TC protects against age-related cognitive dysfunction.* Aging Cell, 2023. **22**(5): p. e13798.
31. Cavalier, A.N., et al., *Accelerated aging of the brain transcriptome by the common chemotherapeutic doxorubicin.* Exp Gerontol, 2021. **152**: p. 111451.
32. Brunt, V.E., et al., *The gut microbiome-derived metabolite trimethylamine N-oxide modulates neuroinflammation and cognitive function with aging.* Geroscience, 2021. **43**(1): p. 377-394.
33. Yan, F., et al., *From reads to insight: a hitchhiker's guide to ATAC-seq data analysis.* Genome Biol, 2020. **21**(1): p. 22.
34. Zhang, Y., et al., *Model-based analysis of ChIP-Seq (MACS).* Genome Biol, 2008. **9**(9): p. R137.
35. Langmead, B. and S.L. Salzberg, *Fast gapped-read alignment with Bowtie 2.* Nat Methods, 2012. **9**(4): p. 357-9.
36. Olesen, M.A., F. Villavicencio-Tejo, and R.A. Quintanilla, *The use of fibroblasts as a valuable strategy for studying mitochondrial impairment in neurological disorders.* Transl Neurodegener, 2022. **11**(1): p. 36.
37. Iannuzzi, F., et al., *Might Fibroblasts from Patients with Alzheimer's Disease Reflect the Brain Pathology? A Focus on the Increased Phosphorylation of Amyloid Precursor Protein Tyr(682) Residue.* Brain Sci, 2021. **11**(1).
38. LaRocca, T.J., A.N. Cavalier, and D. Wahl, *Repetitive elements as a transcriptomic marker of aging: Evidence in multiple datasets and models.* Aging Cell, 2020. **19**(7): p. e13167.
39. Gorbunova, V., et al., *The role of retrotransposable elements in ageing and age-associated diseases.* Nature, 2021. **596**(7870): p. 43-53.
40. Macciardi, F., et al., *A retrotransposon storm marks clinical phenoconversion to late-onset Alzheimer's disease.* Geroscience, 2022. **44**(3): p. 1525-1550.
41. Feng, Y., et al., *Widespread transposable element dysregulation in human aging brains with Alzheimer's disease.* Alzheimers Dement, 2024. **20**(11): p. 7495-7517.
42. Ochoa, E., et al., *Pathogenic tau-induced transposable element-derived dsRNA drives neuroinflammation.* Sci Adv, 2023. **9**(1): p. eabq5423.
43. Guo, C., et al., *Tau Activates Transposable Elements in Alzheimer's Disease.* Cell Rep, 2018. **23**(10): p. 2874-2880.
44. McEntee, C.M. and T.J. LaRocca, *Single-Cell Transcriptome Patterns of Transposable Elements in Alzheimer's Disease.* Mol Neurobiol, 2025.

45. Rivera, L., et al., *Integrative Single-Cell Analysis Reveals the Regulation of Transposable Elements in HSPCs during the Aging Process.* Blood, 2024. **144**(Supplement 1): p. 5647-5647.
46. Sun, W., et al., *Pathogenic tau-induced piRNA depletion promotes neuronal death through transposable element dysregulation in neurodegenerative tauopathies.* Nat Neurosci, 2018. **21**(8): p. 1038-1048.
47. Pal, S. and J.K. Tyler, *Epigenetics and aging.* Sci Adv, 2016. **2**(7): p. e1600584.
48. Martinez, J.C., et al., *cGAS deficient mice display premature aging associated with de-repression of LINE1 elements and inflammation.* bioRxiv, 2024.
49. Wyss-Coray, T., *Ageing, neurodegeneration and brain rejuvenation.* Nature, 2016. **539**(7628): p. 180-186.
50. Guyer, R.A., et al., *Simultaneous single-nucleus RNA sequencing and single-nucleus ATAC sequencing of neuroblastoma cell lines.* Sci Data, 2024. **11**(1): p. 1203.
51. Kaminow, B., D. Yunusov, and A. Dobin, *STARsolo: accurate, fast and versatile mapping/quantification of single-cell and single-nucleus RNA-seq data.* bioRxiv, 2021: p. 2021.05.05.442755.
52. Rodríguez-Quiroz, R. and B. Valdebenito-Maturana, *SoloTE for improved analysis of transposable elements in single-cell RNA-Seq data using locus-specific expression.* Commun Biol, 2022. **5**(1): p. 1063.
53. Hao, Y., et al., *Dictionary learning for integrative, multimodal and scalable single-cell analysis.* Nat Biotechnol, 2024. **42**(2): p. 293-304.
54. Satija, R., et al., *Spatial reconstruction of single-cell gene expression data.* Nat Biotechnol, 2015. **33**(5): p. 495-502.
55. Love, M.I., W. Huber, and S. Anders, *Moderated estimation of fold change and dispersion for RNA-seq data with DESeq2.* Genome Biol, 2014. **15**(12): p. 550.
56. Stuart, T., et al., *Single-cell chromatin state analysis with Signac.* Nat Methods, 2021. **18**(11): p. 1333-1341.

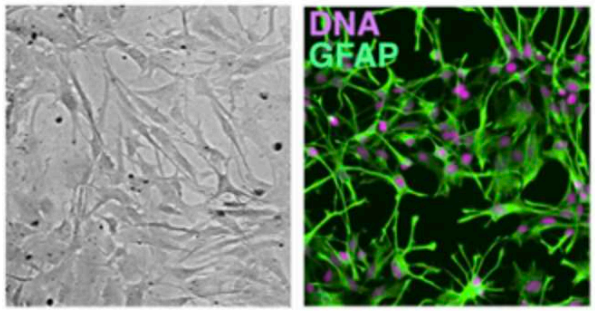


**Figure A.1. Representative image of commercially obtained primary astrocytes used for all experiments.** Left: Phase contrast image of typical astrocyte morphology in the current experiments. Right: positive staining for glial fibrillary acidic protein (GFAP, example courtesy ScienCell).

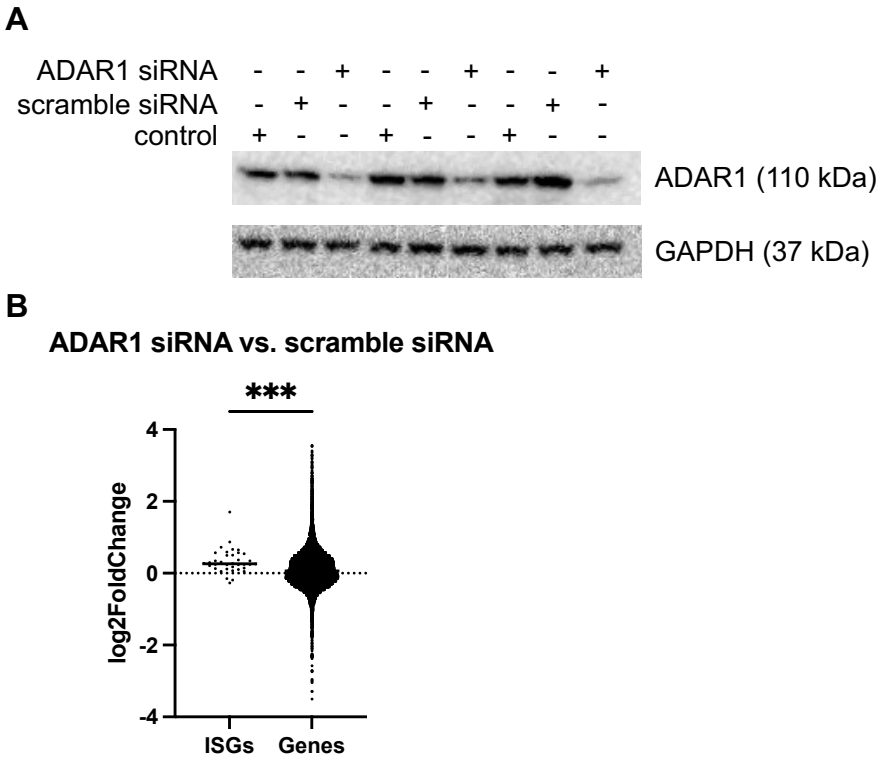


**Figure A.2. ADAR1 knockdown increases interferon stimulated gene expression. (A)** Immunoblots for ADAR1 in control, scramble siRNA, and ADAR1 siRNA transfected cells. **(B)** Increase in average interferon stimulated gene expression with ADAR1 knockdown (mean log2FoldChange vs. that of all other genes). ***p ≤ 0.001, Mann-Whitney test.

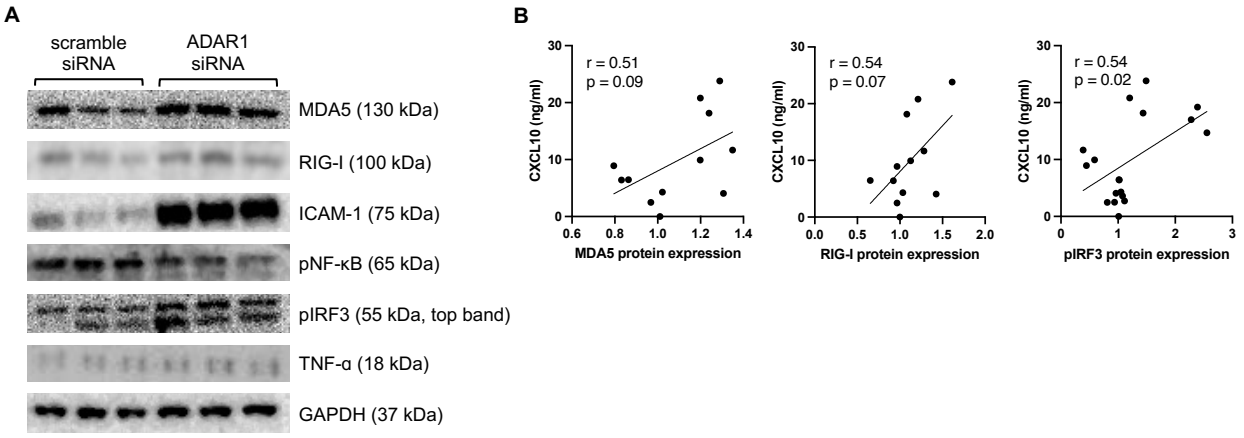


**Figure A.3. Immunoblots showing increases/decreases in proteins following ADAR1 knockdown and correlations among MDA5, RIG-I, pIRF3 protein expression and CXCL10.** **(A)** Immunoblots of dsRNA sensors and pro-inflammatory astrocyte markers after ADAR1 knockdown. **(B)** Correlations between MDA5, RIG-I, and pIRF3 protein expression and CXCL10 concentration. p-values and r values calculated using a simple linear regression.

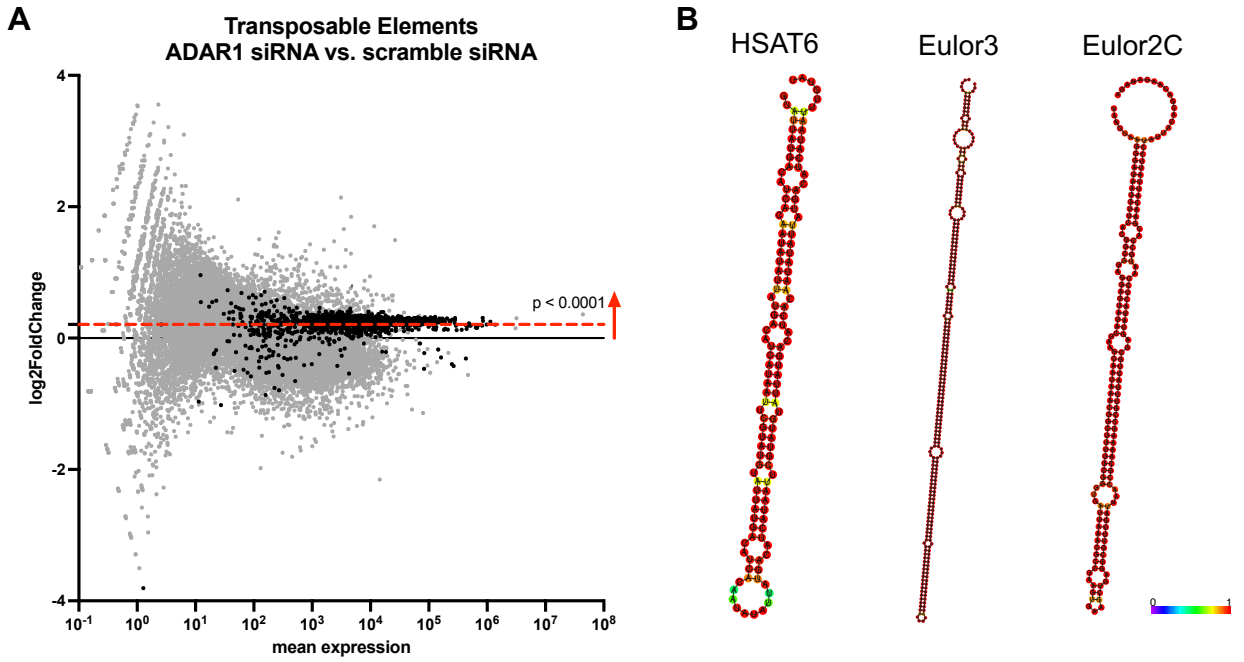


**Figure A.4. Increase in TE transcripts that form intra-stranded dsRNA following ADAR1 knockdown.** **(A)** MA plot showing general increase in TE transcript expression with ADAR1 knockdown. Genes shown in grey, TE transcripts shown in black. Red dashed line indicates shift in average TE transcript log2FoldChange. $p < 0.0001$, Chi-squared test. **(B)** Potential RNA secondary structures of highly increased TE transcripts with ADAR1 knockdown. Red base pairs indicate high base-pairing probabilities.

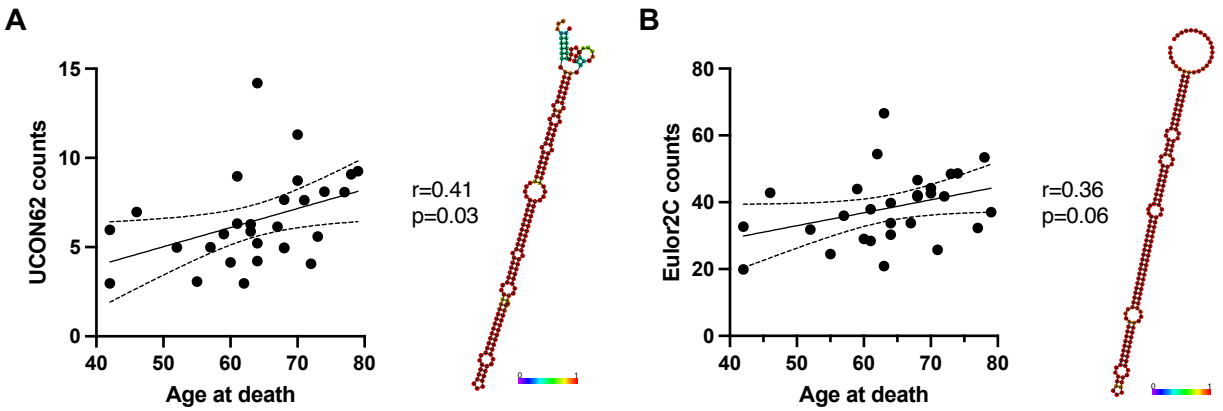


**Figure A.5. Correlations between age and dsRNA-prone TE transcripts that were highly increased with ADAR1 knockdown. (A)** Positive correlation between UCON62 counts vs. age at death, and potential RNA secondary structure of UCON62. **(B)** Positive correlation between Eulor2C counts vs. age at death, and potential RNA secondary structure of Eulor2C. *p*-values and *r*-values calculated using simple linear regression. RNA-seq data derived from Nativio et al., 2020.

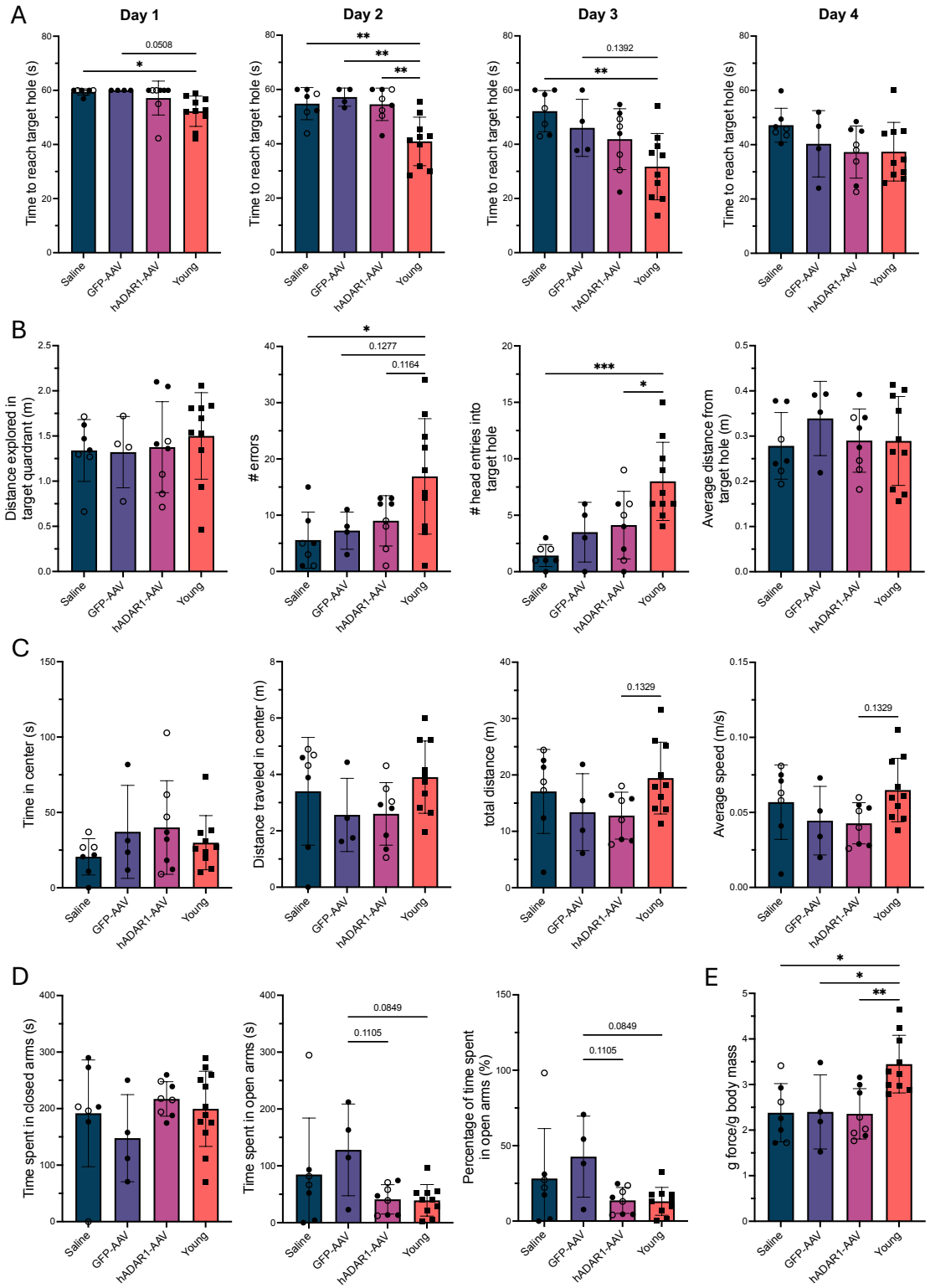
A
Day 1
Day 2
Day 3
Day 4
Time to reach target hole (s)
0.0508
*
**
0.1392
B
Distance explored in target quardrant (m)
# errors
0.1277
0.1164
# head entries into target hole
***
Average distance from target hole (m)
C
Time in center (s)
Distance traveled in center (m)
total distance (m)
0.1329
Average speed (m/s)
D
Time spent in closed arms (s)
Time spent in open arms (s)
0.0849
0.1105
Percentage of time spent in open arms (%)
E
g force/g body mass
Saline
GFP-AAV
hADAR1-AAV
Young

**Figure B.1. Cognitive and physiological function data in old mice treated with the hADAR1 and GFP AAVs. (A)** Time to reach target hole by day in the Barnes maze test. **(B)** Distance and head entry data during the Barnes maze probe trial from left to right: distance traveled, number of errors made (head entries to wrong holes), number of head entries into the target hole, and average distance from target hole. **(C)** Open field data from left to right: time spent in center, distance traveled in center, total distance travelled, and average speed. **(D)** Elevated plus maze data from left to right: time spent in closed arms, time spent in open arms, and percentage of total time spent in open arms. **(E)** Grip strength relative to body mass. *$p \leq 0.05$, **$p \leq 0.01$, ***$p \leq 0.001$; One-way ANOVA with multiple testing. Open circles = cohort 1; closed circles = cohort 2; closed squares = cohort 3 (only young).

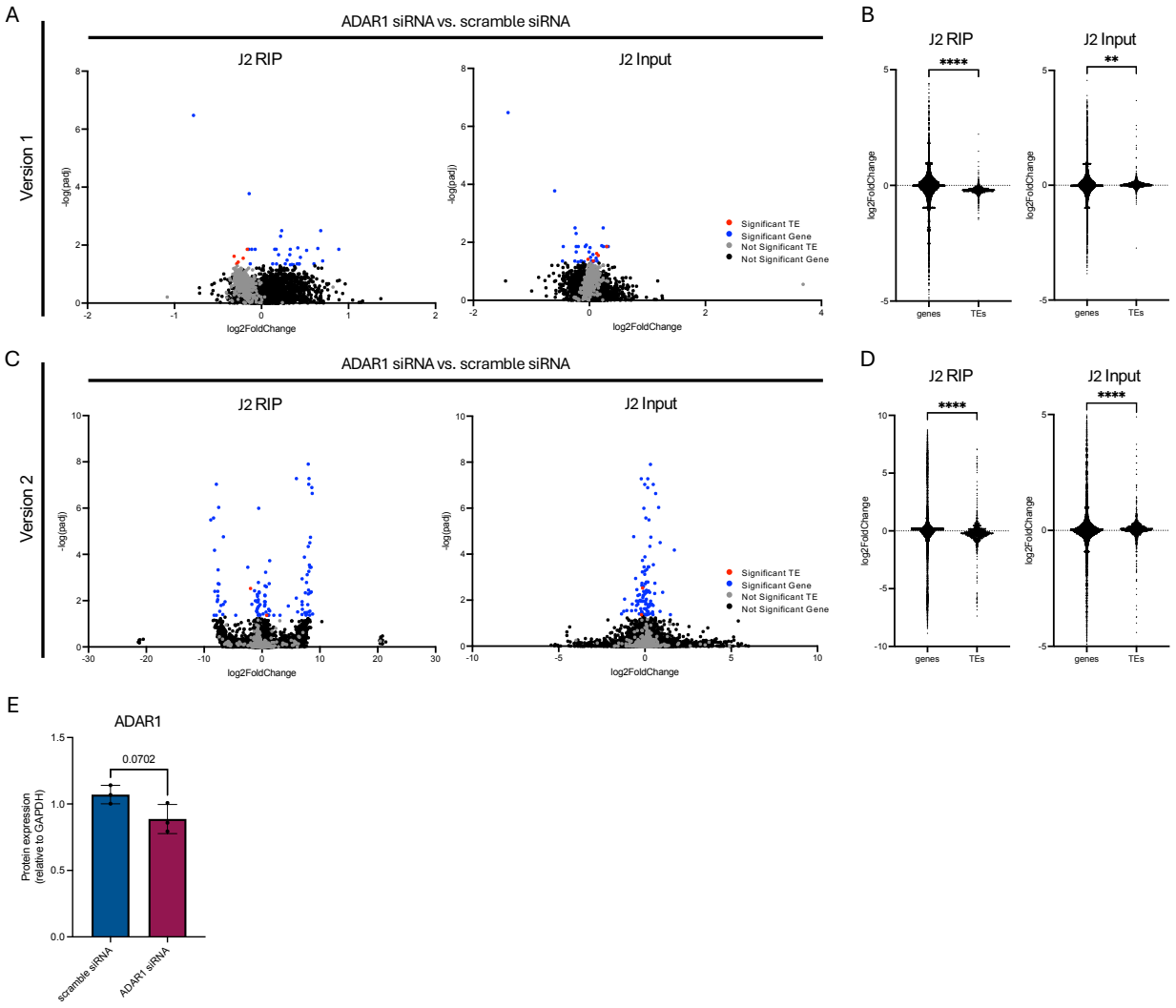


**Figure C.1. Changes in gene and TE transcript expression with J2 RIP and ADAR1 KD.** Volcano plot of J2 RIP and Input RNA-seq data showing changes in genes (black) and TE transcript (grey) expression of astrocytes transfected with ADAR1 siRNA compared to scramble siRNA for **(A)** version 1 and **(C)** version 2. Significant differentially expressed genes and TE transcripts shown in blue and red, respectively (FDR < 0.1); n=3/group. Violin plots comparing median gene and TE transcript expression in ADAR1 siRNA vs. scramble siRNA of J2 RIP and Input RNA-seq for **(B)** version 1, **(C)** version 2, and **(D)** version 3. $^{**}p \leq 0.01$, $^{***}p \leq 0.001$, $^{****}p \leq 0.0001$; Mann-Whitney test. n=3/condition.

**Supplemental Table C.1.** Top 10 genes with the lowest residuals (J2 RIP log2FC – J2 Input log2FC) in primary human astrocytes with ADAR1 is knocked down. Negative residual indicates greater expression in the J2 RIP, and residual < 0 indicates transcripts that are enriched in the RIP.

| Gene Name | Input log2FC | Input FDR | RIP log2FC | RIP FDR | Residual |
|---|---|---|---|---|---|
| SLC16A5 | -0.3100 | < 0.0001 | 9.0839 | < 0.0001 | -9.3939 |
| OLFML1 | -0.5077 | 0.0450 | 8.4221 | 0.0450 | -8.9298 |
| SLC7A3 | 0.0562 | 0.0002 | 8.9126 | 0.0002 | -8.8564 |
| SNORD93 | -0.6224 | 0.0152 | 7.9813 | 0.0152 | -8.6038 |
| SPATA22 | -0.6452 | 0.0360 | 7.8717 | 0.0360 | -8.5169 |
| DUSP27 | -0.2786 | 0.0878 | 8.2326 | 0.0878 | -8.5113 |
| LOC285847 | -0.5026 | 0.0208 | 7.9249 | 0.0208 | -8.4275 |
| LINC00669 | -0.2824 | 0.0173 | 8.1415 | 0.0173 | -8.4239 |
| GPR132 | 0.2057 | 0.0062 | 8.6081 | 0.0062 | -8.4024 |
| CFL1P1 | -0.4279 | 0.0444 | 7.9070 | 0.0444 | -8.3349 |

**Supplemental Table C.2.** Top 10 genes with the lowest residuals in the ADAR1 p110 RIP. Negative residual indicates greater expression in the ADAR1 p110 RIP, and residual < 0 indicates transcripts that are enriched in the RIP.

| Gene Name | Input log2FC | Input FDR | RIP log2FC | RIP FDR | Residual |
|---|---|---|---|---|---|
| LINC01002 | -0.0788 | < 0.0001 | 3.5743 | < 0.0001 | -3.6531 |
| MINOS1P1 | -0.2589 | 0.0001 | 3.1206 | 0.0001 | -3.3795 |
| LINC01588 | 0.4679 | 0.0154 | 3.3397 | 0.0154 | -2.8718 |
| ACPT | 0.0742 | 0.0006 | 2.7903 | 0.0006 | -2.7162 |
| MCM8-AS1 | 0.0670 | 0.0017 | 2.7785 | 0.0017 | -2.7115 |
| LOC100190986 | -0.3982 | 0.0774 | 2.2013 | 0.0774 | -2.5995 |
| AKAP5 | -0.5439 | 0.0070 | 2.0378 | 0.0070 | -2.5818 |
| LOC100996251 | -0.6951 | 0.0064 | 1.8769 | 0.0064 | -2.5720 |
| MIR3648-2 | 0.7575 | 0.0010 | 3.3218 | 0.0010 | -2.5643 |
| FKBP1AP1 | -0.7671 | 0.0643 | 1.7264 | 0.0643 | -2.4935 |
| LINC01002 | -0.0788 | < 0.0001 | 3.5743 | < 0.0001 | -3.6531 |
| MINOS1P1 | -0.2589 | 0.0001 | 3.1206 | 0.0001 | -3.3795 |
| LINC01588 | 0.4679 | 0.0154 | 3.3397 | 0.0154 | -2.8718 |

**Supplemental Table C.3.** Top 10 genes with the lowest residuals in the ADAR1 p150 RIP. Negative residual indicates greater expression in the ADAR1 p150 RIP, and residual < 0 indicates transcripts that are enriched in the RIP.

| Gene Name | Input log2FC | Input FDR | RIP log2FC | RIP FDR | Residual |
|---|---|---|---|---|---|
| ZNF329 | 0.1731 | 0.0001 | 3.1599 | 0.0001 | -2.9868 |
| CCDC117 | -0.1000 | < 0.0001 | 2.5970 | < 0.0001 | -2.6970 |
| WAC-AS1 | 1.1574 | < 0.0001 | 3.6431 | < 0.0001 | -2.4857 |
| MED18 | 0.0224 | < 0.0001 | 2.4566 | < 0.0001 | -2.4343 |

| | | | | | |
|---|---|---|---|---|---|
| FAM46A | -0.1105 | 0.0006 | 2.2898 | 0.0006 | -2.4003 |
| AEN | 1.2971 | < 0.0001 | 3.5450 | < 0.0001 | -2.2479 |
| RAB21 | -0.3417 | 0.0008 | 1.8509 | 0.0008 | -2.1926 |
| FAM53C | 1.0624 | < 0.0001 | 3.2455 | < 0.0001 | -2.1832 |
| ORAOV1 | -0.3205 | 0.0001 | 1.8597 | 0.0001 | -2.1803 |
| BFSP1 | -0.3019 | 0.0137 | 1.8500 | 0.0137 | -2.1519 |

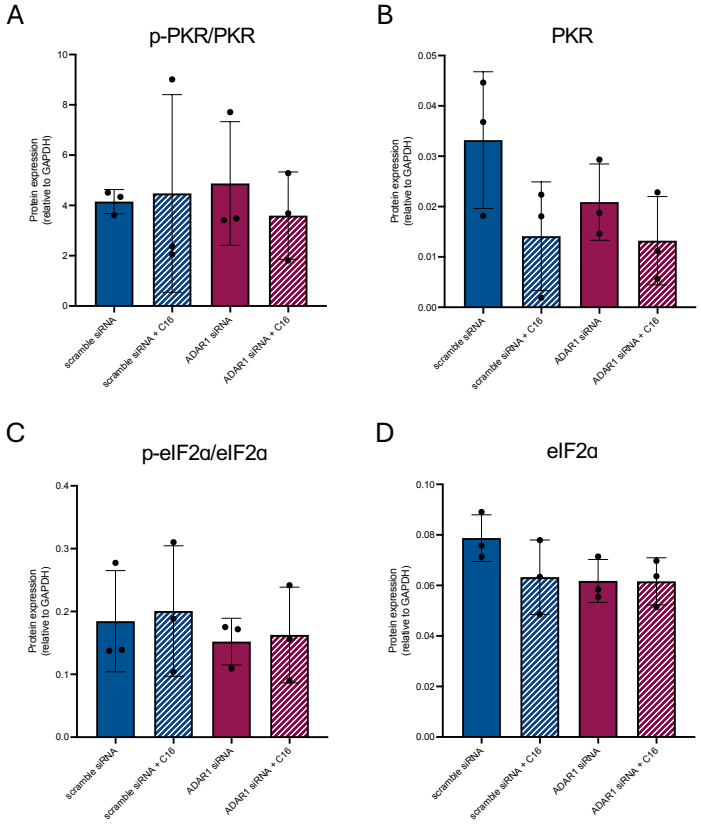


**Figure C.2. Changes in proteins involved in PKR signaling when ADAR1 is suppressed.** Immunoblot data showing **(A)** p-PKR, **(B)** PKR, **(C)** precursor TNF-α, **(D)** p-eIF2α, and **(E)** eIF2α in astrocytes transfected with an ADAR1 siRNA or a scramble siRNA and cotreated with the compound C16 (PKR inhibitor). *$p \leq 0.05$, *$p \leq 0.01$; one-way ANOVA with multiple testing; n=2-3/condition.

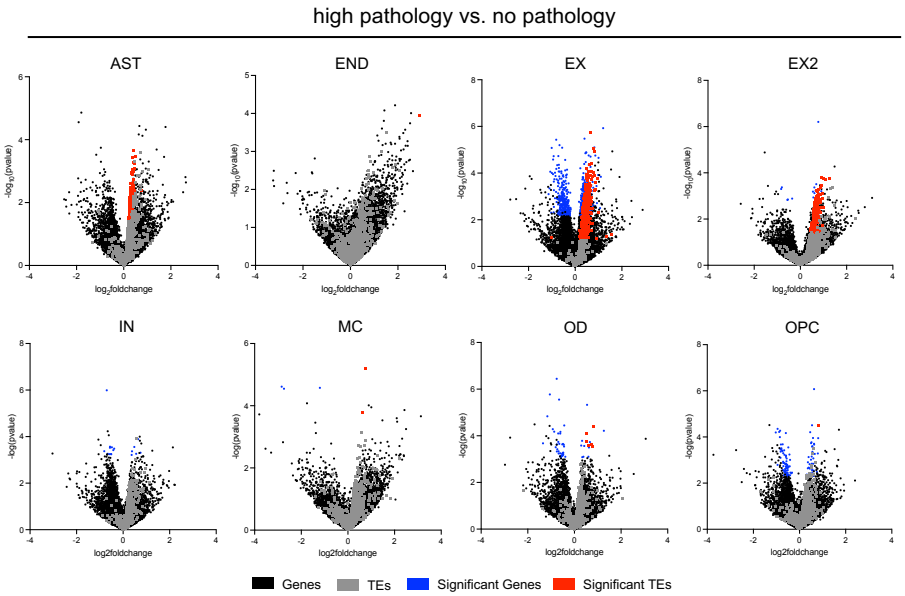


**Figure D.1. Volcano plots showing increases in TE transcript expression in subjects with high pathology.** Differentially expressed genes (black) and TE transcripts (grey) in subjects with high pathology vs. low pathology by each cell type. Significant genes (blue) and TE transcripts (red) with an FDR < 0.1.

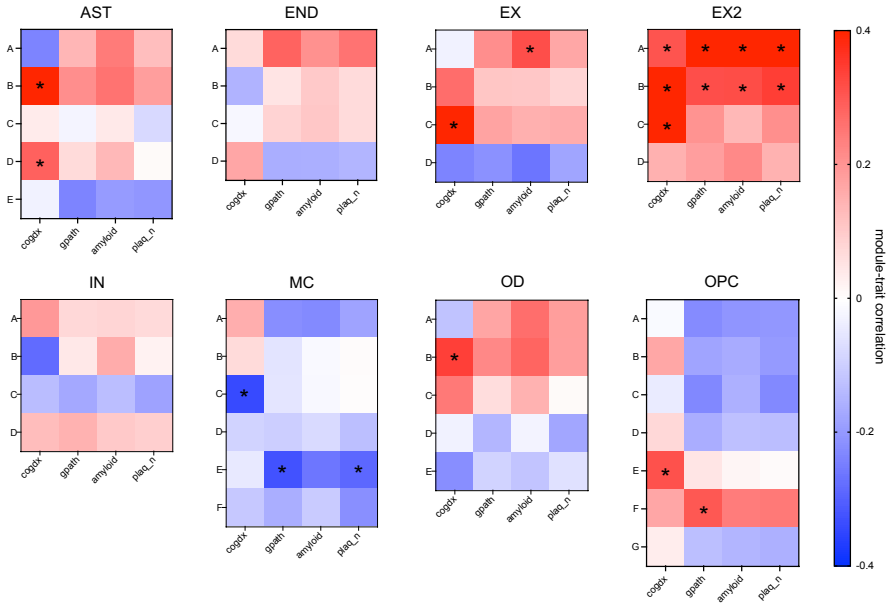


**Figure D.2. Pseudobulked TE WGCNA modules for each cell type**. *$p \leq 0.05$.

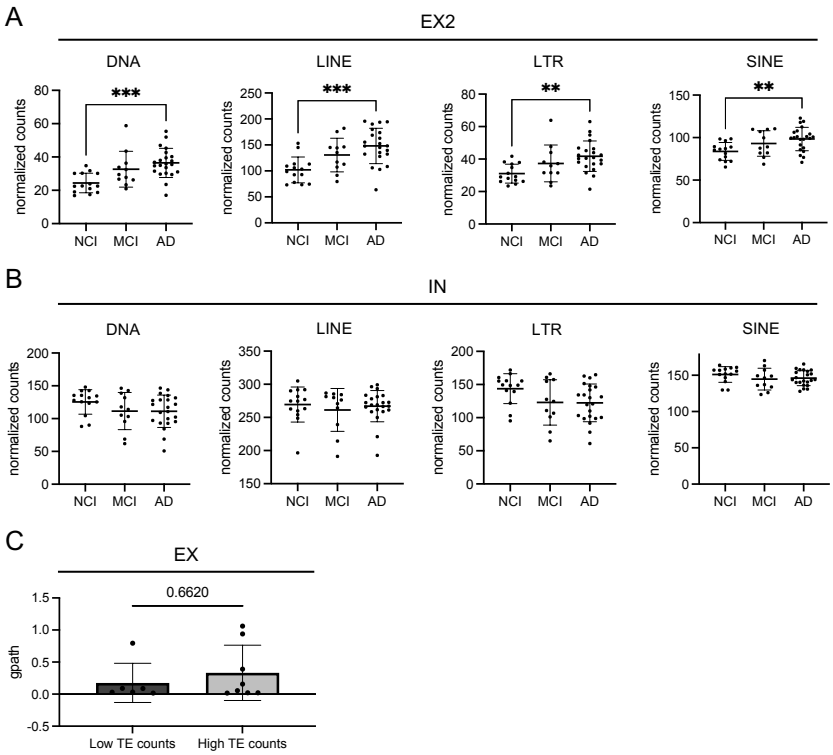


**Figure D.3. Total normalized counts (pseudobulk) of TE transcripts by class. (A)** EX2 and **(B)** IN clusters grouped by final clinical consensus diagnosis of cognitive status (cogdx). ** $p \leq 0.01$, *** $p \leq 0.001$; Kruskal-wallis test. **(C)** Global neocortical pathology (gpath) scores in NCI subjects with low vs. high total normalized TE counts (for all TE types); Mann-Whitney test.

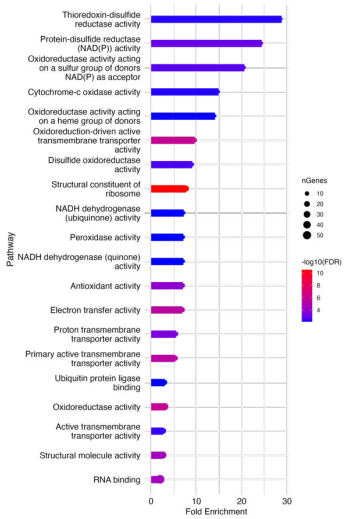


**Figure D.4.** Gene Ontology (GO) analysis of high pathology vs. no pathology differentially expressed genes within the EX cluster correlating with total TE transcript counts in all subjects

**Supplemental Table D.1.** TE transcripts (including subfamily, type, and copy number) that are shared between the astrocyte, excitatory neuron, and excitatory neuron 2 clusters.

| TE | Subfamily | Type | Copy Number |
|---|---|---|---|
| Arthur2 | hAT-Tip100 | DNA | 24 |
| FLAM-C | Alu | SINE | 26386 |
| L1M1 | L1 | LINE | 10243 |
| L1M3b | L1 | LINE | 650 |
| L1M3c | L1 | LINE | 1107 |
| L1M4b | L1 | LINE | 4719 |
| L1MA10 | L1 | LINE | 5264 |
| L1MA3 | L1 | LINE | 9668 |
| L1ME3F | L1 | LINE | 4795 |
| L1P1 | L1 | LINE | 3449 |
| L1P2 | L1 | LINE | 1669 |
| L1P4d | L1 | LINE | 161 |
| L1PA10 | L1 | LINE | 7573 |
| L1PA12 | L1 | LINE | 1912 |
| L1PA15 | L1 | LINE | 10265 |
| L1PA2 | L1 | LINE | 5251 |
| L1PA3 | L1 | LINE | 11401 |
| L1PA4 | L1 | LINE | 12692 |
| L1PA5 | L1 | LINE | 11889 |
| L1PA6 | L1 | LINE | 6297 |
| L1PA7 | L1 | LINE | 13661 |
| L1PA8 | L1 | LINE | 8642 |
| L1PA8A | L1 | LINE | 2571 |
| L1PB1 | L1 | LINE | 13715 |
| L1PBa | L1 | LINE | 2334 |
| L1PBa1 | L1 | LINE | 552 |
| LTR23-int | ERV1 | LTR | 192 |
| LTR37-int | ERV1 | LTR | 1380 |
| MER101 | ERV1 | LTR | 1621 |
| MER5C | hAT-Charlie | DNA | 1380 |
| MER92-int | ERV1 | LTR | 1012 |
| MLT1B-int | ERVL-MaLR | LTR | 592 |

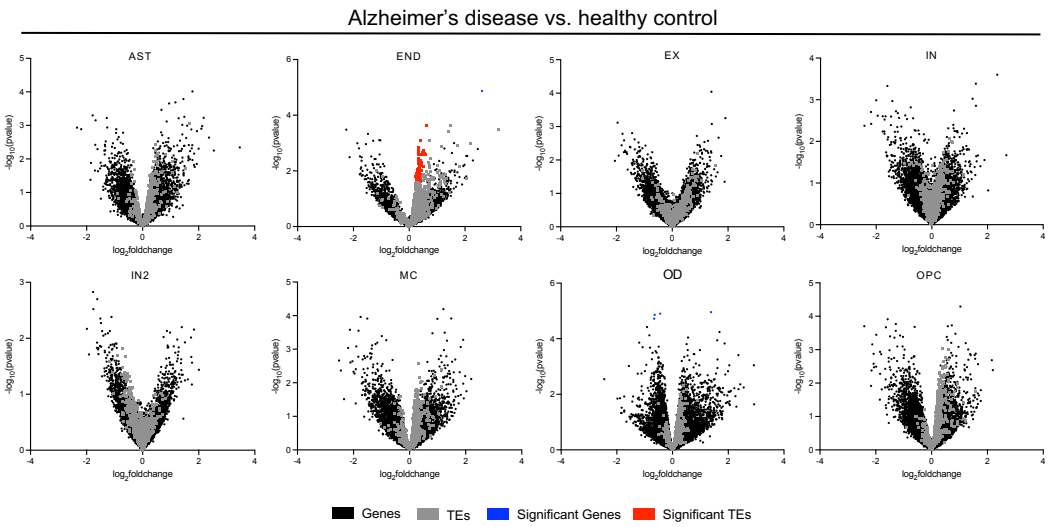


**Figure D.5. Volcano plots showing increases in TE transcript expression in subjects with AD.** Differentially expressed genes (black) and TE transcripts (grey) in AD subjects for each cell type. Significant genes (blue) and TE transcripts (red) with an FDR < 0.1.

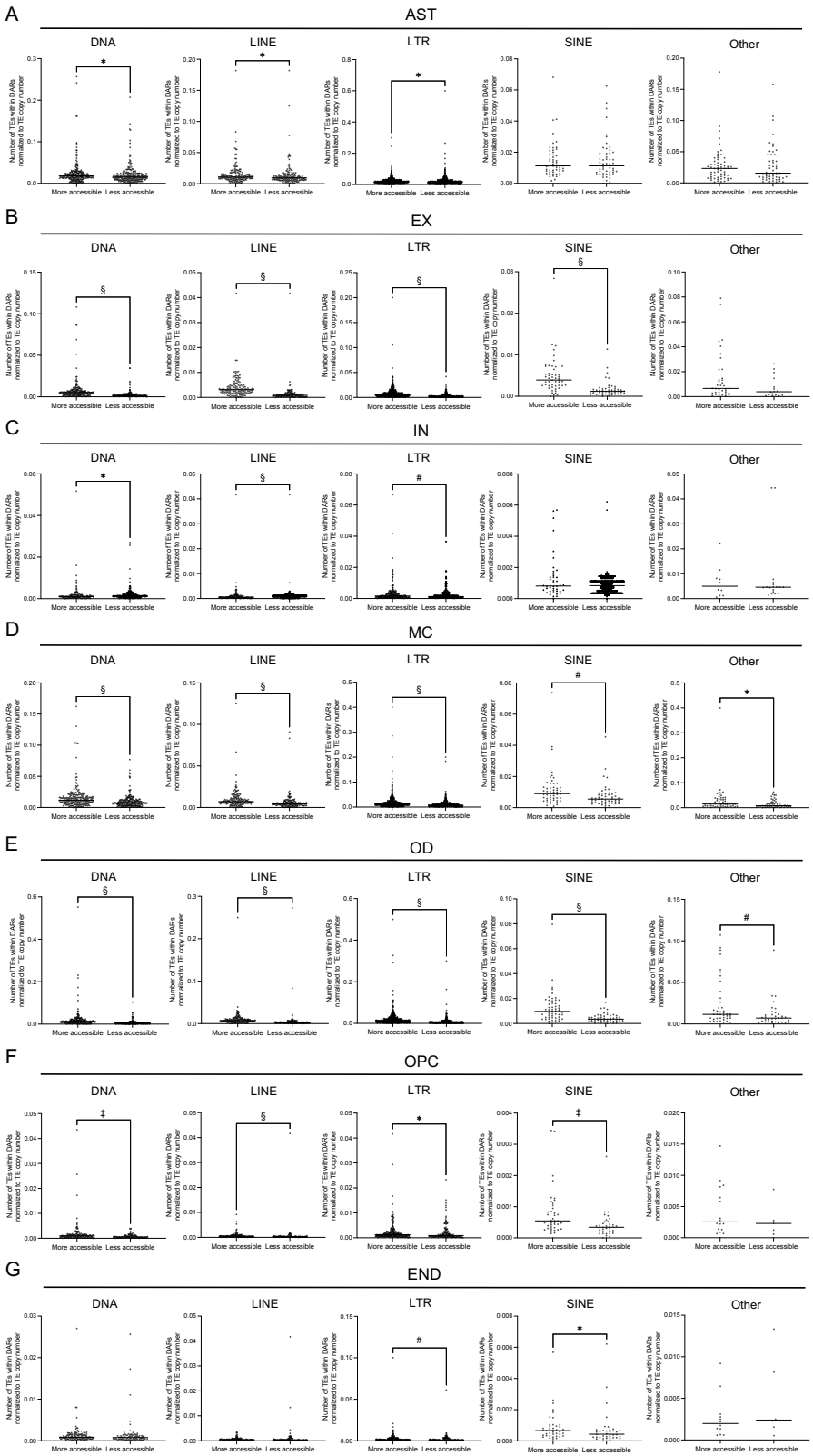


**Figure D.6. Number of TEs normalized to TE copy number for each cell type and TE class in 'more accessible' vs 'less accessible' regions.** *$p \leq 0.05$, #$p \leq 0.01$, ‡p ≤ 0.001, §$p \leq$ 0.0001; Mann-Whitney test.

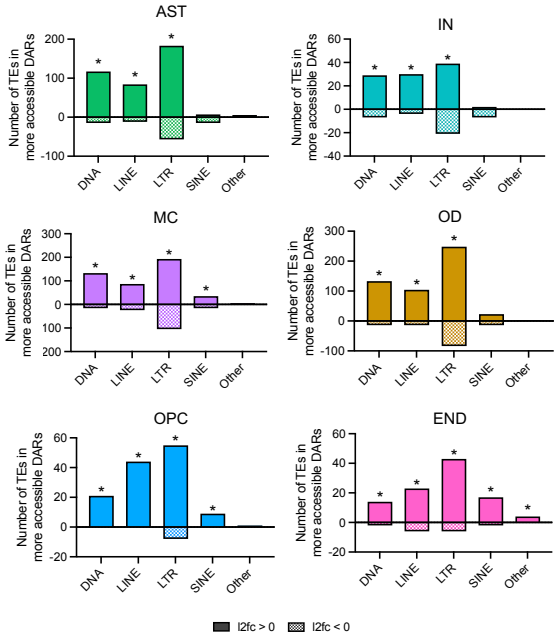


**Figure D.7. Number of TEs in more accessible DARs (TE accessibility ratio > 1).** TE transcript expression log2foldchange > 0 vs. log2foldchange < 0 for AST, IN, MC, OD, OPC, END clusters by class. *$p$ < 0.0001; Chi-square test.

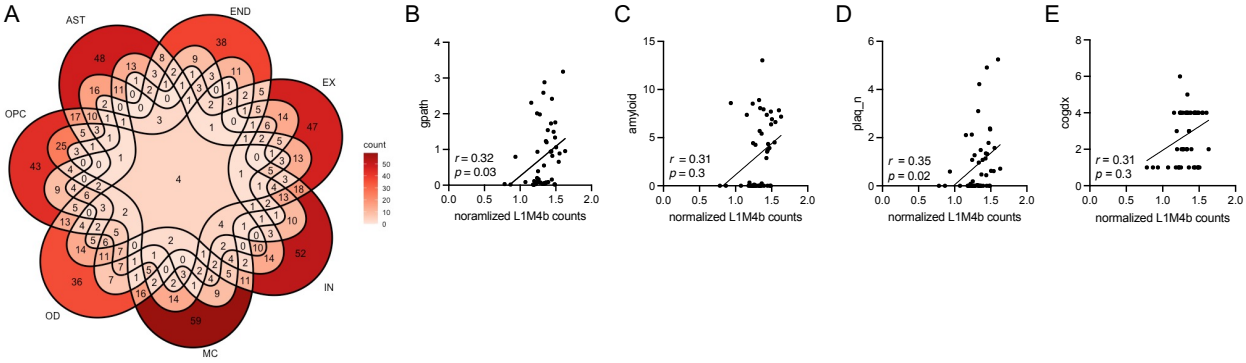


**Figure D.8. Shared TE transcripts across all cell types correlated with AD pathological scoring and cognitive diagnosis. (A)** Shared TE transcripts across all cell types. Simple Pearson correlations between normalized L1M4b counts and the following clinical data in al 48 subjects: **(B)** gpath = global neocortical pathology, **(C)** amyloid = overall amyloid burden, **(D)** plaq_n = neuritic plaque burden, **(E)** cogdx = final consensus cognitive diagnosis.

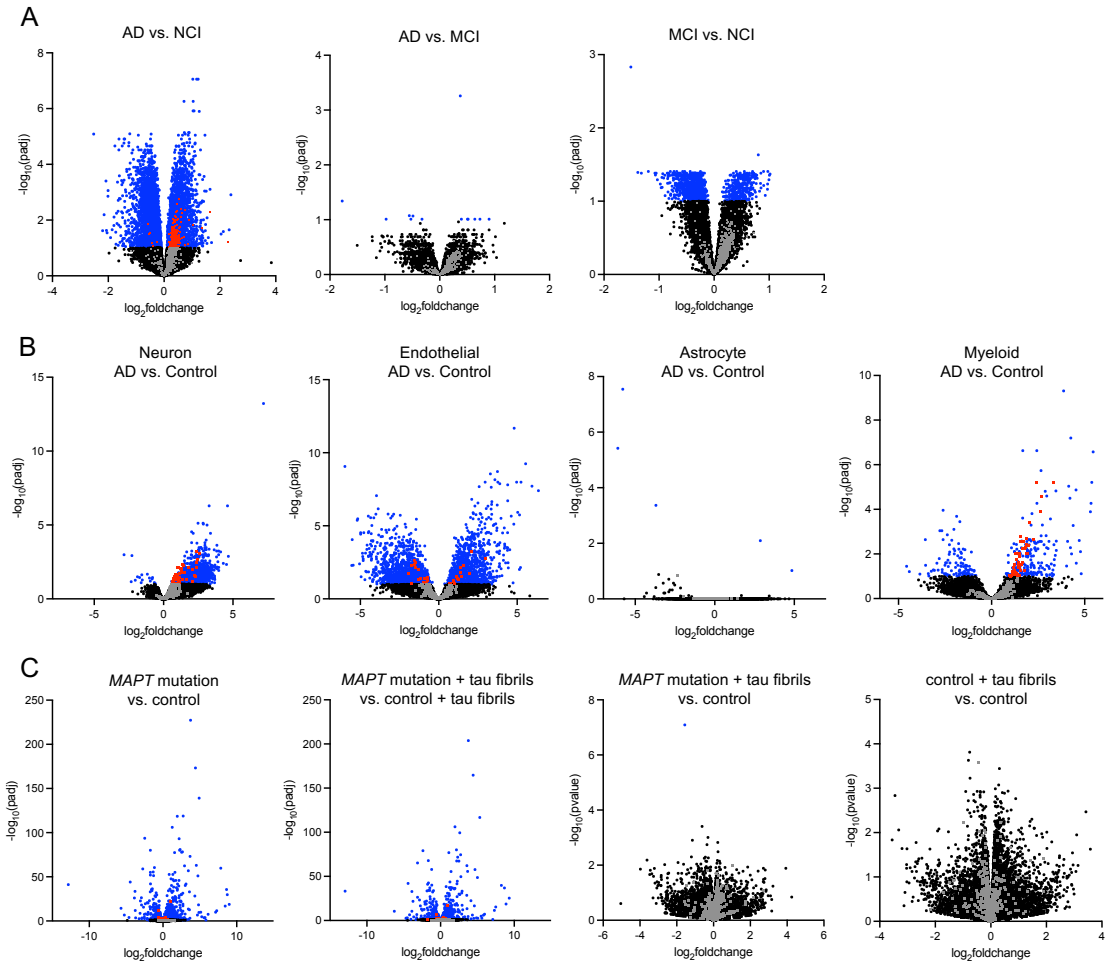


**Figure D.9. Volcano plots of 'neuron-focused' bulk RNA-seq datasets for TE transcripts.** **(A)** Volcano plots showing differentially expressed genes (black) and TE transcripts (grey) in AD patients and MCI subjects. Significant genes (blue) and TE transcripts (red) with an FDR < 0.1. **(B)** Volcano plots showing differentially expressed genes (black) and TE transcripts (grey) in FACS cell types from AD and control brain tissue. Significant genes (blue) and TE transcripts (red) with an FDR < 0.1. **(C)** Volcano plots showing differentially expressed genes (black) and TE transcripts (grey) in 4R tau iPSC-derived neurons with P130S MAPT mutation and with or without the addition of tau fibrils. Significant genes (blue) and TE transcripts (red) with an FDR < 0.1.

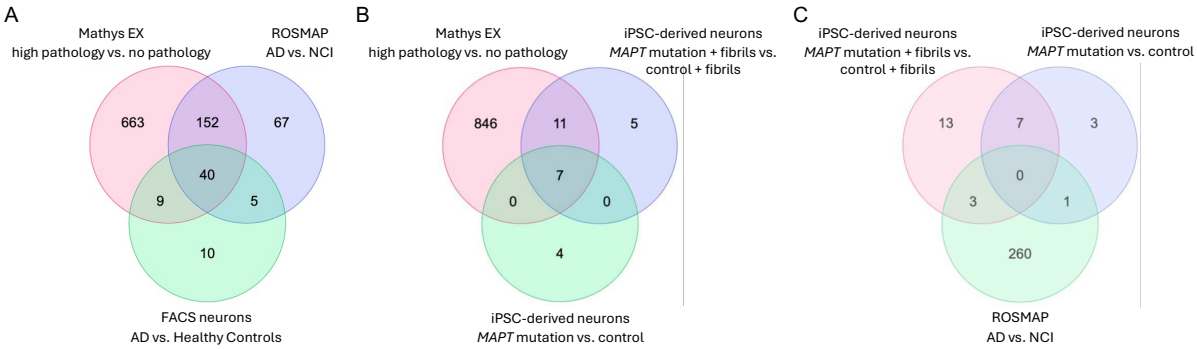

**Figure D.10. Common TE transcripts between snRNA-seq and bulk RNA-seq datasets. (A)** Venn diagram showing TE transcripts shared between the Mathys snRNA-seq EX cluster (high pathology vs. no pathology), ROSMAP bulk RNA-seq (AD vs. NCI), and FACS neurons RNA-seq (AD vs. healthy controls). **(B)** Venn diagram showing TE transcripts shared between the Mathys snRNA-seq EX cluster (high pathology vs. no pathology) and 4R tau iPSC-derived neurons (*MAPT* mutation + tau fibrils vs. control + tau fibrils and *MAPT* mutation vs. control). **(C)** Venn diagram showing TE transcripts shared between the ROSMAP bulk RNA-seq (AD vs. NCI) and 4R tau iPSC-derived neurons (*MAPT* mutation + tau fibrils vs. control + tau fibrils and *MAPT* mutation vs. control). TE transcripts used in these comparisons were significantly (FDR < 0.1) upregulated ($log_2$foldchange > 0) in their respective comparisons.

APPENDIX E – CHAPTER 6 SUPPLEMENTAL DATA

**Supplemental Table E.1.** NIH NeuroBioBank subject characteristics for single-nucleus multi-omics (snRNA/snATAC) study (Chapter 6, Aim 2).

| | **Young (n = 10)** | **Old (n = 10)** | **AD (n = 10)** |
|---|---|---|---|
| Age (years) | 38.7 ± 4.95 | 84.3 ± 3.62* | 85.6 ±1.78* |
| Sex | 5M/5F | 5M/5F | 5M/5F |
| Race | 3W/4B/3NR | 6W/4B | 6W/4B |
| Clinical Brain Diagnosis | No clinical diagnosis found | No clinical diagnosis found | Alzheimer's disease with late onset |
| Neuropathology Diagnosis | Diagnostic pathology not present | Diagnostic pathology not present | Alzheimer's disease with late onset |
| Non-Diagnosis Flag | Normative | Normative | Not Applicable |
| Repository | Mt. Sinai | Mt. Sinai | Mt. Sinai |

Values are reported as mean ± SD.
*$p \leq 0.0001$ compared to Young; One-way ANOVA with multiple comparisons.
W = white, B = black, NR = not reported

**Supplemental Table E.2.** NIH NeuroBioBank subject IDs for single-nucleus multi-omics (snRNA/snATAC) study (Chapter 6, Aim 2).

| **Young (subject ID)** | **Old (subject ID)** | **AD (subject ID)** |
|---|---|---|
| 904597 | 68129 | 49022 |
| 50197 | 393501 | 61631 |
| 23996 | 34913 | 64525 |
| 62622 | 29972 | 38069 |
| 570004 | 2027 | 271116 |
| 63941 | 7698 | 42235 |
| 67963 | 66229 | 33789 |
| 74432 | 85981 | 91903 |
| 74703 | 62537 | 71010 |
| 813923 | 99695 | 65669 |